EFFECT OF PREPARATION AND OPERATION PARAMETERS ON PERFORMANCE OF POLYETHERSULFONE BASED MIXED MATRIX GAS SEPARATION MEMBRANES

A THESIS SUBMITTED TO
THE GRADUATE SCHOOL OF NATURAL AND APPLIED SCIENCES
OF
MIDDLE EAST TECHNICAL UNIVERSITY

BY

ELİF KARATAY

IN PARTIAL FULFILLMENT OF THE REQUIREMENTS
FOR
THE DEGREE OF MASTER OF SCIENCE
IN
CHEMICAL ENGINEERING

AUGUST 2009

Approval of the thesis:

EFFECT OF PREPARATION AND OPERATION PARAMETERS ON PERFORMANCE OF POLYETHERSULFONE BASED MIXED MATRIX GAS SEPARATION MEMBRANES

submitted by **ELİF KARATAY** in partial fulfillment of the requirements for the degree of **Master of Science in Chemical Engineering Department, Middle East Technical University** by,

Prof. Dr. Canan Özgen
Dean, Graduate School of **Natural and Applied Sciences** _____

Prof. Dr. Gürkan Karakaş
Head of Department, **Chemical Engineering** _____

Prof. Dr. Levent Yılmaz
Supervisor, **Chemical Engineering Dept., METU** _____

Assoc. Prof. Dr. Halil Kalıpçılar
Co-supervisor, **Chemical Engineering Dept., METU** _____

Examining Committee Members:

Prof. Dr. Ali Çulfaz
Chemical Engineering Dept., METU _____

Prof. Dr. Levent Yılmaz
Chemical Engineering Dept., METU _____

Prof. Dr. Birgül Tantekin Ersolmaz
Chemical Engineering Dept., ITU _____

Assoc. Prof. Dr. Halil Kalıpçılar
Chemical Engineering Dept., METU _____

Assoc. Prof. Dr. Göknur Bayram
Chemical Engineering Dept., METU _____

Date: 17.08.2009

I hereby declare that all information in this document has been obtained and presented in accordance with academic rules and ethical conduct. I also declare that, as required by these rules and conduct, I have fully cited and referenced all material and results that are not original to this work.

Name, Last name : Elif Karatay

Signature :

ABSTRACT

EFFECT OF PREPARATION AND OPERATION PARAMETERS ON PERFORMANCE OF POLYETHERSULFONE BASED MIXED MATRIX GAS SEPARATION MEMBRANES

Karatay, Elif

M.Sc., Department of Chemical Engineering

Supervisor : Prof. Dr. Levent Yılmaz

Co-supervisor : Assoc. Prof. Dr. Halil Kalıpçılar

August 2009, 126 pages

Membrane processes have been considered as promising alternatives to other competing technologies in gas separation industry. Developing new membrane morphologies are required to improve the gas permeation properties of the membranes. Mixed matrix membranes composing of polymer matrices and distributed inorganic/organic particles are among the promising, developing membrane materials.

In this study, the effect of low molecular weight additive (LMWA) type and concentration on the gas separation performance of neat polyethersulfone (PES) membranes and zeolite SAPO-34 containing PES based mixed matrix membranes was investigated. Membranes were prepared by solvent evaporation method and annealed above the glass transition temperature (T_g) of PES in order to remove the residual solvent and erase the thermal history. They were characterized by single gas permeability measurements of H_2, CO_2, and CH_4 as well as scanning electron microscopy (SEM), thermal gravimetric analysis (TGA), and differential scanning calorimetry (DSC).

Various LMWAs were added to the neat PES membrane at a concentration of 4 wt %. Regardless of the type, all of the LMWAs had an anti-plasticization effect on PES gas permeation properties. 2-Hydroxy 5-Methyl Aniline, HMA, was selected among the other LMWAs for parametric study on the concentration effect of this additive.

The incorporation of SAPO-34 to PES membranes increased the permeabilities of all gases with a slight loss in selectivities. However, the addition of HMA to PES/SAPO-34 membranes increased the ideal selectivities well above the ideal selectivities of PES/HMA membranes, while keeping the permeabilities of all the gases above the permeabilities of both pure PES and PES/HMA membranes.

Keywords: Gas Separation, Mixed Matrix Membrane, Antiplasticization, Polyethersulfone, SAPO-34, 2-hydroxy 5-methyl aniline

ÖZ

POLİETERSÜLFON BAZLI KARIŞIK MATRİSLİ MEMBRANLARIN HAZIRLANMA VE ÖLÇÜM PARAMETRELERİNİN GAZ AYIRIM PERFORMANSINA ETKİLERİ

Karatay, Elif

Yüksek Lisans, Kimya Mühendisliği Bölümü

Tez Yöneticisi : Prof. Dr. Levent Yılmaz

Ortak Tez Yöneticisi : Doç. Dr. Halil Kalıpçılar

Ağustos 2009, 126 sayfa

Gazların membran ayırım süreçleri ile ayrılması sanayide kullanılan diğer uygulamalara göre çok daha umut vaadeden alternatif bir yöntemdir. Bu sebeple, yüksek gaz ayırım performans özelliklerine sahip membranlara olan gereksinim, araştırmaları yeni membran morfolojilerinin ve membran malzemelerinin geliştirilmesi yönünde yoğunlaştırmıştır. Bu kapsamda, polimerik membranların seçici-geçirgen özelliklerini değiştirmek amacıyla, polimere zeolit dolgu maddesinin katılması ile oluşturulan karışık matrisli membranlar geliştirilen malzemeler arasındadır.

Bu çalışmada, düşük molekül ağırlıklı katkı maddeleri (LMWA) türü ve bunların membrandaki farklı derişimlerinin saf polietersülfon ve SAPO-34 zeoliti katkılı karışık matrisli membranların seçici-geçirgen özelliklerine etkileri araştırılmıştır. Membranlar çözücü buharlaştırma yöntemi, ve politersülfon polimerinin camsı geçiş sıcaklığının üzerinde tavlanması ile hazırlanmıştır. Bu sıcaklıkta gerçekleştirilen tavlama membranlarda kalabilecek olan artık çözücüyü uçurma ve membranların ısısal hafızalarını silmek amacı ile

tercih edilmiştir. Membranlar tarama elektron mikroskobu (SEM), fark taramalı kalorimetre (DSC) ve H_2, CO_2, ve CH_4 gazlarının tek gaz geçirgenlik ölçümleri ile karakterize edilmiştir.

Farklı kimyasal yapılara sahip düşük molekül ağırlıklı katkı maddeleri membran hazırlama çözeltilerine ağırlıkça % 4 derişimde eklenerek katkılı PES membranlar üretilmiştir. Kimyasal yapıdan bağımsız olarak tüm katkı maddeleri, membranların gaz geçirgenliklerini düşürerek ve ideal seçiciliklerini yükselterek, yapıda anti-plastizasyon etkisi yaratmıştır. Düşük molekül ağırlıklı katkı maddelerinden, 2-hidroksil-5-metil anilin farklı derişimlerin etkisini araştırmak amacıyla seçilmiştir.

SAPO-34 zeoliti katkılı karışık matrisli membranlar saf polietersülfon membranlar kıyasla ideal seçiciliklerde az bir kayıpla daha yüksek gaz geçirgenlikleri göstermişlerdir. Ancak SAPO-34 zeoliti katkılı karışık matrisli polietersülfon membranlara düşük molekül ağırlıklı katkı maddesi 2-hidroksil-5-metil anilinin eklenmesi ile hem gaz geçirgenlikleri hem de ideal seçicilikleri PES/HMA membranlara göre geliştirilmiştir.

Anahtar sözcükler: Gaz ayırımı, Karışık Matrisli Membran, Antiplastizasyon, Polietersülfon, SAPO-34, 2-hidroksil-5-metil anilin.

To my mother Emel Karatay

ACKNOWLEDGEMENTS

I wish to express my sincere gratitude to my supervisor Prof. Dr. Levent Yılmaz for his guidance and interest throughout this study. I would also like to thank my co-supervisor Assoc. Prof. Dr. Halil Kalıpçılar for his suggestions, criticisim and helps.

I would like to thank the financial supports from The Scientific and Technological Research Council of Turkey (TUBITAK) through the grant number 106M179 and Prof. Dr. Birgül Tantekin Ersolmaz for her guidance and supervision throughout this project. I would also gratefully acknowledge TUBITAK for the bursary provided to me during my M.Sc. education.

I would like to thank to thermal analysis specialists Doç. Dr. Necati Özkan, Ayşenur Özkan, and Mihrican Açıkgöz for their helps in Differential Scanning Calorimetric analysis. I wish also thank specialist Burcu Akata for her helps in Scanning Electron Microscopic analysis.

I also thank to the technicians of Chemical Engineering Department of Middle East Technical University.

I would like to thank my colleague Değer Şen for her helps, suggestions, solutions to my problems, and conveying her invaluable laboratory experiences to me. I would like to thank also to all of my friends, especially Berker Fıçıcılar not only their endless support and understanding but also for their very special intimacy. Thanks also to all my lab mates for their helpful and enjoyable friendships throughout this study.

I am indebted to my mother Emel Karatay for her continuous encouragement, understanding and endless support.

TABLE OF CONTENTS

ABSTRACT iv

ÖZ iv

ACKNOWLEDGEMENTS ix

TABLE OF CONTENTS x

LIST OF TABLES xiii

LIST OF FIGURES xvii

LIST OF SYMBOLS AND ABBREVIATIONS xxii

CHAPTER

1. INTRODUCTION 1

2. LITERATURE SURVEY 6

2.1 Polymeric Gas Separation Membranes 6

2.2 Polymer/Additive Gas Separation Membranes 9

2.3 Mixed Matrix Membranes 13

2.3.1 Mixed Matrix Membranes Prepared with Rubbery Polymers 14

2.3.2 Mixed Matrix Membranes Prepared with Glassy Polymers 15

2.4 Possible Interface Morphologies and Attempts to Improve Mixed Matrix Membranes'Performance 18

3. EXPERIMENTAL 26

3.1 Membrane Preparation 26

3.1.1 Materials for Membrane Preparation 26
3.1.2 Determination of Solubilities of Low Molecular Weight Additives 28
3.1.3 Membrane Preparation Methodology 28
3.2 Membrane Characterization 32
3.2.1 Thermal Characterization 32
3.2.2 Scanning Electron Microscopy (SEM) Characterization 33
3.2.3 Carbon-Nitrogen-Sulphur Elemental Analysis 33
3.2.4 Single Gas Permeability Measurements 33
3.2.4.1 Single Gas Permeability Set-Up and Procedure 33
3.2.4.2 Single Gas Permeability Calculations 37
4. RESULTS AND DISCUSSION 39
4.1 Selection of Membrane Preparation Materials 39
4.2 Effects of Measurement and Preparation Methodology 44
4.2.1 Reproducibility in Permeability Measurements and Membrane Preparation 47
4.2.2 Effects of Membrane Preparation Parameters 48
4.2.2.1 Modifications on Annealing 50
4.3 PES/LMWA Blend Membranes 54
4.3.1 Effect of LMWA Type on PES/LMWA Blend Membranes 54
4.3.2 Effect of LMWA Loading on PES/LMWA Blend Membranes 62
4.4 Development of SAPO-34 Filled Mixed Matrix Membranes 67
4.4.1 PES/SAPO-34 Mixed Matrix Membranes 67
4.4.2 PES/HMA/SAPO-34 Mixed Matrix Membranes 68
4.4.2.1 Effect of Zeolite Loading on PES/HMA/SAPO-34 Mixed Matrix Membranes 75

4.5 Characterization of Membranes 77

4.5.1 TGA Experiments 77

4.5.2 DSC Experiments 79

4.5.3 Morphological Characterization of Membranes 81

4.5.4 Characterization of Membranes by Carbon-Nitrogen-Sulphur Elemental Analysis 86

5. CONCLUSIONS 89

REFERENCES 91

APPENDICES

A. AMOUNTS OF MATERIALS IN MEMBRANE PREPARATION 98

B. REPRODUCIBILITY EXPERIMENTS FOR SINGLE GAS PERMEABILITY MEASUREMENTS 99

C. SAMPLE DSC THERMOGRAMS OF THE PREPARED MEMBRANES 105

D. DETERMINATION OF SOLUBILITY PARAMETERS BY HOY'S METHOD 116

E. THERMAL GRAVIMETRIC ANALYSIS GRAPHS 118

F. ELEMENTAL ANALYSIS 124

LIST OF TABLES

TABLES

Table 2.1 Potential applications of gas separation membranes 7

Table 2.2 Comparison of additives incorporated to polymeric membranes 12

Table 2.3 Selected studies on MMMs prepared by several glassy polymers..... 16

Table 2.4 Several methods proposed to enhance polymer/zeolite interface..... 23

Table 3.1 Chemical structures of low molecular weight additives used in membrane preparation..... 27

Table 3.2 LMWA/PES ratio for various membrane solutions..... 29

Table 4.1 Three component Hansen solubility parameters of the selected polymer and solvent candidates..... 41

Table 4.2 Selected LMWAs with their chemical structure and physical properties together with their experimental solubilities in three candidate solvents... 43

Table 4.3 Permeability and selectivity results of pure PES membranes casted and tested at different times measured at 35 ^{o}C, feed side preesure is 2 bar, and permeate side is at vacuum 47

Table 4.4 Permeabilities of dense homogeneous PES membranes in literature 49

Table 4.5 Effect of annealing conditions on pure PES membrane gas separation performance..... 51

Table 4.6 Permeability and selectivity results for PES/LMWA membranes..... 56

Table 4.7 T_g of PES membranes prepared with different LMWAs 57

Table 4.8 Kinetic diameters of studied gases 58

Table 4.9 Solubility Parameters Values of Polyethersulfone and Additives 60

Table 4.10 Permeabilities and ideal selectivities of PES/SAPO-34 mixed matrix membranes including 20 w/w % SAPO-34 67

Table 4.11 Single gas permeabilities through PES/SAPO-34/HMA MMMs..... 69

Table 4.12 Ideal Selectivity values of PES/SAPO-34/HMA MMMs..... 70

Table 4.13 Effect of zeolite loading on the gas permeabilities for PES/SAPO-34/HMA MMMs 76

Table 4.14 Effect of zeolite loading on the ideal selectivities for PES/SAPO-34/HMA MMMs 77

Table 4.15 Effect of HMA/PES ratio on the glass transition temperatures of PES/HMA blend membranes..... 80

Table 4.16 Comparison of glass transition temperatures of mixed matrix membranes with pure PES and PES/HMA blend membranes 82

Table 4.17 Weight percentages of carbon, nitrogen, and sulphur elements in the PES/HMA membranes obtained by CNS elemental analysis and calculated theoretically 87

Table 4.18 Estimations of HMA contents of PES/HMA membranes based on the amount of nitrogen element detected by CNS elemental analysis 88

Table A.1 Actual weights of polymer and additive and volume of the solvent used during pure polymer, and polymer/additive membranes 98

Table A.2 Actual weights of polymer and zeolite and volume of the solvent used during polymer/zeolite and polymer/zeolite/additive mixed matrix membranes 98

Table B.1 Reproducibility data for pure PES membranes 99

Table B.2 Reproducibility data for PES/HMA (2 w/w %) membranes 100

Table B.3 Reproducibility data for PES/HMA (4 w/w %) membranes 100

Table B.4 Reproducibility data for PES/HMA (7 w/w %) membranes 100

Table B.5 Reproducibility data for PES/SAPO-34 membrane 101

Table B.6 Reproducibility data for PES/SAPO-34(20 w/w %)/HMA(4 w/w %) membrane 101

Table B.7 Reproducibility data for PES/SAPO-34(20 w/w %)/HMA(7 w/w %) membrane 101

Table B.8 Reproducibility data for PES/SAPO-34(20 w/w %)/HMA(10 w/w %) membrane 102

Table B.9 Reproducibility data for PES/SAPO-34(10 w/w %)/HMA(10 w/w %) membrane 102

Table B.10 Reproducibility data for PES/SAPO-34(30 w/w %)/HMA(10 w/w %) membrane 102

Table B.11 Reproducibility data for PES/SAPO-34(40 w/w %)/HMA(10 w/w %) membrane 103

Table B.12 Data for pure PES membrane, above T_g annealed and gas permeated at feed pressure of 3.7 bar with a initially vacuum permeate side pressure ... 103

Table B.13 Data for PES/pNA (4 w/w %) membranes 103

Table B.14 Data for PES/ANP (4 w/w %) membranes 103

Table B.15 Data for PES/AMP (4 w/w %) membranes..... 104

Table B.16 Data for PES/Mia (4 w/w %) membranes 104

Table B.17 Data for PES/AHMP (4 w/w %) membranes 104

Table B.18 Data for PES/HMA (4 w/w %) membranes 104

Table D.1 Values of increment of molar functions for Hoy's system 117

Table D.2 Estimated solubility parameter components for HMA 117

Table F.1 Carbon-Nitrogen-Sulphur Elemental Analysis Results 124

Table F.2 Weight percentages of elements in polymer and additive..... 126

Table F.3 Amounts of elements in PES/HMA (4 % (w/w)) membrane. 126

LIST OF FIGURES

FIGURES

Figure 1.1 Upper bound trade-off curve 2008 for the hydrogen methane gas pair 3

Figure 2.1 Possible interfacial morphologies for MMMs and effect on CO_2/CH_4 gas transport properties 19

Figure 2.2 Cross sectional SEM image of a polysulfone-zeolite 4A MMM, "sieve-in-a-cage" morphology 21

Figure 3.1 Repeating unit of polyethersulfone 26

Figure 3.2 Flow chart of the casting membrane solution preparation procedure for PES/LMWA blend membranes 30

Figure 3.3 Flow chart of the casting membrane solution preparation procedure for PES/SAPO-34 and PES/SAPO-34/LMWA membranes 30

Figure 3.4 Flow chart of membrane preparation procedure of all type of membranes after the casting membrane solution preparation 32

Figure 3.5 Schematic view of both of the single gas permeation systems 34

Figure 3.6 Schematic of front view of the home made membrane cell..... 35

Figure 3.7 Schematic of the Millipore membrane cell 36

Figure 4.1 Permeate side pressure increase with time for pure PES membrane, feed side pressure is 2 bar, permeate side pressure is at vacuum 45

Figure 4.2 Effect of spontaneous change of temperature on permeate side pressure for pure PES membrane 46

Figure 4.3 TGA graph of membranes (a) annealed at 110 ^{o}C for 24 hour (b) annealed at 130 ^{o}C, 160 ^{o}C, 190 ^{o}C for 3 days, 225 ^{o}C for 8 hours, respectively 52

Figure 4.4 SEM images of PES/AHMP, indicating the AHMP agglomerations (a) Top view (b) Cross-sectional..... 56

Figure 4.5 Reduction in H_2 permeability with increasing HMA/PES ratio in the membrane casting solution..... 63

Figure 4.6 Reduction in CO_2 permeability with increasing HMA/PES ratio in the membrane casting solution..... 63

Figure 4.7 Reduction in CH_2 permeability with increasing HMA/PES ratio in the membrane casting solution..... 64

Figure 4.8 Effect of increasing HMA/PES ratio in the casting membrane solution on H_2/CO_2 ideal selectivity..... 65

Figure 4.9 Effect of increasing HMA/PES ratio in the casting membrane solution on CO_2/CH_4 ideal selectivity 66

Figure 4.10 Effect of increasing HMA/PES ratio in the casting membrane solution on H_2/CH_4 ideal selectivity..... 66

Figure 4.11 Effect of HMA loading on the gas permeabilities of H_2, CO_2, and CH_4 69

Figure 4.12 Comparison of increasing HMA/PES ratio (w/w %) on (a) H_2 permeability (b) H_2/CH_4 ideal selectivity between PES/HMA and PES/SAPO-34 (20%)/HMA membranes 71

Figure 4.13 Effect of increasing HMA/PES ratio (w/w %) on CO_2/CH_4 ideal selectivity for PES/SAPO-34 (20%)/HMA and PES/HMA membranes 72

Figure 4.14 Effect of increasing HMA/PES ratio (w/w %) on H_2/CO_2 ideal selectivity for PES/SAPO-34 (20%)/HMA and PES/HMA membranes 73

Figure 4.15 Comparison of TGA graphs of pure PES and various PES/LMWA membranes annealed at 225 ^oC for 8 hours 78

Figure 4.16 Thermogravimetric analysis of PES/SAPO-34 membranes performed between room temperature and 850 ^oC 79

Figure 4.17 Cross-sectional SEM images of (a) pure PES, (b) PES/pNA, (c)PES/HMA and (d) PC/ANP membranes. 83

Figure 4.18 Cross sectional SEM image of PES/HMA membrane (HMA/PES ratio = 25 w/w %) 83

Figure 4.19 Cross sectional SEM images of PES/SAPO-34 (a), PES/SAPO-34/HMA membranes at a HMA/PES ratio of 4 w/w % (b), 7 w/w % (c),

10 w/w % (d) 89

Figure 4.20 Cross sectional SEM images of PES/SAPO-34 (a), PES/SAPO-34/HMA membranes at zeolite loadings of (a) 10 w/w %, (b) 20 w/w % ,

(c) 30 w/w % ,(d) 40 w/w % 84

Figure 4.21 Cross sectional SEM images of PES/SAPO-34 MMMs at higher magnifications X50.000 (a) PES/SAPO-34(20 w %) MMM and (b) PES/SAPO-34 (20 w %)/HMA (10 w %) MMM 86

Figure C.1 The DSC graph of pure PES membrane 105

Figure C.2 The DSC graph of PES/HMA (2%) membrane blend..... 106

Figure C.3 The DSC graph of PES/HMA (4%) membrane blend..... 106

Figure C.4 The DSC graph of PES/HMA (4%) membrane blend..... 107

Figure C.5 The DSC graph of PES/HMA (7%) membrane blend..... 107

Figure C.6 The DSC graph of PES/HMA (7%) membrane blend..... 108

Figure C.7 The DSC graph of PES/HMA (10%) membrane blend..... 108

Figure C.8 The DSC graph of PES/HMA (15%) membrane blend..... 109

Figure C.9 The DSC graph of PES/HMA (25%) membrane blend..... 109

Figure C.10 The DSC graph of PES/SAPO-34 (20 w %)..... 110

Figure C.11 The DSC graph of PES/SAPO-34 (20 w %)/ HMA (4 w %) MMM 110

Figure C.12 The DSC graph of PES/SAPO-34 (20 w %)/ HMA (7 w %) MMM 111

Figure C.13 The DSC graph of PES/SAPO-34 (20 w %)/ HMA (10 w %) MMM 111

Figure C.14 The DSC graph of PES/SAPO-34 (10 w %)/ HMA (10 w %) MMM 112

Figure C.15 The DSC graph of PES/SAPO-34 (30 w %)/ HMA (10 w %) MMM 112

Figure C.16 The DSC graph of PES/SAPO-34 (40 w %)/ HMA (10 w %) MMM 113

Figure C.17 The DSC graph of PES/Mia (4 %) membrane..... 113

Figure C.18 The DSC graph of PES/ANP (4 %) membrane 114

Figure C.19 The DSC graph of PES/pNA (4 %) membrane 114

Figure C.20 The DSC graph of PES/AMP (4 %) membrane 115

Figure E.1 TGA thermogram of above T_g annealed pure PES membrane 118

Figure E.2 TGA thermogram of pure PES membrane (Annealing at 130 ^oC for 3 days) 119

Figure E.3 TGA thermogram of pure PES membrane (Annealing at 160 ^oC for 3 days) 119

Figure E.4 TGA thermogram of pure PES membrane (Annealing at 190 ^oC for 3 days) 120

Figure E.5 TGA thermogram of PES/HMA(2 w/w %) membrane 120

Figure E.6 TGA thermogram of PES/AHMP (4 w/w %) membrane 121

Figure E.7 TGA thermogram of pure PES membrane prepared by only solvent evaporation (without annealing) 121

Figure E.8 TGA thermogram of powder (AMP) 122

Figure E.9 TGA thermogram of powder (Mia)..... 122

Figure E.10 TGA thermogram of powder (TAP)..... 123

Figure E.11 TGA thermogram of powder (AHMP)..... 123

LIST OF SYMBOLS AND ABBREVATIONS

A	: Effective membrane area (cm^2)
dn/dt	: Molar flow rate (mol/s)
dp/dt	: Pressure increase
J	: Flux ($cm^3/cm^2.s$)
K	: adjustable parameter
M	: Molecular weight of the gas
P	: Permeability (Barrer)
p_f	: Feed side pressure (cmHg)
p_p	: Permeate side pressure (cmHg)
R	: Ideal gas constant
T	: Temperature (°C)
T_g	: Glass transition temperature (°C)
T_{ga} and T_{gp}	: Glass transition temperatures of additive and polymer
V_d	: Dead volume (cm^3)
w_a and w_p	: Weight fractions of additive and polymer

Greek Letters

δ	: Solubility Parameter
α	: Selectivity
β and λ	: Empirical parameters
ρ	: Density of the gas
ν	: Volumetric flow rate (cm^3/s)
Δp	: Transmembrane pressure difference (cmHg)

Abbreviations

ANP	: 4-amino 3-nitro phenol
CA	: Cellulose acetate
CMS	: Carbon molecular sieve
DBP	: Di-butyl phythalate
DCM	: Dichloromethane
DHM	: Dense homogenous membrane
DSC	: Differential scanning calorimetry
EPDM	: Ethylene-propylene rubber
FTIR	: Fourier transform infrared
HBP	: 4-hydroxy benzophenone
HMA	: 2-hydroxy 5-methyl aniline
HPA	: Heteropolyacid
LMWA	: Low molecular-weight additive
MMM	: Mixed matrix membrane
NBR	: Nitrile-butadiene rubber
PC	: Polycarbonate
PDMS	: Poly(dimethylsiloxane)
PEI	: Polyetherimide
PEI/BMI	: Polyetherimide-bismaleimide
PES	: Polyethersulfone
PI	: Polyimide
pNA	: *p*-nitroaniline
PPO	: Poly(phenyleneoxide)
PSF	: Polysulfone
PVAc	: Poly(vinylacetate)
SEM	: Scanning electron microscopy
STP	: Standard temperature and pressure
TAP	: 2,4,6-triamino pyrimidine
TGA	: Thermal gravimetric analyzer

CHAPTER 1

INTRODUCTION

Membrane based gas separation is a technique introduced commercially in the late 1970s. Technical and economical advantages of membrane processes over other competing technologies like cryogenic separations, and pressure adsorption have been reported in many industrial applications [1-3]. Advantages of membrane separation technologies include low capital investment, simplicity and ease of installation and operation, low maintenance requirements, low weight and space requirements and high processability [1].

A membrane is a semipermeable barrier between two phases. It allows the passage of some molecules, called permeate, and reject the others, called retentate with the aid of a driving force such as pressure or concentration difference. The membrane performance depends on physical and chemical properties of the membrane material and the permeating components. The permeability or flux through a membrane and the selectivity of the membrane to a component over another are the key parameters to evaluate the performance of a membrane [2, 3].

For gas separation membranes, permeability is defined as the flux of a permeate gas through a membrane per unit transmembrane driving force multiplied by membrane thickness and is expressed as,

$$P = \frac{J.\delta}{p_f - p_p} \tag{1.1}$$

where J is flux of gas through the membrane, p_f and p_p are the partial pressures of the gas on the feed and permeate side, respectively; and δ is the thickness of the membrane. The

conventional unit for expressing permeability, *P*, is Barrers, where 1 Barrer is equal to 10^{-10} cm^3 (STP).cm / cm^2.s.cm-Hg.

Selectivity is a measurement of a membrane's ability to separate the components of a mixture. Ideal selectivity (α_{ij}) is the ratio of permeabilities of single gases and is defined by the relation,

$$\alpha_{ij} = \frac{P_i}{P_j} \tag{1.2}$$

The membranes most commonly used in gas separation processes are polymeric and nonporous. The separation is based on a solution-diffusion mechanism. This mechanism involves molecular scale interactions of the permeating molecule with the membrane polymer. The mechanism assumes that each molecule is sorbed by the membrane at one interface, transported by diffusion across the membrane through the voids between the polymeric chains (or called free volume), and desorbed at the other interface. According to the solution - diffusion model, the permeation of molecules through the membranes is controlled by two major parameters: diffusivity coefficient (D) and solubility coefficient (S) [2, 3]. Diffusivity is a measure of the mobility of individual molecules passing through the voids between the polymeric chains in a membrane material. The solubility coefficient equals the ratio of sorption uptake normalized by some measure of uptake potential, such as partial pressure [4]. Permeability (P) defined in equation (1.1), represents the ability of molecules to permeate through a membrane:

$$P = DS \tag{1.3}$$

Although recently intense research has been directed towards the development of inorganic membranes which have more favorable trades-off between selectivity and permeability such as more rigid carbons and zeolites as membrane materials, gas separation membranes are traditionally composed of synthetic polymeric materials as indicated earlier. Polymers provide a range of desirable properties that are important for gas separation processes including low cost, high permeability, good mechanical stability, and ease of processability [4]. For separations of permanent gases, these polymers tend to be glassy because of their mechanical properties and better size-dependent separation characteristics as a class compared to rubbery polymers [5]. Glassy polymers have stiffer polymer backbones and therefore let smaller molecules such as H_2 and He pass more

quickly, and larger molecules such as hydrocarbons permeate the membrane slowly [4]. To increase the membrane selectivity, either the diffusivity or the solubility needs to be enhanced; however, polymers that are more permeable are generally less selective and vice versa. Polymeric membranes suffer from a trade-off between their permeability, and selectivity [4, 5]. This trade- off was illustrated first by Robeson in 1991, where he plotted polymer selectivity versus permeability in what has become known as the "upper-bound trade-off" curves [6]. There have been few reports of *processable* polymers with properties above the 1991 upper-bound, hence owing to these improvements during the last decade, Robeson revisited the upper bound curves in 2008 [7]. Trade-off curve for H_2/CH_4 gas pair is illustrated in Figure 1.1.

The trade off line represented in Figure 1.1 depicts the permeability-selectivity relation for conventional polymers, and this linear relation has originated from empirical model parameters depending on the kinetic diameters and solubility coefficients of gases. The slope of the trade-off lines are gas pair specific, and altering this slope by chemical modifications of the polymers or polymer blending is not possible [6, 23-25].

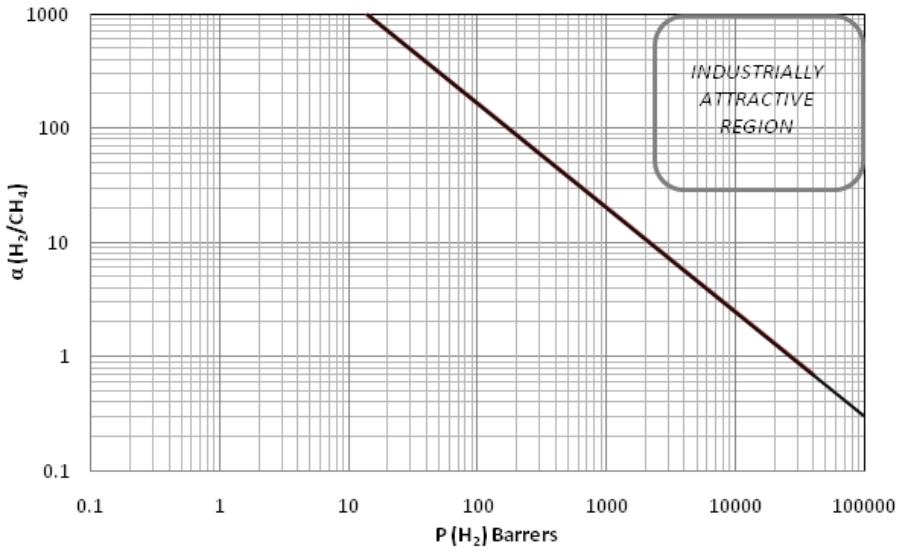

Figure 1.1: Upper-bound trade-off curve (2008) for the hydrogen – methane gas pair [7].

A substantial research effort has been directed to overcome the limit imposed by the upper bound not only from the point of membrane material of construction but also from the point of structure and morphology of membranes. The membrane structure may determine the separation mechanism and hence the application; thus, membrane

morphology is one of the most important parameters that affects the performance [2]. A dense homogeneous polymeric membrane has the simplest morphology, which is composed of a nonporous, dense, single polymer layer that is homogeneous in all directions. Therefore, it is the most suitable structure for material screening in other words to investigate different polymers and the effect of chemical modification [8]. High permeability with low selectivity is encountered for rubbery polymers. Glassy polymers provide high selectivity, but the rate of transport of the gases are usually low [9]. Since permeation rate varies inversely with membrane thickness, permeation properties can be optimized by minimizing the effective membrane thickness [2]. This approach brought the concept of asymmetric membranes consisting of two structurally distinct layers, one of which is a thin, dense selective skin or barrier layer, and the other a thick, porous matrix (substructure) whose main function is to provide a physical support for the thin skin. Two general classes of asymmetric membranes are universally recognized. They are integrally skinned and thin film composite types [9]. Composite membranes utilize two or more different polymeric materials in their construction.

For membranes to be used in practical applications, it is necessary for them to be constructed into a useful morphology [10]. In addition, improvement in both the selectivity and permeability of the membrane material is desired to overcome the limit imposed by the upper bound. Despite all the improvements, polymeric membranes cannot overcome the upper bound limit, and reach the industrially attractive region represented in Figure 1.1. On the other hand, some inorganic membranes offer much higher permeability and selectivity than polymeric membranes but they suffer from poor processability. Based on the need of a more efficient membrane than polymeric and inorganic membranes, a new type of membranes has been developed [4, 5, 8, 12, 13]. This new type of membrane material emerging with the potential for future applications is mixed matrix membranes composed of homogeneously interpenetrating polymeric and inorganic particles. Compared to original polymeric membranes, significant improvement in separation properties with trivial loss in membrane flexibility is expected for the resultant mixed matrix membranes (MMMs) [11]. Generally the literature has focused on the incorporation of inorganic particles like zeolites, carbon molecular sieves, and non-porous silica particles [11] as dispersed inorganic phase into a polymer matrix. The incorporation of the inorganic particles to the polymer matrix can have three effects on the permeabilities; they can act as molecular sieves altering the permeabilities, they can disrupt the polymeric structure increasing permeabilities and they can act as barriers reducing permeabilities [10].

However, it has been found that there is an obstacle to the successful introduction of inorganic molecular sieve materials into an organic polymer matrix since a number of studies share the view that the performance of MMMs is not a simple addition of the intrinsic properties of individual phase. Many variables may seriously affect MMM performance, making it difficult to understand. Currently, the major concerns in research on MMM are a suitable combination of polymers and particles, the physical properties of the inorganic fillers (e.g., particle size and particle agglomerations), and the polymer/particle interface morphologies [11]. One of the main proposed polymer/particle interface scenario is the detachment of polymer chains from the particle surface, causing interfacial voids. The poor polymer/inorganic filler contact could result in these voids, presumed to be the major cause for the more or less deteriorated performance as gas molecules pass through this non-selective and less resistant by-pass [11-14].

Many alternate methods concerning the poor polymer/inorganic filler contact were proposed to improve the MMM overall performance. These methods can be classified into two major groups; polymer flexibility promotion during membrane formation [12, 14, 15, 19], and compatibility improvement between zeolite and polymer [16-18, 20, 21]. Annealing the membranes above the glass transition temperature of the polymer is an example to the methods regarding the flexibility promotion. Research on compatibility improvement includes the examples of chemical or physical interaction of the polymer and the zeolite via the addition of coupling agents or low molecular weight additives, respectively.

In this study, the effect of low molecular weight additive (LMWA) type and loading on neat polyethersulfone (PES) membranes was investigated. Various LMWAs such as p-nitroaniline (pNA), 4-amino 3-nitro phenol (ANP), 2-Hydroxy 5-Methyl Aniline (HMA) are added to the membrane formulation. One of them, HMA was selected to be used in the parametric study of loading effect on PES, and PES/SAPO-34 membranes. HMA was incorporated into SAPO-34 containing polyethersulfone mixed matrix membranes as a compatibilizer agent between SAPO-34 and PES. The membranes were annealed above the glass transition temperature of PES. SAPO-34 particles were used to prepare the MMMs. The performance of the membranes was determined by single gas permeation measurements, and characterized via scanning electron microscopy (SEM), and differential scanning calorimetry (DSC).

CHAPTER 2

LITERATURE SURVEY

Gas separation occupies a central position in the chemical feed stock industry [11], basically oxygen and nitrogen enrichment, hydrogen recovery, natural gas separation, the removal of volatile compounds from effluent streams are current applications. Gas separation by membranes has acquired great significance in terms of economical considerations. Some examples of potential applications for membrane based gas separation are summarized in Table 2.1. One of the major problems confronting the use of membrane-based gas separation processes in a wide range of applications is the lack of membranes with high flux and high selectivity [22].

Therefore, in order to improve gas separation performance of membranes, extensive research has been conducted over several decades.

2.1 Polymeric Gas Separation Membranes

Polymers are attractive membrane materials mainly owing to their processability. There are two types of polymeric membranes. Those that are referred to as glassy polymeric membranes having a glass transition temperature higher than application temperature. In contrast, those that are referred to as rubbery polymeric membranes having a glass transition temperature well below application temperature.

As Robeson [6] indicated, it is possible to find polymers that exhibit high selectivity and low permeability, and vice versa, in addition to those that combine low selectivities with low permeabilities. There do not, however, appear to be any polymers that show the desired trend to large values for both permeability and selectivity. Nonetheless, glassy polymeric materials are advantageous to their rubbery counterparts, because of their

superior mechanical properties and overall permeability-selectivity tradeoffs being closer to the upper bound line. As indicated earlier, the selectivity of a large fraction of glassy polymeric membranes depends largely on their ability to discriminate gas species by size and diffusivities through the membrane structure [26]. Common glassy polymeric materials focused on as membrane materials include polysulfones, polyimides, polyaramides and polycarbonates, polyphenylene oxides, and cellulose derivatives.

Table 2.1 Potential applications of gas separation membranes, adopted list from [5] (HC=Hydrocarbon)

Category	Gas Pair	Application
Hydrogen	H_2/N_2	Ammonia purge gas
	H_2/CH_4	Refinery hydrogen recovery
	H_2/CO H_2/CO_2	Synthesis gas ratio adjustment
	H_2/O_2	Fuel Cells
Air	O_2/N_2	O_2-enriched air for combustion
Acid Gases	CO_2/CH_4	Landfill and natural gas sweetening
	H_2S/CH_4	Sour gas sweetening
	CO_2/N_2	Digester gas treatment
Drying	H_2O/HC	Hydrocarbon drying
	H_2O/Air	Air drying
Hydrocarbons	HC/Air	Pollution control; stack gas or solvent recovery
	HC/N_2	Upgrading low-BTU gas
Helium	He/HC	Helium recovery from gas wells
	He/N_2	Helium recovery from diving air

Substantial effort has been put on for the polymeric membranes achieve both high permeability and selectivity values. One of the proposed strategies to alter the trade off relation was chemical modifications of classical polymers. Sridhar et al. [28] prepared poly (phenylene oxide) (PPO) membranes and sulfonated PPO membranes using chlorosulfonic acid. However, both before and after the chemical modification, PPO membranes lay very below the upper bound line. The performance of CO_2 selectivity (27.2) for sulfonated PPO membranes was 2.2 times higher than PPO membranes, while CO_2 permeability (43.7) decreased by a factor of 2.4.

One another strategy is polymer blending. Kapantaidakis et al. [27] aimed to improve the gas separation properties of polyethersulfone (PES) and polyimide (PI) by preparing PES/PI (20/80), (50/50), (80/20) w/w blends. However the results indicated that no significant improvement was observed in selectivites for blends having different compositions. Ideal selectivity of CO_2/N_2 gas pair reported as 40 for PES/PI (20/80) blend and as 39 for PES/PI (80/20), being both close to the selectivity values of single polymers.

Aforementioned studies imply that simple modifications in the polymer structure often lead only to a trade-off: One of the parameters is improved, while the other is simultaneously affected negatively [6]. Therefore, such measures only shift the compromise between permeability coefficient and selectivity, but do not constitute a real improvement. The Robeson's trade-off is shown as a linear relation of permeability and selectivity by Robeson (Figure 1.1);

$$\log \alpha_{ij} = \log \beta_{i/j} - \lambda_{ij} \log P_i \tag{2.1}$$

P_i is the fast gas permeability, α_{ij} is selectivity of species i to j, λ_{ij} is an empirical model parameter depending on the kinetic diameters of the permeating species. The position of the upper bound line, $\beta_{i/j}$, depends on gas molecule size as well as solubility;

$$\beta_{i/j} = \frac{S_i^{1+\lambda_{ij}}}{S_j} \exp\left\{-\lambda_{ij}\left[b - f\left(\frac{1-a}{RT}\right)\right]\right\} \tag{2.2}$$

where $S_{i,j}$ are solubility coefficients of the gases. The values of parameters a, and b are constant for glassy polymers (a=0.64, b=11.5). According to Freeman [23], only adjustable parameter is f that characterizes the product of energy to open a gap to allow a penetrant to diffuse and the equilibrium interchain spacing. The permeability/selectivity trade off relations is to be evaluated with free volume viewpoint [24]. Based on this concept, changing the structure of the polymer by introducing packing-disrupting units into the polymer backbone, thereby manipulating the free volume is required for significant enhancement of the performance of the polymers [24, 25].

2.2 Polymer / Additive Gas Separation Membranes

Another alternative to alter the gas separation performance of membranes is the incorporation of organic additives into glassy polymers. Many researchers observed anti-plasticization effect of certain additives [20, 29-33, 35]; whereas some observed the plasticization effect [15, 16]. Table 2.2 summarizes results of several studies using different polymer/additive pairs together with the function of the additives in the polymer matrix.

The incorporation of additives is expected to increase the membrane performance [29-34] by modifying the membrane structure, and by especially changing the free volume of the polymer [29]. There are numerous different types of additives employed for those purposes. Long aliphatic and polyaromatic based compounds, 4,4'-dichlorodiphenylsulfone (DDS) was used with 10 w% in polysulfone matrix by Robeson [29]. Single gas permeability measurements revealed that DDS acted as anti-plasticizer since the CO_2 permeability decreased from 5.76 to 2.16 with the addition of 10 w % DDS. He suggested that DDS filled the free volume of polymer and reduced the permeability.

Maeda and Paul [30-31] further examined the effects of additives on the membrane structure not only by gas permeation performance but also by thermal analysis. 4,4'-dichlorodiphenyl sulfone, N-phenyl-2-naphtylamine, tricreysl phosphate and different type of sebacates were added into polysulfone (PSF) and poly(phenylene oxide) (PPO) in the concentration range of 10-30 w%. Similar to Robeson [29], they observed a decrease in gas permeabilities with significant increase in selectivities. They also measured the glass transition temperatures of membranes including the mentioned additives. They observed a significant decrease in the glass transition temperature of PSF from 185 ^{o}C to 50 ^{o}C with 30 wt % addition.

Ruiz-Trevino and Paul [32] selected derivatives of naphthalene-, bisphenol-, and fluorene- as additives, based on their interaction capabilities with bisphenol A polysulfone (PSF). Gas permeation experiments again revealed anti-plasticization effect enabling them to speculate that the compounds which have hydroxyl groups and polar atoms in their structure showed interactions with PSF. This led to a reduction in free volume by bringing the polymer chains closer. They also observed a decrease in the glass transition temperatures as did Maeda and Paul [30-31] and proposed that there is a relation between reduction in Tg and antiplasticization effect. They used an antiplasticization model relating

the glass transition of blend to the weight fractions and glass transition temperatures of the pure components, the Gordon-Taylor model;

$$T_g = \frac{w_A T_{gA} + K w_P T_{pP}}{w_A + K w_P} \tag{2.3}$$

where K is an adjustable parameter that depending on the polymer and additive, w is the weight fractions of the components, the subscripts "A" and "P" stands for the additive and the polymer respectively. Ruiz-Trevino and Paul [32] found that the model and experimental results for T_g of the membranes are compatible.

A similar study was performed by Larrocco and Pessan [33] employing polyetherimide (PEI) as the polymer and halogen containing polyaromatic derivatives as the additives. They also observed the anti-plasticization effect of these additives, which decreased both the glass transition temperature and gas permeabilities of polyetherimide. They used a solubility parameter based approach in the selection of the additives, and claimed that as the difference between solubility parameters of PEI and additive decrease, the level of interaction between polymer and additive or in other words the level of antiplasticization of polymer increased.

Vidotti and Pessan [34] further employed the solubility parameter based approach in polyethersulfone (PES), Hexafluoro-bisphenol A (HFBPA), N-phenyl-2-naphthylamine (PNA) system. They determined the solubility parameters of the polymer and the additives by Hoy's method [35] and used to estimate the level of interaction between additives and PES. On the basis of this criterion, small differences in the values of solubility parameter (δ) (<5 J/cm^3) indicate high interaction between polymer and additive. The experimental results including thermal characterization for T_g together with the solubility parameter based approach revealed better interaction of PNA with PES rather than HFBPA. The Δδ values for PES–PNA mixtures and for PES-HFBPA mixtures were 4.20 (<5 J/cm^3) and 14.77 (>5 J/cm^3) respectively.

As the aforementioned studies indicate, physical incorporation of several types of additives to different polymers was investigated, and the effect of these additives was analyzed according to gas permeation and thermal analyses. In addition to these analyses, effect of these additives was also analyzed mainly by Fourier transform infrared spectroscopy (FTIR), mechanical strength testing, and free volume determination. Sridhar

et al. [28] physically modified the poly(phenylene oxide) membranes by the incorporation of phosphotungstic acid (HPA, heteropolyacid). They suggested physical interactions like hydrogen bonding between HPA and PPO based on the FTIR results. They observed a slight decrease in tensile strength, and a dramatic decrease in CO_2 permeability with the addition of HPA to PPO.

Based on FTIR analysis, Yong et al. [20] reported that amine groups of 2, 4, 6-triaminopyrimidine (TAP) interacted with polyimide by means of hydrogen bonding. The incorporation of 21 w% TAP to polyimide membrane resulted in a decrease of N_2 permeability to 0.0022 from 0.218, whereas an increase in O_2/N_2 selectivity to 15.40 from 6.88.

Şen et al. [36] also incorporated different types of low molecular weight compounds (LMWCs) having multifunctional groups as additives to polycarbonate (PC). These LMWCs are cathecol, *p*-nitroaniline (pNA), 4-amino 3-nitro phenol (ANP) and 2-hydroxy 5-methyl aniline (HMA) and their concentrations in the membrane were changed between 1 and 10 % (w/w), which was significantly low as opposed to the additive concentration applied in the previous studies [20, 29-34]. Polycarbonate membranes including LMWCs revealed higher ideal selectivities but reduced permeabilities. It was concluded that the selected LMWCs anti-plasticized the PC even at low concentrations. LMWC containing membranes had lower glass transition temperatures compared to dense PC membranes. In addition, the interaction between PC chains and LMWAs was apparent in FTIR spectra of membranes. Among the LMWAs, pNA was the most effective anti-plasticizing additive, which provided the highest selectivity and lowest T_g reduction.

Mahajan et al. [16] utilized a polymer-additive pair in which the plasticization effect of the additive was observed rather than the anti-plasticization effect. Incorporation of the additives RDP Fyroflex, Di-Butyl Phthalate (DBP), and 4-Hydroxy Benzophenone (HBP) to Matrimid led to significant decrease in the T_g of the polymeric film from 305 °C to 161°C, 150°C, and 144°C respectively. From the gas separation viewpoint, plasticization behavior was observed; with the addition of DBP, N_2 permeability increased to 0.227 from 0.183 whereas N_2/O_2 selectivity decreased to 6.60 from 7.20. They proposed the addition of plasticizers as a method to improve the zeolite polymer interface since they promote the flexibility of the polymer by decreasing the glass transition temperatures.

Table 2.2 Comparison of additives incorporated to dense polymeric membranes

Study	Additive	Function	Loading (w %)	Polymer	Permeability (Barrer)				Ideal Selectivity (α)		
					O_2	N_2	CO_2	CH_4	O_2/N_2	CO_2/CH_4	CO_2/N_2
Ruiz Trevino et al [32]	N-PNA Fluorene TMBPA	anti-plasticizer	-	PSF	1.39	0.248	-	-	5.60	-	-
				PSF/N-PNA	0.13	0.016	-	-	8.13	-	-
				PSF/Fluorene	0.33	0.048	-	-	6.88	-	-
			20	PSF/TMBPA	0.18	0.024	-	-	7.50	-	-
Larocca et al. [33]	N-PNA TBBPA BHT	anti-plasticizer	-	PEI	0.60	-	-	-	-	-	-
			23	PEI/N-PNA	0.15	-	-	-	-	-	-
			32	PEI/TBBPA	0.16	-	-	-	-	-	-
			23	PEI/BHT	0.32	-	-	-	-	-	-
Sridhar et al. [28]	HPA	anti-plasticizer	-	PPO	-	-	43.7	3.6	-	12.1	-
			1.22	PPO/HPA	-	-	28.2	1.36	-	20.6	-
Yong et al. [20]	TAP	anti-plasticizer compatibilizer	-	PI	1.50	0.218	8.34	6.86	6.88	1.22	38.30
			21	PI/TAP	0.035	0.00224	0.194	0.00231	15.40	84	86.60
Şen et al. [36]	pNA ANP HMA Catechol	anti-plasticizer compatibilizer	-	PC	1.45	0.265	5.45	-	5.60	-	20.60
			1	PC/ANP	1.45	0.160	5.77	-	9.10	-	36.10
			1	PC/HMA	1.41	0.160	6.10	-	8.80	-	38.10
			1	PC/Catechol	1.63	0.180	6.62	-	9.10	-	36.80
			1	PC/pNA	1.21	0.130	4.78	-	9.30	-	36.80
			2	PC/pNA	1.00	0.100	3.60	-	10.00	-	36.00
			5	PC/pNA	0.90	0.070	3.50	-	12.90	-	50.00
			10	PC/pNA	0.40	0.040	1.40	-	10.00	-	35.00
Mahajan et al. [16]	DBP	plasticizer flexibility promotion	-	Matrimid	1.32	0.183	-	-	7.20	-	-
			33	Matrimid/DBP	1.50	0.227	-	-	6.60	-	-

2.3 Mixed Matrix Membranes

Robeson plot reveals that materials with permeability/selectivity combinations above and to the right of the upper bound line (Figure 1.1) are in the industrially attractive region however they are exceptionally rare. As mentioned in the previous sections, extensive research has been carried out to develop membranes having combinations of permeability and selectivity above the trade-off. However, when polymers modified based on the structure–property relation, the resultant polymers have permeability and selectivity tracking along this line instead of exceeding it. Mixed matrix membranes containing a bulk continuous phase and a dispersed phase have the potential to achieve higher selectivity with equal or higher permeability compared to existing polymer membranes. The bulk continuous phase is conventionally polymer. Numerous types of solid fillers used as dispersed phase such as; carbon molecular sieves, mesoporous molecular sieves, metal organic frameworks, activated carbons, layered materials, silica, but mostly microporous molecular sieves (zeolites) [4].

Vu et al. [46] attempted to show that encouraging selectivity and permeability enhancements can be achieved using carbon molecular sieves (CMS) in MMMs. The CMSs formed by pyrolysis of a polyimide (Matrimid) and ball-milled to fine particles were incorporated into Matrimid 5218 and Ultem® 1000. For Ultem® CMS mixed matrix membrane films, pure gas permeation tests showed enhancements by as much as 40% in CO_2/CH_4 selectivity and 8% in O_2/N_2 selectivity over the intrinsic selectivity values of the pure Ultem® polymer matrix. Likewise, for Matrimid–CMS mixed matrix films, enhancements by as much as 45% in CO_2/CH_4 selectivity and 20 % in O_2/N_2 were observed.
Balkus and his co-workers [48] synthesized metal–organic framework 5 (MOF-5) nanocrystals and added to Matrimid® at different loadings (10, 20, and 30 w%) to form mixed-matrix membranes for gas separations. The membranes were tested using H_2, CO_2, O_2, N_2, and CH_4 gases. No increase in ideal selectivity for any gas pairs was reported, however, increase in permeability was obtained due to the porosity of the MOF-5 nanocrystals. For membranes including 30 w% MOF-5, an increase up to a 120% for the permeability of H_2 was reported, to 53.8 from 24.4 Barrer.

In addition to the utilization of porous fillers in MMMs, studies regarding the incorporation of non-porous fillers such as nano-sized silica particles to polymers is another leading way in MMM research. The function of these non-porous fillers is to manipulate

the molecular packing of polymer chains [11]. Polyimides, in particular, 6FDA-6FpDA-DABA, 6FDA-6FpDA, poly (4-methyl-2-pentyne) (PMP), and polydimethyl siloxane (PDMS) are widely used base polymers in these studies, since these polymers are considerably more permeable compared to classical polymers.

2.3.1 Mixed Matrix Membranes Prepared with Rubbery Polymers

Transport of permanent gases based on the mixed matrix membrane approach was first investigated in 1973 by Paul and Kemp [37]. They have investigated the incorporation of zeolite 5A into silicone rubber. According to Paul and Kemp, the incorporation of zeolite 5A into silicone rubber did not improve the separation properties of the polymer.

Jia et al. [38] studied the permeation properties of He, H_2, O_2, CO_2, N_2, CH_4 and C_4H_{10} through silicalite-1 filled poly-dimethylsiloxane (PDMS) membranes. They proposed that silicalite-1 functioned as molecular sieve since the permeabilities of He, H_2, O_2 and CO_2 increased, while those of N_2, CH_4 and C_4H_{10} decreased.

Duval et al. [39] systematically studied several polymer/zeolite combinations, using poly- dimethylsiloxane (PDMS), ethylene-propylene rubber (EPDM), polychloroprene (PCP) and nitrile butadiene rubber (NBR) as continuous phase, and silicalite-1, zeolites 13X, KY, 3A, 4A, 5A as the dispersed phase. Improvement was only reported for the combination of NBR and 46 v% zeolite KY for CO_2/CH_4 gas pair as the selectivity increase from 13.5 to 35, and for EPDM rubber with 53 v % silicalite-1 for O_2/N_2 gas pair as the selectivity increase from 3.0 to 4.7. However, no improvement was reported for the membranes filled with zeolite 3A, 4A, and 5A.

Tantekin et al. [40] examined the separation performance of PDMS/silicalite-1 MMMs and the effect of different particle sizes (0.1, 0.4, 0.7, 0.8, 8.0 μm) of silicalite-1 in PDMS. Addition of silicalite-1 enhanced the permeability of the membranes compared to neat PDMS polymer membrane; however only slight improvement in the CO_2/N_2, O_2/N_2 and CO_2/O_2 ideal selectivities were reported.

Way et al. [49] utilized the zeolite SAPO-34 as dispersed inorganic filler in mixed matrix membranes for the first time. The methoxy ethoxy ethanol (MEE) substituted

polyphosphazene (PPZ) rubbery polymer used in the formulation of mixed-matrix membranes as the base polymer. 25 w % SAPO-34 incorporated PPZ membranes were tested using CO_2, H_2, CH_4, and N_2 gases. Although scanning electron microscopy (SEM) images signals the good interface contact between the molecular sieve particles and the polymer due to substituted PPZ's rubbery nature, no significant improvements was recorded in terms of gas permeation characteristics. Gas permeation experiments at 22 ^oC, reveal a decrease in CO_2 permeability to 48 from 71 Barrer with the addition of SAPO-34. The ideal selectivities slightly decreased to 7.3 from 8.5 for CO_2/H_2 gas pair, whereas a small increase in ideal selectivities to 53 from 42 for CO_2/N_2 gas pair, and to 17.5 from 15.3 for CO_2/CH_4 gas pair.

Rubbery polymers locate very below the upper bound curve due to their less selective nature compared to their glassy counterparts. As the above results indicate, selectivity promotion was only observed in rubbery polymer-zeolite mixed matrix membranes for high zeolite loadings. Even though, the addition of zeolites at high loadings of 40-50 w % could not improve the gas permeation properties of these polymers to the industrially attractive region remarked in Robeson plot. Therefore, rubbery polymers are less attractive compared to the glassy polymers. Due to the facts that glassy polymers possess properties closer to the upper bound and they are mechanically more stable enabling them to be spun into hollow fiber morphologies to achieve favorable economics make these rigid glassy polymers attractive compared to rubbery polymers, researchers have focused on a way to prepare mixed matrix membranes with glassy polymers.

2.3.2 Mixed Matrix Membranes Prepared with Glassy Polymers

The usage of glassy polymers as the matrix polymer in zeolite filled MMMs can be advantageous due to their restricted segmental motions and hence their higher intrinsic diffusion selectivities compared to rubbery polymers [37, 46]. Various kinds of glassy polymers such as cellulose acetate, polyethersulfone, polycarbonate, polyimide, polyetherimide have been investigated over the last decade. A list of selected studies on mixed matrix membranes prepared by several glassy polymers can be seen in Table 2.3. The effects of zeolite type and loading on membrane performance are the parameters typically investigated.

Table 2.3 Selected studies on MMMs prepared by several glassy polymers, where PES: Polyethersulfone, PI: Polyimide, PC: Polycarbonate, PEI: Polyetherimide

Polymer	Zeolite			Permeability (Barrer)			Selectivity (α)	
	Type	*Loading (w/w%)*	*Avg. Particle Size*	N_2	O_2	CO_2	O_2/N_2	CO_2/CH_4
PES [41]	13X	0	Micron	0.140	0.52	2.60	3.71	-
		16.6		0.088	0.33	1.80	3.75	-
		33.3		0.097	0.37	2.70	3.81	-
		50.0		0.120	0.50	5.20	4.17	-
	4A	16.6		0.120	0.47	2.30	3.92	-
		33.3		0.097	0.41	2.00	4.23	-
		50.0		0.250	1.10	10.70	4.40	-
PES [1]	AgA	0	Micron (1-2 μm)	-	-	2.70	-	32.00
		20		-	-	1.60	-	39.00
		30		-	-	1.40	-	48.00
		50		-	-	1.00	-	60.00
PES [42]	4A	0		0.129	0.773	3.38	5.99	30.18
		20	Nano (50-100 nm)	0.091	0.583	2.32	6.43	31.22
		20	Micro (1-5 μm)	0.058	0.363	1.56	6.26	31.14
PES [43]	β	0	Nano (100-300 μm)	0.129	0.77	3.38	5.99	30.20
		10		0.133	0.81	4.22	6.06	37.00
		20		0.141	0.83	4.13	5.85	34.10
		30		0.236	1.39	6.82	5.89	36.70
PI [43]	β	0	Nano (100-300 μm)	0.254	1.68	6.50	6.61	33.50
		10		0.322	2.25	9.42	6.99	33.90
		20		0.573	3.65	13.40	6.37	31.80
		30		0.972	4.16	16.40	4.28	18.60
PI (Ultem) [16]	4A	0	Micron (1-3 μm)	0.049	0.38	-	7.80	-
		15		0.039	0.38	-	9.70	-
		35		0.022	0.28	-	12.90	-
PI [20]	4A	0	Micron (0.6-4 μm)	0.218	1.50	8.34	6.88	1.22
		43		0.455	1.91	9.36	4.20	2.23
	13X	43		1.350	6.58	33.40	4.87	6.86
PC [44]	4A	0	Micron (3 μm)	0.267	1.81	8.80	6.80	23.60
		5		0.249	1.77	8.40	7.10	31.60
		10		0.211	1.79	8.20	8.50	32.80
		20		0.202	1.77	7.80	8.80	32.50
		30		0.179	1.55	7.00	8.70	37.60
PEI [12]	Silicalite	0	Micron	-	-	1.50		61.00
		50		-	-	14.60	-	34.00
PI Matrimid [45]	4A	0	Micron	0.18	1.32	-	7.20	-
		20 (v %)		0.56	4.00	-	7.20	-

The majority of the work on zeolite filled polymeric membranes utilizes synthetic zeolites, such as zeolite A, X, Y and silicalite, especially zeolite 4A. Zeolite loading is usually changed in the range of 15 and 50 w % of the polymer. When the zeolite content of the membranes was increased, either increased permeabilities with decreased selectivities [12, 20, 43] or decreased permeabilities with increased selectivities [1, 16, 41, 42, 44] were observed as shown in Table 2.3.

For glassy polymer matrix filled with zeolite, one of the earliest research is done by Süer et al. [41], who studied the permeation rates of N_2, O_2, Ar, CO_2 and H_2 of polyethersulfone (PES) membranes filled with zeolites 13X and 4A. They concluded that both increased permeability and selectivity was obtained at a zeolite loading of 50 w %. With increasing zeolite loading, permeabilities decreased in both PES-13X and PES-4A membranes. However, after a certain loading permeabilities started to increase. For PES-13X membranes, permeability showed a recovery for zeolite loadings above 8 w %. However, the permeability recovery of PES-4A membranes was observed to for zeolite loadings above 25 w %. This result was interpreted by the fact that zeolite 13X crystals seemed to be more discrete, whereas zeolite 4A crystals were partly aggregated forming wider cavities which was probably the result of partial incompatibility between polymer and zeolite. For mixed matrix membranes, formation of microvoids was observed.

Tsapatsis and his co-workers [47] selected polybenzimidazole (PBI) as continuous phase due to its promise as a membrane material being located on the trade-off curve for H_2/CO_2 gas pair. PBI based composite membranes were prepared with the incorporation of AMH-3 (layered silicates with nanoporous layers). Particles of proton-exchanged AMH-3 (hereafter named as PAMH) and swollen AMH-3 (hereafter, SAMH) were incorporated in different weight percentages. The single gas permeation results at 100 ^{o}C indicated that addition of these fillers reduced the permeabilities. Only slight increase in selectivity for H_2/CO_2 observed with the addition of 3 w % SAMH and 14 w % PAMH. The probable reason of reduction in permeabilities was attributed to the large aspect ratio of the silicates increasing the tortuosity of the gas transport path.

Considering the mentioned results together with the ones in Table 2.3, some improvements in membrane performance relative to the neat polymeric membranes are evident; however the reported performance properties of those MMMs still do not exhibit the expected performance which are predicted using model membrane structures and

Maxwell type equations [12, 13, 53]. This is mainly due to the fact that the incorporation of zeolites into glassy polymer membranes has proven much more difficult than for the rubbery counterparts [5].This case is generally attributed to poor interface between polymer and zeolite, and achieving better gas separation properties of resultant MMM by means of improving the interfacial region remains as a challenge. According to Chung et al. [11], currently, the major concerns in research on MMM are a suitable combination of polymers and particles, the physical properties of the inorganic fillers including, particle size and particle agglomeration, and the polymer/zeolite interface morphologies.

2.4 Possible Interface Morphologies and Attempts to Improve Mixed Matrix Membranes' Performance

The strategy for the development of mixed matrix membranes is to combine the advanced features of polymers and inorganic materials. However, as discussed in the previous sections, the performances of some of the existing MMMs are below the expected attractive region in Robeson plot, and variables tailoring the MMMs' performance including the selection of appropriate polymer/filler combinations and the polymer/filler interface morphologies are under investigation [4-5].

It is known that the permeability of a gas through a zeolite filled polymeric membrane depends on the properties of the zeolite and the polymer and on the interaction between them [50]. Hence selecting appropriate polymer–filler combinations is complicated since performance of MMMs is not a simple addition of the intrinsic properties of these phases. The properties of each phase are potentially affected by the presence of the other and possibly by components of the feed gases [44].

Tailoring interfacial morphology is a difficult problem frequently encountered in composite materials, but it is especially challenging for gas separation membranes since small changes in interfacial morphology can lead to dramatic changes in transport properties [4, 5, 11]. Research has shown that the interfacial region is of particular importance in successful mixed matrix membrane formation [4]. Extensive research has been carried out to improve the overall morphology and hence the performance of mixed matrix membranes.

Several scenarios at the interface region between the zeolite and polymer are discussed during the last decades, such as sieve-in-a cage, matrix rigidification, and pore blockage [4]. Gas permeation experiments and the effect of the mentioned possible interface morphologies are discussed on Robeson plot in Figure 2.1.

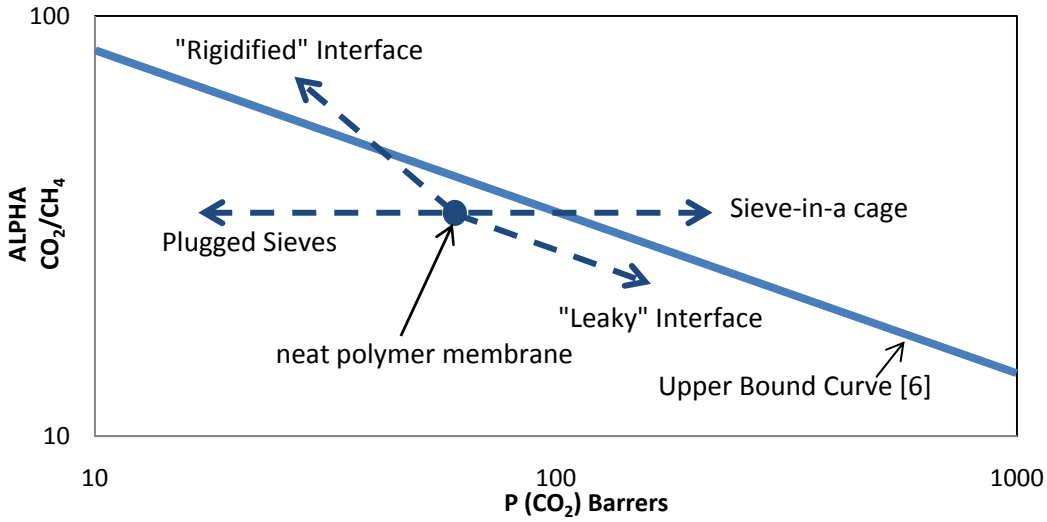

Figure 2.1 Possible interfacial morphologies for mixed matrix membranes and their effect on CO_2/CH_4 gas transport properties, adopted from reference [4]

Even from the first attempt to combine zeolites with polymers formation of non-selective voids were reported at the interface [51]. Poor contact of the polymer with zeolite resulting from material incompatibility has been noted as the reason of these voids, presumably the major cause for the more or less deteriorated performance as gas molecules take this non-selective and less resistant by-pass instead of passing through pores in the particle [11-14]. The formation of these voids is usually named as *sieve-in-a cage* morphology, resulting in increased permeabilities with reduced selectivity as represented in Figure 2.1 [45].

In addition to formation of non-selective voids, other possible interface morphologies are matrix rigidification and pore blockage [16, 52-53]. If sieve-polymer interfacial adhesion is good, but a reduction in free volume is believed to occur near the sieve surface [52, 53], the result is termed as *matrix rigidification*. It is believed that the layer of rigidified polymer surrounding the sieves displays a lower permeability than the bulk polymer matrix, possibly resulting in an overall reduced permeability. The enhancement in selectivity caused by the sieving phase should not be affected significantly

by matrix rigidification, unless the rigidified polymer permeability is so low that it starves the zeolites.

The effect of a rigidified polymer region around zeolite particles on the performance properties of MMMs has been demonstrated in different systems, such as zeolite 4A dispersed in polyethersulfone. Li et al. [52] observed such a trend in PES-zeolite 4A MMM system. They reported an increment in T_g of PES with increasing zeolite 4A loading. The T_g of PES increased from 215 to 217°C and 219°C with the addition of 30 % and 50 % (w/w) zeolite 4A, respectively. They also reported a decrease in the H_2, O_2 and N_2 permeabilities of PES membrane with the addition of zeolite 4A particles. Li and his colleagues attributed these results to matrix rigidification. PES-zeolite 4A MMM system was also studied by Suer et al. [41]. However, they reported the formation of voids, and the glass transition temperature of the membranes remained the same after the incorporation of zeolite 4A. These type of different observations for same polymer-zeolite systems demonstrate the importance of membrane preparation parameters.

In MMM studies using porous fillers, blockage of the fillers' pores by the polymer chains is also reported [19, 45, 52, 53]. Depending on the pore size of the filler, the polymer chain can fill the pore in various degrees; this is usually termed as *partial pore blockage* [11]. Pore blockage is often reported to be accompanied by chain rigidification although there is no experimental design to completely differentiate the influence of these two factors. Since no characterization technique to definitively assess pore blockage is available, it remains as an assumption [11]. This interpretation may be valid for the other proposed interface morphologies; sieve in a cage and matrix rigidification. In most studies, scanning electron microscopy (SEM) is used to characterize prepared membranes and compare the interface morphologies of the membranes prepared by different approaches. Figure 2.2 shows a SEM image of a zeolite 4A filled polysulfone MMM, which is interpreted to have a sieve in-a-cage morphology [19].

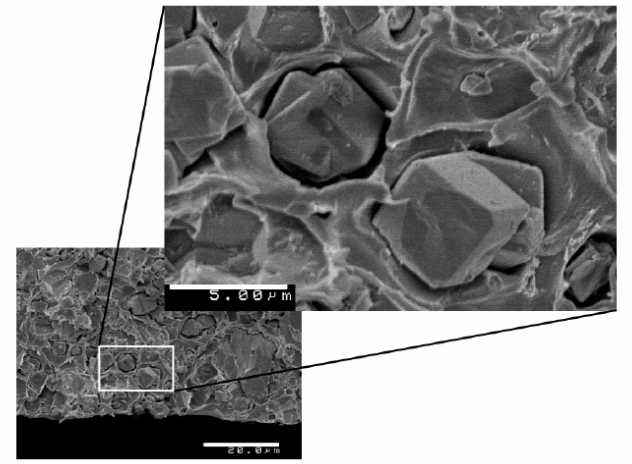

Figure 2.2 Cross sectional SEM image of a polysulfone-zeolite 4A MMM, “sieve in-a-cage” morphology [19]

Whichever scenario is proposed for the interfacial region, improper materials selection or failure to eliminate defects may likely result in unfavorable performance [50], and it is essential to improve the overall morphology of the MMM and hence the gas separation properties. There are several strategies proposed for this purpose;

- Utilization of a polymer with a flexible backbone [15],
- Fabrication of the MMM above T_g of the neat polymer [12-14],
- Modification of the external zeolite surface by silylation [16]
- Usage of modification agents to create special zeolite surface having whiskers or asperities [17],
- Utilization of coupling agents that can react with both the zeolite and the polymer [18],
- Incorporation of plasticizers to decrease the glass transition temperature of the matrix [19],
- Incorporation of low molecular weight additives that can interact with both of the phases [20, 21].

Several researchers suggested fabricating or processing an MMM containing glassy polymer at temperatures above T_g [12, 13, 19], since stress induced during the solvent evaporation from a matrix polymer of a higher T_g is severe, and can pull the polymer chains away from the particle [11]. Li et al. [52] prepared zeolite 3A, 4A, and 5A filled polyethersulfone (PES) membranes 30 ^{o}C above the glass transition temperature of

PES, at 250 ^{o}C to eliminate the void between two phases but with an exception; after annealing, the membranes were cooled down to room temperature naturally instead of quenching. Their results indicated that the gas separation performance of mixed matrix membranes with natural cooling is superior to that of mixed matrix membranes with immediate quenching probably because natural cooling can make polymer chains better adhere on the zeolite surface proved by SEM micrographs. They concluded that natural cooling avoided the detachment of polymer chains from the zeolite surface as polymer chains are suddenly cooled, resulting in the formation of voids between polymer and zeolite phases because of their different thermal coefficients of expansion.

Mahajan et al. [16] proposed to maintain the polymer flexibility during the membrane formation by decreasing T_g of the neat polymer PI (matrimid) having a high T_g of 305 ^{o}C by means of the incorporation of a plasticizer into the polymer matrix. PI membranes filled with zeolite 4A and plasticizer di-Butyl Phthalate (DBP) resulted in a decrease of O_2 permeability to 1.10 from 1.32 with a decrease in O_2/N_2 selectivity to 7.10 from 7.20 when compared to neat PI membranes. The addition of plasticizer lowered the gas separation performance of polymeric materials. Therefore choosing glassy polymers with an intermediate T_g should be a more appropriate alternative for this solution.

Another strategy was proposed by Zhang et al. [54] recently. Mixed-matrix membranes were prepared from PI (Matrimid) and mesoporous ZSM-5 nanoparticles containing crystalline ZSM-5. The ideal selectivity for O_2/N_2 separation increased from 6.64 for pure PI to 10.35 at 20 w% loading, while the selectivity of CO_2/CH_4 increased from 34.71 for pure PI to 66.07 at 20 w% loading. The results suggest that the mesopores of the ZSM-5 material provide good contact between the nanoparticles and the polymer, since the polymer chains can penetrate into the mesopores.

The single gas permeation results for the other strategies including zeolite surface modification, and utilization of reactive polymers are summarized in Table 2.4. The results for these methods illustrated in Table 2.4 show that the gas permeation performance of the membranes could not be improved after the chemical modifications and no clear explanation was reported in these studies. It was only assumed that voids still remained after silylation.

Table 2.4 Several Methods Proposed to Enhance the Polymer/Zeolite Interface

#	Strategy	Membrane	Permeability (Barrer)		Selectivity	
			O_2	CO_2	O_2/N_2	CO_2/CH_4
1	Flexibility Promotion via Annealing Above T_g [42]	PES	0.77	-	5.99	-
		PES/zeolite 4A (20 w%)	0.34	-	5.91	-
2	Flexibility Promotion via Incoporation of Placticizer [16]	PI	1.32	-	7.20	-
		PI/DBP (25 w%)	1.50	-	6.60	-
		PI/DBP (25 w%)/4A (15 w%)	1.10	-	7.10	-
3	Zeolite Surface Modification Via Silane-Coupling Agent [45]	PI	1.32	-	6.40	-
		PI/unmodified 4A (20 v%)	4.00	-	7.20	-
		PI/modified 4A (20 v%)	1.40	-	6.40	-
4	Synthesis of Zeolites Including Mesopores and Micropores [54]	PI	1.40	7.29	6.64	34.71
		PI/ZSM-5 (20 w%)	1.80	8.65	10.35	66.07
		PI/ZSM-5 (30 w%)	2.82	14.61	8.49	56.48
5	Synthesis of Reactive Polymers with Specific Groups [45]	reactive fluorinated PI	22.00	-	4.20	-
		PI/ zeolite 4A (15 w%)	14.00	-	4.50	-
6	Incorporation of LMWA [20]	PI	1.50	8.34	6.80	1.22
		PI/TAP (21 w%)/4A (43 w%)	0.0346	0.194	15.40	84.00
		PI/zeolite 4A (43 w%)	1.91	9.36	4.20	2.23
		PI/TAP (21 w%)/4A (43 w%)	0.033	0.19	18.20	617.00
6	Incorporation of LMWA [21]	PC	1.81	8.80	6.80	23.60
		PC/pNA (5 w%)	0.85	3.90	10.80	53.40
		PC/zeolite 4A (20 w%)	1.77	7.80	8.80	32.50
		PC/pNA (5 w%)/4A (20 w%)	0.92	4.11	7.40	37.20
7	Combination of Strategy no 1 & 3 [45]	PI	0.50	-	7.10	-
		PI/unmodified 4A (20 v%)	0.47	-	9.40	-
		PI/modified 4A (20 v%)	0.37	-	12.40	-

Mahajan et al. [45] concluded that the formation of bonds between sieve and polymer can lead to good adhesion and mechanical strength at the interface, nevertheless, the membranes produced by the mentioned procedure will not be effective for gas separation if the interface is slightly larger than the size of the gas molecules. In fact, filling the space between zeolite particles and polymer chains would be more convenient and effective than surface treatment of zeolites from the viewpoint of both permeation properties of the membranes and ease of membrane preparation [39].

Alternatively, Yong et al. [27] suggested adding a low molecular-weight organic compound, which is likely to link the polymer chain to the zeolite crystals, to the membrane formulation as a third component. These compounds may interact both with polymer and zeolite, thus, they may act as "compatibilizer" between polymer and zeolite. They suggested 2,4,6-triaminopyrimidine (TAP) as a compatibilizer. As shown in Table 2.4, O_2/N_2 selectivity was increased nearly three-fold and CO_2/CH_4 selectivity was increased substantially to 617 from 1.22 compared to neat PI membranes. Permeability of O_2 and CO_2 decreased at least forty-fold. They concluded that TAP enhanced the contact between the zeolite particles and polymer chains presumably by forming hydrogen bonding between them and increased the separation performance of MMMs. However, the TAP concentration in the membrane matrix was so high that TAP was indeed one of the main components in the membrane rather than an additive and decreased the permeabilities considerably.

Şen et al. [21] introduced another low molecular weight additive, para-nitroaniline (pNA). The pNA and zeolite 4A concentrations in the casting solutions were changed between 1-5% (w/w) and 5-30% (w/w), respectively. Pure PC and PC/pNA dense homogeneous membranes, and PC/zeolite 4A and PC/pNA/zeolite 4A mixed matrix membranes (MMM) were prepared. A significant improvement was achieved in selectivities with the addition of only 1 % and 2 % (w/w) pNA to the PC/zeolite 4A MMMs with a zeolite loading of 20 % (w/w). The H_2/CH_4 and CO_2/CH_4 selectivities of PC/pNA (1%)/zeolite 4A (20%) membrane were 121.3 and 51.8, respectively, which were three times higher than those of pure PC membrane. The contribution of pNA to interaction of PC and zeolite 4A was also observed by DSC analysis. DSC analysis of the membranes showed that incorporation of zeolite 4A particles into PC/pNA increased the glass transition temperatures, T_g, but incorporation of them to pure PC had no effect on the T_g, suggesting that pNA was a necessary agent for interaction between zeolite 4A and PC matrix.

These studies imply that zeolite filled glassy polymer MMMs can be appreciated as a favorable way to prepare high permeability and high selectivity gas separation membranes. Nonetheless, the poor interaction between glassy polymers and zeolite particles and the limit imposed by the upper-bound curve requires intense research activity. These considerations lead to the combination of two strategies in this study; incorporation of low molecular weight organic additives to the MMM formulation and annealing the membranes above the glass transition temperature of the neat polymer for flexibility promotion during preparation.

CHAPTER 3

EXPERIMENTAL

3.1 Membrane Preparation

3.1.1 Materials for Membrane Preparation

The polymer used for membrane preparation was a commercial Radel A-100 grade polyethersulfone (PES) provided by Solvay. The polymer (PES) has a weight average molecular weight of 53,000 and glass transition temperature (T_g) of about 220 ^oC. Figure 3.1 shows the repeating unit of polyethersulfone.

Analytical grade dimethylsulfoxide (DMSO) was purchased from J.T. Baker and used as solvent. Dimethylsulfoxide has a normal boiling point of 189 ^oC and a melting point of 18 ^oC.

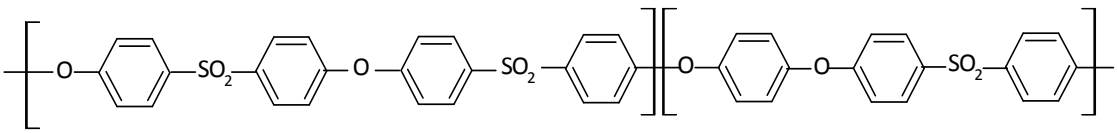

Figure 3.1 Repeating unit of polyethersulfone

Table 3.1 lists the low molecular weight organic compounds selected to be added to the membrane formulations. Analytical grade low molecular weight additives (LMWA) were purchased from Acros Organics and used without any further purification. All of the LMWAs are solid at room temperature.

Table 3.1 The chemical structures of low molecular weight additives used in membrane preparation

Name	Acronym	Chemical Structure
para-Nitroaniline	pNA	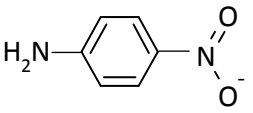
2-Hydroxy 5-Methyl Aniline	HMA	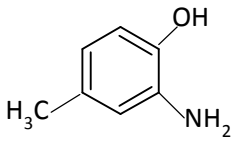
4-Amino 3-Nitro Phenol	ANP	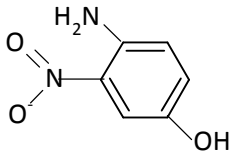
2-Amino-4-hydroxy-6 Methyl Pyrimidine	AHMP	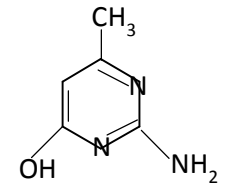
2-Amino-4-methylpyrimidine	AMP	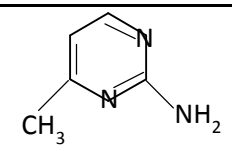
2-Methyldimidazole	Mia	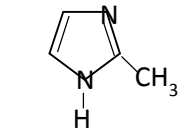
2,4,6 Triaminoprymidine	TAP	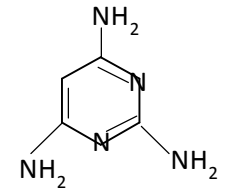
Melamine	MEL	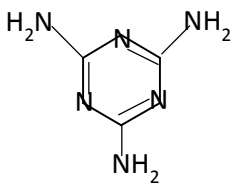

SAPO-34 type zeolite was used as the inorganic filler material in the membrane. Home-made SAPO-34 zeolite crystals were synthesized in our laboratory. The average particle size of the SAPO-34 zeolite crystals was half micron. Before using SAPO-34 in membrane preparation, they were dried at 250 ^{0}C for 24 h.

3.1.2 Determination of Solubilities of Low Molecular Weight Additives

The approximate solubilities of low molecular weight additives in DMSO were determined at room temperature before membrane preparation. The following procedure was used: 0.1 g of LMWA was added to 10 ml of DMSO, the mixture was stirred by a magnetic stirrer at room temperature for at least 3-4 h. If the solution was not clear, the amount of compatibilizer was decreased and the same procedure was repeated. If a clear solution was obtained, the amount of compatibilizer was gradually increased and the same procedure was repeated.

3.1.3 Membrane Preparation Methodology

Membranes were prepared by solvent evaporation method. Throughout this study, four types of membranes were prepared; pure polymeric PES membranes, PES membranes including low molecular weight additives, PES membranes including SAPO-34 zeolite crystals, and PES membranes including both LMWA and SAPO-34. The concentration of PES in DMSO was kept constant at 20 w/v % for all membranes. Casting of the membrane solution, solvent evaporation, annealing steps are the same for all of the membranes but their casting solution preparation steps are different. The preparation of casting solutions of PES/LMWA and PES/SAPO-34/LMWA membranes are explained in the following subsections, and summarized in Figures 3.2 and 3.3. The steps that are common for all of the membranes are explained in the subsection for pure PES membrane preparation below and also summarized in the flow chart given in Figure 3.4.

Casting Solution Preparation for PES/LMWA membranes:

For LMWA including PES membranes, the organic additive was dissolved in DMSO at a specified concentration and the solution was continuously stirred for 2 hours. One fifth of the PES necessary to obtain 20 w/v % PES solution is added to the LMWA-DMSO solution and stirred for 8 hours until a clear solution is observed. The rest of PES was added to the solution step by step in order to prevent the resultant mixture to be so viscous that makes

mixing too difficult. Stepwise addition of PES is also expected to minimize the aggregation of organic additives and to enhance the dispersion of LMWA in the LMWA-PES solution. This type of membrane mixture preparation is called priming of the polymer [44]. The LMWA / PES ratio in the solution was changed between 1 and 25 w/w % depending on the type of the LMWA. The type of additive and LMWA/PES ratios in the membrane solutions are shown in Table 3.2. It should be noted that the represented LMWA loadings are LMWA/PES ratios in the membrane casting solution, not necessarily in the membrane itself. LMWA/PES membrane mixture preparation is summarized in a flow chart (Figure 3.2). The actual weights of the components in the membrane preparation are tabulated in Appendix A. Membrane casting, evaporation, and annealing steps, which are same for all membranes, are given in Figure 3.4.

Table 3.2 LMWA / PES ratio for various membrane solutions.

Membrane	**LMWA**	**LMWA / PES ratio, w/w %**
PES/HMA	HMA	2, 4, 7, 10, 15, 25
PES/pNA	pNA	2, 4
PES/ANP	ANP	4
PES/AHMP	AHMP	1, 2, 3, 4
PES/AMP	AMP	4
PES/Mia	Mia	4
PES/TAP	TAP	4
PES/MEL	MEL	4

Casting Solution Preparation for PES/SAPO-34 and PES/SAPO-34/LMWA membranes:

SAPO-34 was dispersed in DMSO by continuous stirring for 24 hours on a magnetic stirrer. For PES/SAPO-34/LMWA membrane preparation, the solution was continuously stirred for 24 hours after the addition of LMWA at a specified concentration. For both PES/SAPO-34 and PES/SAPO-34/LMWA membrane mixtures, the solution was ultrasonicated for an hour to improve the dispersion of zeolite particles. One fifth of the total PES amount to be added to the solution to obtain 20 w/v % PES solution is added to the SAPO-34/ DMSO and/or LMWA / SAPO-34 / DMSO solution and stirred for 24 hours until a clear solution is observed and afterwards ultrasonicated for an hour to enhance the homogeneity. The rest of PES was primed similarly as explained previously. The details regarding the preparation of PES/SAPO-34 and PES/SAPO-34/LMWA membrane casting

solutions are summarized in Figure 3.3. When the PES/SAPO-34 and PES/SAPO-34/LMWA membrane mixtures were prepared according to the method explained, they were cast, solvent evaporated and annealed with the same conditions for all type of membranes summarized in Figure 3.4. The weights of the components in the membrane preparation are tabulated in Appendix A.

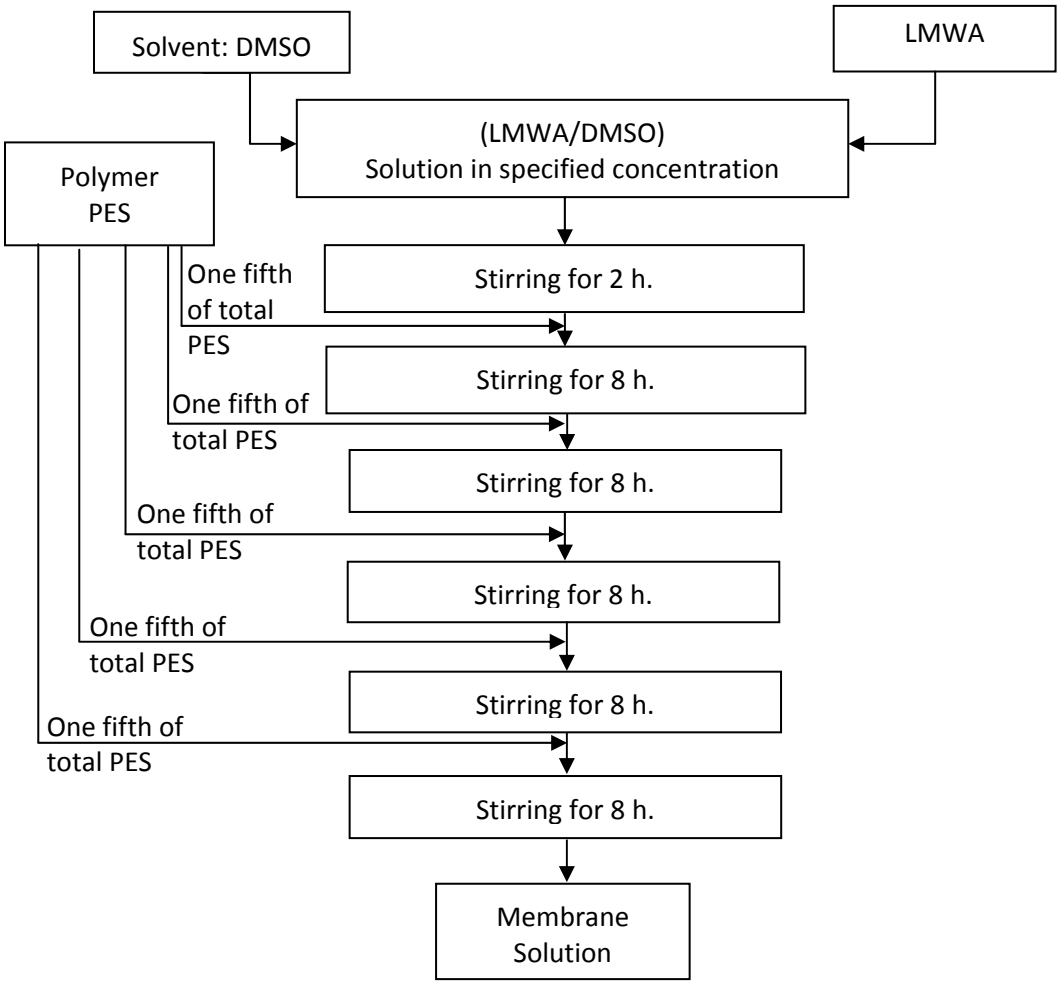

Figure 3.2 Flow chart of the casting membrane solution preparation procedure for PES/LMWA blend membranes

Membrane Preparation:

Membrane solutions were ultrasonicated (Branson 2510, 40 kHz) for an hour before casting. The solutions were drop cast on a Petri dish with a diameter of 12 cm in air atmosphere. Since DMSO is a dipolar aprotic, water miscible solvent, solutions were drop casted inside the oven with a temperature of 45 ± 5 ^{0}C to decrease the exposure of the solutions to the humidity. The films were dried at 80 ^{0}C in 0.2 atm N_2 atmosphere for 24 hours. The films were peeled off the glass Petri dish and placed between two metal frames

in a way that both the upper and below cross section of the film does not touch a surface in order to enhance the solvent removal from both sides of the membrane. The films were annealed for 8 hours at 1 atm N_2 atmosphere and 225 ^oC which is above the glass transition temperature (T_g) of PES in order to remove the residual solvent.

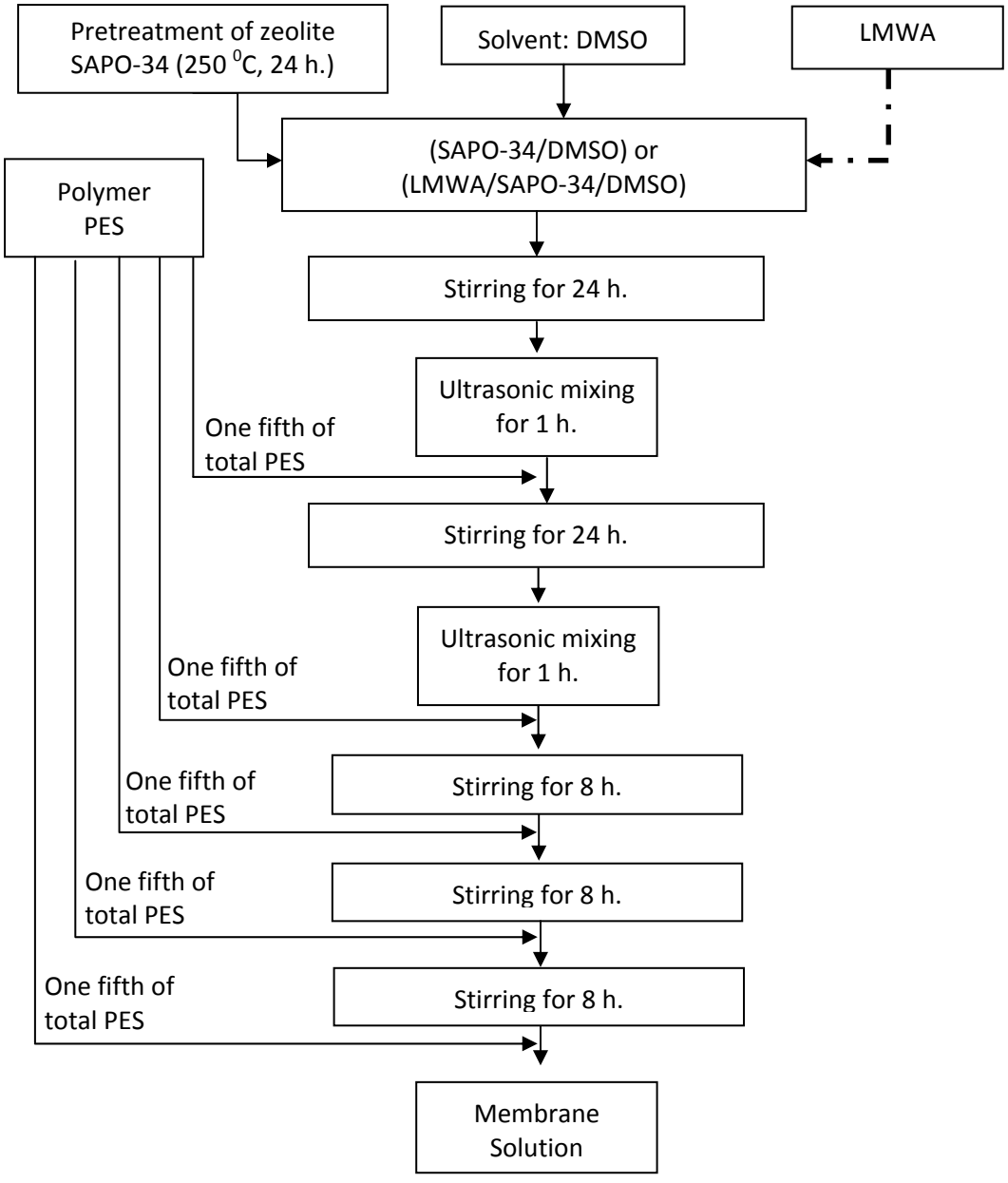

Figure 3.3 Flow chart of the casting membrane solution preparation procedure for PES/SAPO-34 and PES/SAPO-34/LMWA membranes

In order to prevent quenching, the annealed membranes were left in oven in N_2 atmosphere for natural cooling to room temperature. Prepared membranes were kept in a desiccator filled with desiccant silica gel at room temperature. The thicknesses of all

membranes were measured with a micrometer and these thickness measurements were checked with SEM micrographs. The thicknesses were in the range of 100-150 µm. All of the membranes were mechanically stable for the gas permeation experiments.

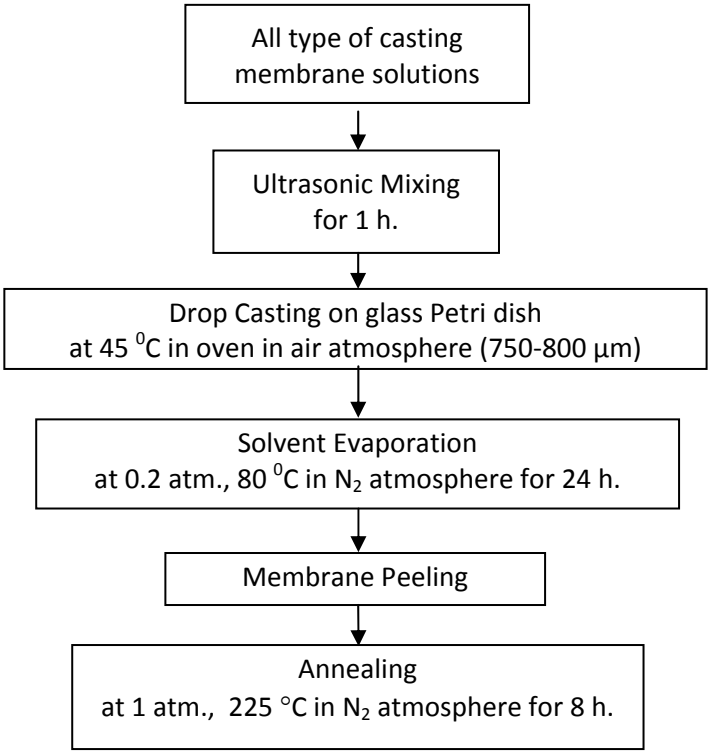

Figure 3.4 Flow chart of membrane preparation procedure of all type of membranes after the casting membrane solution preparation

3.2 Membrane Characterization

3.2.1 Thermal Characterization

Membranes were analyzed by Perkin – Elmer Diamond Differential Scanning Calorimeter (DSC) to determine the glass transition temperatures (T_g) of membranes. A small piece of membrane was heated to 250 ^{0}C which is above the glass transition of pure PES membrane (220 ^{0}C) in 10 ml/min N_2 flow with a heating rate of 10 ^{0}C/min. Then, the sample was naturally cooled to room temperature and heated again to 250 ^{0}C with the same conditions as the first scan. The T_g was determined from second scan. Membranes were also analyzed by Perkin – Elmer Pyris Thermal Gravimetry Analyzer to determine the thermal stability and the amount of residual solvent. The samples were heated at a rate of 10 ^{0}C/min in N_2 atmosphere. The nitrogen flow rate was 10 ml/min.

3.2.2 Scanning Electron Microscopy (SEM) Characterization

The membrane morphology was analyzed by Scanning Electron Microscopy (SEM) on a JEOL JSM-6400. Membranes were fractured in liquid nitrogen to obtain smooth and clean cross section SEM micrographs. The samples were stuck vertically or horizontally on to a circular aluminum sample holder depending on whether the cross section or the top view micrograph of the membrane is desired. Samples were coated with gold in order to provide an electrically conductive layer. After coating, the membranes were analyzed at various magnifications of 1500x – 100,000x.

3.2.3 Carbon- Nitrogen- Sulphur Elemental Analysis

The carbon, nitrogen, and sulphur content of the membranes were analyzed by LECO type CHNS-932 elemental analyzer. The instrument has carbon, hydrogen, nitrogen, and sulphur detectors. Approximately 2 mg of homogeneous solid samples are placed in the instrument. CHN analysis is accomplished by combustion analysis. In this technique, sample is burned in an excess of oxygen, and various traps collect the combustion products. The weights of these combustion products can be used to calculate the composition of the unknown sample. The weight percentages of the elements are recorded for the samples.

3.2.4 Single Gas Permeability Measurements

3.2.4.1 Single Gas Permeability Set-up and Procedure

Single gas permeability measurements of the membranes were performed using constant volume-variable pressure technique. This technique was used previously in our laboratory [36, 41, 55, 60]. Based on this technique, permeation systems was previously designed and used by our research group [36, 41, 55, 60]. According to this technique, membrane was placed in a constant volume membrane module where the pressurized feed gas permeates through the membrane to increase the dead end upstream pressure. The set-up consists of a membrane cell, a pressure transducer, a gas tank and a vacuum pump (Figure 3.5).

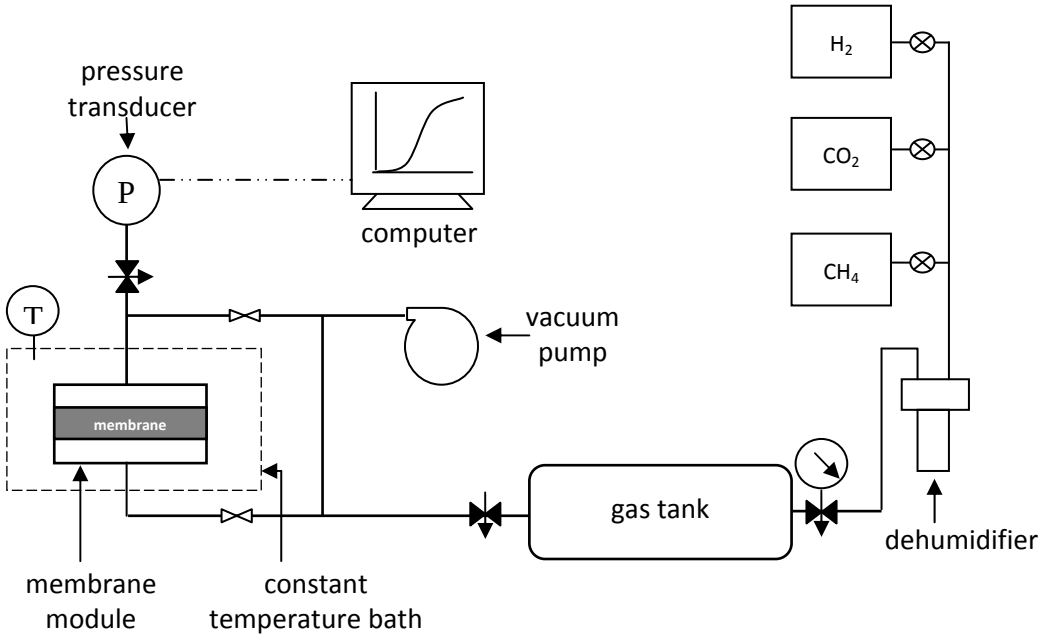

Figure 3.5 Schematic view of both of the single gas permeability systems

In this study, the permeation set-up was reconstructed based on same principles with previously designed constant volume-variable pressure permeation systems used in our laboratory. All of the piping and fittings were renewed and stainless steel Swagelok trade mark ¼ inch pipes and fittings were used. Besides, two types of membrane modules were used, a home-made one and a Millipore filter holder. The set-up fulfills the requirements of ASTM D1435-82.

One of the membrane modules is home made and used by our research group previously. As described elsewhere [6-8], it consists of two horizontal stainless steel flanges which are 10 cm. in diameter and 1.5 cm thick, as shown in Figure 3.6. Circular depressions are machined in each flange, so that a cylindrical cavity is formed. The membrane is clamped between two flanges by means of six equally spaced bolts. The membrane is supported by several sheets of filter paper on both sides of the membrane (Whatman 41, 125 mm Dia, No: 144125). Two synthetic rubber gaskets ensure pressure-tight seal between the membrane and flanges. The effective membrane area was 19.6 cm^2. The dead volume of the set-up, which is described as the volume between permeate side of the membrane cell and the pressure transducer, was measured as 6 cm^3 [36, 41, 55]. The increase of permeate side pressure was measured with a pressure transducer (Data Instruments, Model SA, 0–100 psia pressure range) with a sensitivity of 0.01 psia.

The other membrane module was a stainless steel Millipore filter holder (Millipore, part no.XX45 047 00) with a double Viton O-ring seal, as shown in Figure 3.8. The effective membrane area was 9.6 cm^2. The dead volume of the set-up, which is the volume occupied by the permeate gas from permeate side of the membrane cell to pressure transducer was measured as 7.1 cm^3 by filling the described volume by water. The increase of permeate side pressure was measured with a pressure transducer (BD Sensors, DMP331, 0–4 bar pressure range) with a sensitivity of 0.001 bar.

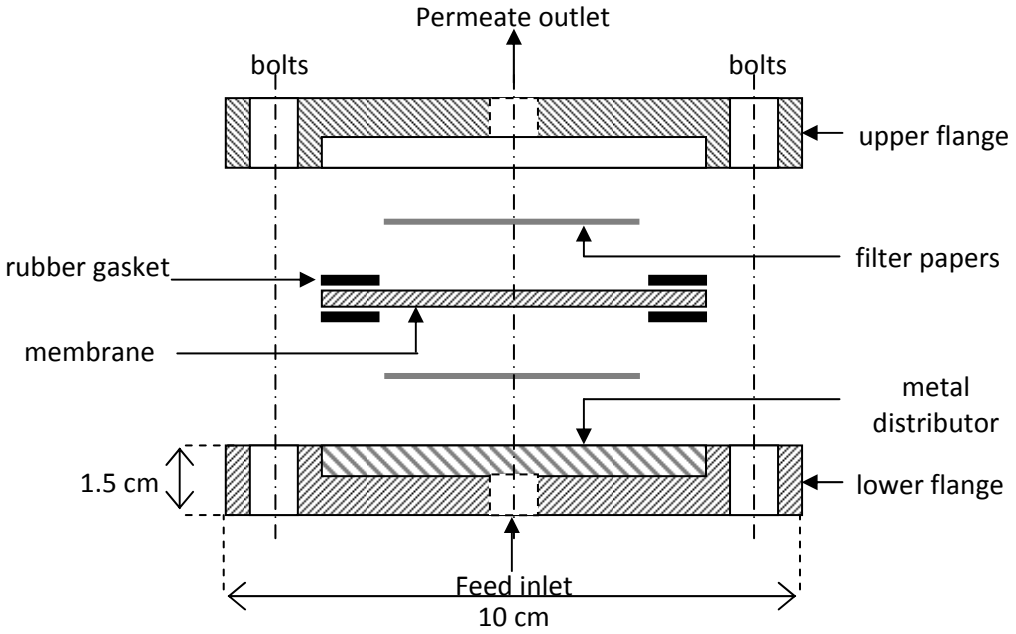

Figure 3.6 Schematic of front view of the home made membrane cell, adopted from [36]

As can be seen in Figure 3.5, the membrane module was placed in a constant temperature silicone oil bath. Single gas permeability of all gases were measured at 35 ^{0}C. The gases were purchased from a local company (Oksan). The gas was sent to the gas chamber after passing through the dehumidifier which was filled with activated zeolite 4A. Passing the dehumidifier, the feed gas was filled into the gas chamber at a specified pressure. Then, this pressurized feed gas was sent to the membrane module. The pressure rise at the permeate side of the membrane was determined by the pressure transducer. The analog data of the pressure transducer was sent to a data acquisition system and sent to the computer as digital data to record the experimental data as pressure and time.

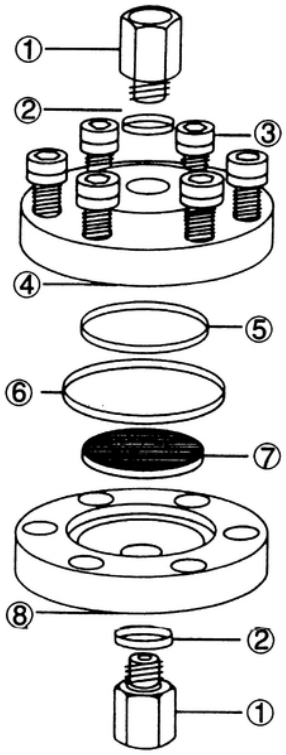

Figure 3.7 Schematic of the Millipore membrane cell; Replacement Parts: 1. Inlet/Outlet Adapter, 2. Adapter O-ring, 3. Hex-cap Screw, 4. Top Plate, 5. Inner O-ring, 6. Outer O-ring, 7. Support Screen, 8. Bottom Plate

For all of the single gas permeability measurements, the initial transmembrane pressure difference was kept constant at 2 bar. During the measurements performed with home made membrane module, the pressure in the gas chamber was 2.9 bar. Then, the gas was fed to the membrane cell where the permeate side pressure was set to the barometric pressure (~ 0.9 bar) by opening the valve at the permeate side to the atmosphere. During the measurements performed with Millipore filter holder, the pressure in the gas chamber was 2 bar, and the gas was fed to the membrane cell where the permeate side was at vacuum.

Before and after each measurement, both feed and permeate sides were evacuated to less than 0.1 bar by a 2-stage mechanical vacuum pump (Model E2M5, Edwards High Vacuum Pump) and kept in vacuum for two hours. Measurements through each membrane were carried out at least twice. The average of all measurements was reported as the permeability and expressed in a unit of Barrer. (1 Barrer = 10^{-10} cm^3 (STP) cm/cm^2 s cmHg).

3.2.4.2 Single Gas Permeability Calculations

Permeability of a single gas through a membrane was calculated from Equation 3.1,

$$P = \frac{v_{STP}.\delta}{\Delta p.A} \tag{3.1}$$

where,

P = permeability (Barrer), 1Barrer = 10^{-10} cm^3 (STP).cm / cm^2.s.cmHg

v_{STP} = volumetric flow rate of the permeate gas through the membrane (cm^3/s) at STP

A = effective membrane area (cm^2)

δ = thickness of the membrane (cm)

Δp = transmembrane pressure difference (cmHg)

The increase of pressure in the module is recorded and plotted as a function of time. Pressure vs. time data points were fit to a straight line by linear regression method. The slope of this line (dp/dt) was used to find the molar flow rate by assuming the ideal gas law holds.

$$\frac{dn}{dt} = \frac{dp}{dt}.\left(\frac{V_d}{R.T_{exp}}\right) \tag{3.2}$$

Where V_d is the dead volume, T is the absolute experimental temperature, and R is the universal gas constant. The experimental volumetric flow rate of the permeate gas can be found by,

$$v_{exp} = \frac{dn}{dt}.\left(\frac{M}{\rho}\right) \tag{3.3}$$

Where dn/dt is the molar flow rate of the permeate gas calculated by equation 3.2, ρ is the density of the permeate gas and M is the molecular weight of the gas. Density of permeate gas is calculated by assuming ideal gas law (eqn. 3.4).

$$\rho = \frac{p_{avg}.M}{R.T} \tag{3.4}$$

where p_{avg} is taken as the average of initial and final pressures at the permeate side. Since permeability unit Barrer is defined at standard temperature of 273.15 K and pressure of 1atm, the volumetric flow rate calculated in equation 3.3 needs to be multiplied by a STP correction factor;

$$v_{STP} = v_{exp}.\frac{T_{STP}}{P_{STP}} \tag{3.5}$$

By means of Equation 3.5, v_{STP} is calculated and can be used in Equation 3.1 to calculate the permeability.

The ideal selectivity of a membrane for a gas over another is defined as the ratio of single gas permeabilities, which can be expressed as;

$$\alpha_{ij} = \frac{P_i}{P_j} \tag{3.6}$$

CHAPTER 4

RESULTS AND DISCUSSION

4.1 Selection of Membrane Preparation Materials

Material selection is a critical factor affecting mixed matrix membrane morphology and transport properties. Hence, selection of suitable polymer matrix, solvent, additives and molecular sieve is a very important aspect. This section discusses the selection of these materials.

Rubbery polymers might lack mechanical stability and desirable inherent transport properties relative to rigid glassy polymers. Therefore, rigid glassy polymers, which possess properties closer to the upper bound, are preferred as the base of mixed matrix membrane. However, the problem for polymers with crystalline structure and/or very high glass transition temperatures is the unnecessarily hard and rigid structure. One may consider decreasing T_g by incorporating a plasticizer into the polymer matrix. However, the study conducted by Mahajan et al. [16] showed that the addition of plasticizer also lowered the gas separation performance of polymeric materials. Therefore, choosing glassy polymers with an intermediate T_g should be a more appropriate alternative for this solution.

The high performance engineering thermoplastic Radel A 100 Polyethersulfone which is supplied by Solvay Plastics was selected as polymer in this study. PES is an attractive commercially available polymer having excellent properties; such as high chemical resistance, stable to oxygen and to thermal degradation. PES has a glass transition temperature of 225°C and thus is a glassy polymer at preparation and application temperature. These properties have made PES a popular membrane material [41, 55].

Previous studies conducted by Suer et al. [41] and Battal et al. [55] showed that PES is an appropriate polymer for preparing mixed matrix membranes. It allows fast gas permeation rates with reasonable selectivities [1, 41, 52, 55]. Robeson's plot is usually used as a tool to evaluate the performance of polymeric membranes. The permeability and selectivity values of PES lies near the upper bound line on the middle region of Robeson's plot for attractive gas pairs like CO_2/CH_4, H_2/CH_4. For example, it shows H_2 and CO_2 permeabilities of 5.85 and 2.61 Barrer, respectively, with H_2/CH_4 and CO_2/CH_4 selectivities of 53.66 and 23.95 [55].

In addition to being an appropriate polymer for investigation of membrane preparation parameters, PES enables wide possibility of low molecular weight additives. Since PES can be dissolved in wide range of solvents including dipolar aprotic solvents having good dissolving power, the selected solvent upon the polymer would not limit the low molecular weight additive alternatives. Solvent was selected among a number of dipolar aprotic solvents such as; dimethylformamide (DMF), dimethylacetamide (DMAc), and dimethylsulfoxide (DMSO), which have strong dissolving power for many components.

Solvent type strongly influences configuration of polymer chains in solution. A solvent might be a good solvent for a polymer, which leads to extension, a poor solvent for a polymer, which leads to satellite effect that is the polymer segments attract each other in solution more strongly than they attract surrounding solvent molecules, or a theta solvent, which leads to ideal mixture [56]. Main criterion for evaluation of solvation power and polymer-solvent interaction is solubility parameter [35, 57]. Table 4.1 represents the three component Hansen solubility parameters of the selected polymer and solvent candidates. Solubility parameter approach is widely used for correlating polymer solvent interactions. The square root of cohesive energy density is called solubility parameter (δ). As a refinement, three solubility parameter components can be distinguished, representing dispersion (δ_d), polar (δ_p), and hydrogen (δ_h) bond interactions [35].

$$\delta^2 = \delta_d^2 + \delta_p^2 + \delta_h^2 \qquad (4.1)$$

In accordance with the general rule that chemical and structural similarity favors solubility, as the difference between the total solubility parameters of the polymer and solvent increases, tendency towards dissolution decreases. Hence the requirement of small differences between these parameters became a rule of thumb in solvent selection. It was

also concluded that substances with a Δδ < 7.0 $MPa^{1/2}$ are likely to be miscible, whereas those with Δδ > 10$MPa^{1/2}$ are likely to be immiscible [57]. Equation 4.2 shows the calculation of Δδ, where the subscripts p and s stands for polymer and solvent respectively.

$$\Delta\delta = \left[\left(\delta_{d,p} - \delta_{d,s}\right)^2 + \left(\delta_{p,p} - \delta_{p,s}\right)^2 + \left(\delta_{h,p} - \delta_{h,s}\right)^2\right]^{1/2} \quad (4.2)$$

Table 4.1 Three Component Hansen Solubility Parameters of the Selected Polymer and the Solvent Candidates [57]

	δ*	**δp**	**δh**	**δd**	**Δδ**	**Normal Boiling Point (°C)**
PES	24.20	10.80	9.20	19.60	-	-
DMSO	26.68	16.40	10.20	18.40	5.81	189
DMF	24.86	13.70	11.30	17.40	4.20	153
DMAc	22.77	11.50	10.20	16.80	3.05	164

*Unit of solubility parameters are $MPa^{1/2}$

Table 4.1 reveals that all of the solvent candidates satisfy the rules of thumb for polymer-solvent miscibility, as expected. Using solubility parameter approach only as an initial estimate, the selected solvent should also satisfy other criteria.

Secondly, the boiling point of the solvent was considered. A solvent having a low boiling point is not practical during the preparation of the films since they are highly volatile. A solvent having a very high boiling point is again not preferable due to the difficulty in solvent removal. Khulbe et al. [15] reported that the permeability increases and the selectivity decreases with the increase in boiling points of the solvents, probably due to the residual solvent amounts in the final membranes. Therefore, a solvent having a boiling point too high or too low is not preferable. Since, as discussed in chapter 3 and in section 4.3.2.1, annealing above the glass transition temperature of PES (220 ^{o}C) was used throughout this study, hence the solvent candidates represented in Table 4.1 together with their normal boiling points are appropriate from this aspect.

As a third criterion, the solvent to be selected should dissolve not only the polymer but also the selected low molecular weight additives. Table 4.2 shows the results of the solubility measurements for three solvent candidates, and also the chemical structures of the selected LMWAs. Solubility experiment measurements showed that DMSO is more suitable among DMF and DMAc, having a better dissolving power to dissolve the selected LMWAs and PES. At the stage of determining the solvent, these criteria were considered and dimethylsulfoxide (DMSO) was selected as the solvent.

Several organic compounds were considered to select the low molecular weight additives which can act as a kind of compatibilizer between the polymer and zeolite. Therefore, the selected LMWAs have at least bifunctional groups, one is for the interaction with the polymer side and the other is for the solvent side, but multifunctional ones were preferred.

Apart from the number of functional groups, their type and position are also important and noted as important parameters in interacting the polymer and zeolite in literature [12, 16, 20, 32, 36, 45]. In the selection of LMWAs, one of the main factors was the possession of amine, nitro, and hydroxyl functional groups. Hydroxyl groups can bind the compatibilizer to the zeolite surface [12, 16, 45] and the compatibilizer may attach to polymer chain from amine and nitro groups by hydrogen bonding [20]. Yong et al. claimed that the carbonyl group of polyimide and the amine group of 2,4,6-triaminopyrimidine forms hydrogen bond. Paul et al. [32] modified polysulfone membranes with fluorene based additives, such as fluorene bisphenol which has two phenol groups superimposed on fluorene. The polymer and the additive linked to each other by hydrogen bonding through the hydroxyl groups of additives. Şen et al. [36] showed the interaction between the amine functional groups of pNA and carbonyl groups of PC using the FTIR spectra of the membranes. Further, they commented that nitro being directive and activating group may extend the hydrogen bonding capability of pNA with PC. Şen et al. [36] employed compatibilizers other than pNA also; these are 4-amino 3-nitro phenol (ANP) and 2-hydroxy 5-methyl aniline (HMA) all of them including amine and hydroxyl groups in different ortho and para positions. Based on the aforementioned studies, low molecular weight additives possessing the mentioned multi-functional groups selected for their possible interacting capability.

In addition to these considerations, all of the LMWAs should be solid and stable at room temperature, and soluble in the solvent of the polymer to be practical in membrane formation. Low molecular weight additives selected are tabulated in Table 4.2 with their chemical structures, melting points, molecular weights, and solubilities.

Table 4.2 Selected LMWAs with their chemical structure and physical properties together with their experimental solubilities in three candidate solvent

Acronym	Chemical Structure	Molecular Weight	Melting Point (°C) [58]	Solubility in DMF (w/v)	Solubility in DMAc (w/v)	Solubility in DMSO (w/v)
pNA	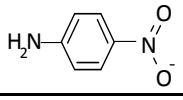	138.13	148.5	5.2	4.1	7.2
HMA	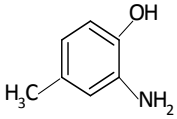	123.16	137	>20	>20	>20
ANP	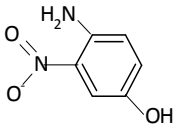	154.11	154	-	-	-
AHMP	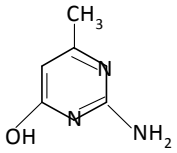	125.13	>250	0.3	0.6	1.9
AMP	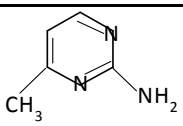	109.13	160	8.5	8.9	9.9
Mia	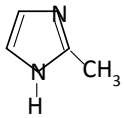	82.10	145	9.8	1.9	9.9
TAP	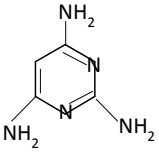	124.00	250	4.7	< 0.1	9.1
MEL	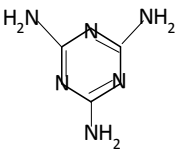	126.12	>250	-	-	-

pNA: para-nitroaniline, HMA: 2-hydroxy 5-methyl aniline, ANP: 4-amino 3-nitro phenol
TAP: 2, 4, 6-Triaminopyrimidine, AHMP: 2-Amino-4-hydroxy-6-methylpyrimidine,
AMP: 2-Amino-4-methylpyrimidine, Mia: 2-Methyldimidazole, MEL: Melamine

As mentioned in Chapter 2, the majority of the work on zeolite filled polymeric membranes utilizes synthetic zeolites, such as zeolite A, X, Y and silicalite, especially zeolite 4A. Only the study conducted by Way et al. [49] is a pioneer work that utilizes the zeolite SAPO-34 as dispersed inorganic filler in mixed matrix membranes. Although no significant improvements were recorded in terms of gas permeation characteristics, the results may be explained with the rubbery nature of their base polymer, methoxy ethoxy ethanol (MEE) substituted polyphosphazene (PPZ).

SAPO-34 zeolite which is a silicoaluminophosphate with the composition $Si_xAl_yP_zO_2$, where x is in between 0.01 and 0.98, y is in between 0.01 and 0.60, z is in between 0.01 and 0.52, and x + z = y [59]. SAPO-34 molecular sieves have pores that are similar in size to CH_4 approximately 0.38 nm, which can act as the cut-off diameter for the CH_4 molecule. But not only the molecular sieving potential of SAPO-34 makes this novel inorganic additive attractive, but also the relatively higher CO_2 sorption affinity compared to conventional zeolite 4A [49].

4.2 Effects of Measurement and Preparation Methodology

All membranes were tested by measuring the single gas permeabilities of H_2, CO_2, and CH_4 in a dead-end system described in Section 3.2.3 at constant 35 ^oC. During the experiments regarding the development of membrane preparation procedure and the investigation of effect of low molecular weight additive type on PES/additive blend membranes, H_2 and CO_2 were used as test gases, for these experiments the feed side pressure was always kept at 3.7 bar, and the permeate side pressure was initially at atmospheric pressure (~ 0.9 bar). During the experiments regarding the investigation of effect of low molecular weight additive loading on PES/additive blend membranes and SAPO-34 filled PES membranes, H_2, CO_2, and CH_4 were used as test gases, for these experiments the feed side pressure was always kept at 2 bar, and the permeate side pressure was initially at vacuum (< 10^{-8} bar). For this operating conditions, the pressure rise at the permeate side with time is shown in Figure 4.1 for pure PES membrane.

The permeate side pressure increased steadily for all gases. For pure PES and PES/SAPO-34 membranes starting from vacuum at the permeate side and 2 bar at the feed side, the pressure reached 40 mmHg in approximately 60 min during the hydrogen permeation, in 130 min during the carbon dioxide permeation, however, this period was

about 2800 min for methane. On the other hand, for PES/LMWA and PES/LMWA/SAPO-34 membranes gas permeation periods were much longer than the above mentioned periods depending on the LMWA type and concentration in the membrane formulation. Permeabilities were calculated by fitting all pressure-time data on a straight line by linear regression method. The slope of the linear steady state section of this line was calculated in the permeate side pressure range of 10 to 40 mmHg when the permeation started at vacuum permeate side, 670 to 800 mmHg when the permeation started at atmospheric permeate side pressure. This slope was used to find membrane's permeability as described in Section 3.2.4.

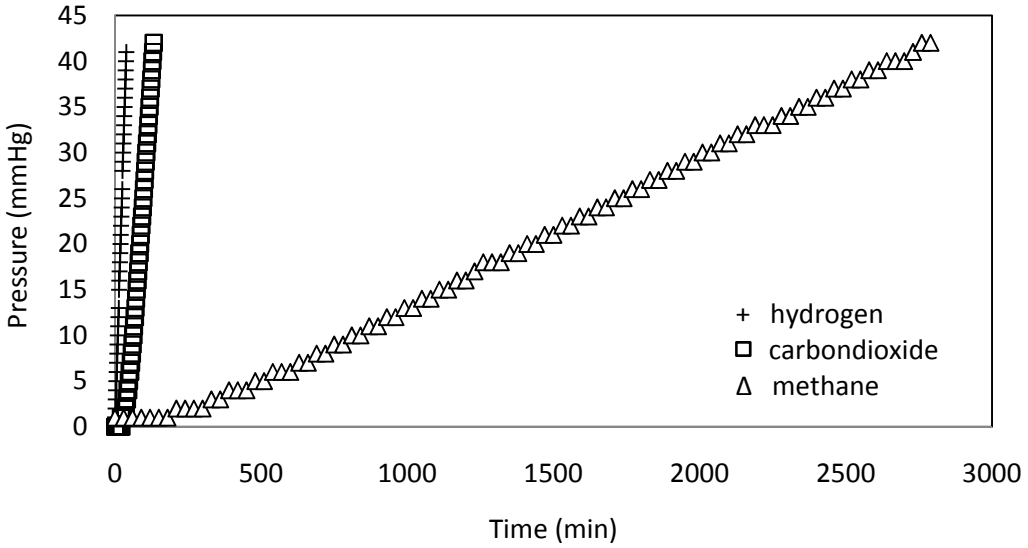

Figure 4.1 Permeate side pressure increase with time for pure PES membrane, feed side pressure is 2 bar, permeate side pressure is at vacuum (< 10^{-8} bar)

As Figure 4.1 represents the pressure increase curves of the solution-cast pure PES membranes for three different gases, these curves have two sections in the given ranges. At the initial region of the curves, permeate pressure does not increase for a while owing to the time required for sorption of the gas molecules. When the permeation is started at time is equal to zero, there is a certain amount of time for each gas to increase the pressure at the permeate side due to the sorption-diffusion mechanism. Sorption time is larger for bulkier molecules like CO_2 and CH_4. The linear section in Figure 4.1 shows the pseudo-steady state pressure rise in the permeate side, and the pressure-time data within this region are used in permeability calculations. The shape of the permeate side pressure increase curves are in agreement with the ones reported in literature [5, 12, 36, 44].

The single gas permeation experiments were performed at a constant temperature of 35 ^{o}C, in order to avoid experimental errors resulting from temperature variations when a lower, so called room, temperature was used. 35 ^{o}C is a commonly used temperature in gas permeation [41, 55]. Figure 4.2 reveals that gas permeation properties of a membrane are strongly related to testing temperature. Figure 4.2 reveals the effects of spontaneous change of temperature on permeate side pressure during CO_2 permeation through pure PES membrane. When CO_2 permeation had been performed at 16 ^{o}C, the membrane module was suddenly placed in a medium at constant temperature 35 ^{o}C. As Figure 4.2 shows, the rate of increase of permeate side pressure increased abruptly with the step change in permeation temperature. The temperature of the permeation cell was controlled, and during the constant temperature periods in pressure time plot below, the pressure increase was calculated for the linear regions, which are also remarked on the Figure 4.2. Permeate side pressure increased at a rate of 0.32 mmHg/min, and 0.41 mmHg/min for 16 ^{o}C and 35 ^{o}C respectively. Low-testing temperature usually led to low gas permeability as expected; at 16 ^{o}C, CO_2 permeability was found to be 2.50 Barrer whereas at 35 ^{o}C, it was found to be 3.44 Barrer. This trend may be explained with the enhanced diffusivities of the gases with the increase in temperature.

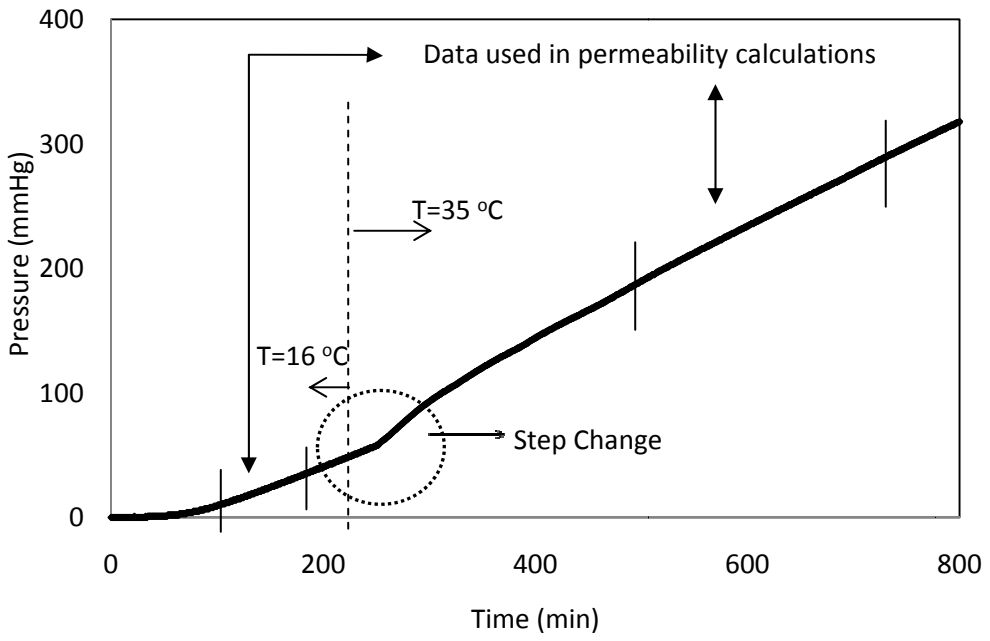

Figure 4.2 Effect of spontaneous change of temperature on permeate side pressure for pure PES membrane

4.2.1 Reproducibility in Permeability Measurements and Membrane Preparation

Reproducible membrane preparation and repeatable permeability measurements are substantial issues in preparation and testing of membranes with complex structures, since it shows the reliability and robustness of membrane preparation procedure [60, 61]. For this purpose, for a particular membrane formulation at least two membranes were prepared at different times with same procedure. Permeabilities of all gases through any membrane were measured at least two times except CH_4 due to its very long permeation duration (between two and ten days depending on the membrane formulation). Therefore, both the repeatability of permeability measurements and the reproducibility of membrane preparation were examined. The results for pure PES membranes are shown in Table 4.3 together with the average results of the three membranes tabulated. The thickness of the membranes changes between 100-150 µm. The difference in permeability measurements between successive two runs vary from 0.15 % to 1.53 % and from 0.33 % to 0.67 % for H_2 and CO_2 gases respectively. The difference in permeability measurements between two membranes with same formulation which are casted at different times is all smaller than % 10 for all gases, which are completely acceptable in literature [21, 36, 41, 60]. These small differences imply that the measurements are accurate and reproducible. Results of reproducibility experiments for the all membranes prepared are tabulated in Appendix B.

Table 4.3 Permeability and selectivity results of pure PES membranes casted and tested at different times measured at 35 ^{o}C, feed side preesure is 2 bar, and permeate side is at vacuum.

Membrane Number	Successive Runs	Permeability			Selectivity		
		H_2	CO_2	CH_4	H_2/CO_2	CO_2/CH_4	H_2/CH_4
M1 (145 µm)	1	6.64	2.60	0.084	2.55	30.95	79.05
	2	6.63	2.59				
	Avg	6.64	2.60	0.084			
	% Δ (Runs)	0.15	0.38	-			
M2 (100 µm)	1	6.96	3.05	0.105	2.28	29.05	65.95
	2	6.89	3.04				
	Avg	6.93	3.05	0.105			
	% Δ (Runs)	1.01	0.33	-			
M3 (100 µm)	1	7.17	2.97	0.105	2.39	28.42	67.76
	2	7.06	2.99				
	Avg	7.12	2.98	0.105			
	% Δ (Runs)	1.53	0.67	-			
AVERAGE		6.89	2.88	0.098	2.40	29.34	70.34

Table 4.4 represents permeability and selectivity data for pure PES membranes from literature, and the results obtained in this study. For the test gases used in this study, the fastest gas is hydrogen, and the slowest is methane. The permeability values are in the range of 5.30-8.96 Barrer for H_2, 2.51-3.80 Barrer for CO_2, and 0.083-0.129 Barrer for CH_4. The permeabilities through pure PES membranes prepared in this study are comparable with those reported in the literature. The significant differences in the reported data in literature may be attributed to the differences in gas permeation experiments or the differences in membrane preparation procedure. As mentioned in the previous section, and as can be seen in Table 4.4, temperature is an important parameter affecting the gas permeation properties of a membrane. Despite this fact, in some studies the permeation temperature is not reported or simply claimed that the permeation is held at room temperature [41, 55]. In addition, as Hacarlıoglu et al. [60] investigated the effects of type and concentration of casting solvent, solvent evaporation duration and temperature, annealing duration and temperature on pure polycarbonate membranes, and concluded that the performance of membranes strongly depends on preparation parameters, the values for these parameters have not been reported in many studies.

4.2.2 Effects of Membrane Preparation Parameters

The solvent-evaporation method was used to prepare all membranes throughout this study. The membranes were drop casted and solvent evaporated at 80 ^{o}C for 24 hours in 0.2 atm N_2 environment. The solvent evaporation temperature and pressure was selected according to vapor-pressure data of the solvent used. DMSO has a boiling point of 125 ^{o}C at 0.15 atm [58], hence any temperature and pressure selected as the solvent evaporation parameters near 125 ^{o}C and 0.15 atm could be resulted in bubbling and foaming of the solvent during the evaporation step which is not desired in preparing defect free nonporous gas separation membranes. Hence a pressure greater than the vapor pressure of DMSO and lower temperature than the saturation temperature of DMSO were chosen to avoid this phenomena for the solvent evaporation step. Annealing was modified and adopted to our polymer-zeolite-solvent system and the effect of parameters such as the duration and temperature were investigated.

Table 4.4 Permeabilities of dense homogeneous PES membranes in literature

Reference	Permeation Temperature (°C)	Polymer Grade	Procedure	Annealing Conditions	Polymer Concentration (w/v %)	Permeability (Barrer)					
						H_2	CO_2	CH_4	O_2	N_2	Ar
[62]	35	Radel A-300	Casting in NMP	-	NR	-	2.51	0.084	0.48	0.082	-
[42]	35	Amoco	Casting in NMP/DCM	In 1 atm N_2 for 12 hours at 250 °C	2	8.96	3.38	0.112	0.77	0.129	-
[27]	25	Sumikaexcel	Compression molding	-		-	3.80	-	-	-	-
[63]	35	Victrex	Casting in NMP	-	29.4	8.00	-	-	0.75	0.110	-
[52]	35	Radel A-300 PES	Casting in NMP	In 1 atm N_2 for 12 hours at 250 °C	20	6.47	-	-	0.47	0.083	-
[1]	35	Radel A-300 PES	Casting in NMP	In 1 atm N_2 for 12 hours at 250 °C	NR	-	2.63	0.083	-	-	-
[64]	25	Victrex	Casting in MC	Vacuum drying at 168 °C for 3 days	10	-	3.28	-	-	-	-
[65]	25	Imperial Chem. Ind.	Casting in DMF	In 1 atm air at 60 °C	15	-	-	-	0.63	0.097	0.229
[41]	NR	Victrex	Casting in DMF	In 1 atm N_2 for 8 hours at 100 °C	NR	6.50	2.60	-	0.52	0.140	0.180
[55]	NR	BASF E2010	Casting in DMF	In 1 atm N_2 for 8 hours at 100 °C	70 wet basis	5.85	2.61	0.109	0.59	0.094	0.234
		BASF E6010	Casting in DMF			5.30	2.55	0.129	0.53	0.090	0.235
[66]	35	Radel A-300	Casting in NMP	In 1 atm N_2 for 12 hours at 250 °C	NR	6.28	2.64	0.084	0.50	0.081	-
[67]	35	NR	Compression Molding	-		-	2.80	0.100	-	-	-
This study	35	Radel A-100	Casting in DMSO	In 1 atm N_2 for 8 hours at 225 °C	20	6.89	2.88	0.098	-	-	-

NR: Not Reported, NMP: N-methyl-2-pyrrolidone, DCM: Dichloromethane, DMF: Dimethylformamide, DMSO: Dimethylsulfoxide, MC: Methyl Chloride

4.2.2.1 Effect of Annealing Parameters

The strong effect of membrane preparation parameters on the performance of the membranes formed the basis of the need for improving membrane preparation method. Membrane preparation conditions have been studied by several researchers, often in relation with type and amount of residual solvent [60, 68-72, 76]. Therefore some preliminary experiments were performed with pure PES membranes fabricated at different annealing conditions. Table 4.5 represents the single gas permeation results for the pure PES membranes annealed at different temperatures and durations. Membrane preparation procedure developed only using pure PES membranes. Due to the fact that, dense homogeneous polymeric membrane has the simplest morphology, which is composed of a polymer layer that is homogeneous in all directions; hence it is the simplest and most suitable structure to investigate parameters [60].

Table 4.5 reveals that as the annealing temperature and duration increased the permeability values of the membranes increased significantly for both H_2 and CO_2, accompanied by a moderate increase in H_2/CO_2 ideal selectivity. Similar observations were also reported by Joly et al [68] and Chang et al [76]. Joly et al [68] investigated the effect of residual solvent on the gas permeation properties of the membranes and permeability increase with the decrease in residual solvent was reported. Chang et al [76] performed a molecular simulation study investigating the effects of residual solvent on free volume of the membranes and validated their model results with the results of Joly et al [68]. Both studies reported the improved sorption and permeability coefficients with the removal of residual solvent molecules.

Hacarlıoğlu et al. [60] also investigated the effect of annealing period on neat PC membranes. The solvent used in this study had a boiling point of 44 ^{o}C and a molar volume of 64 cm^3/mol. The films annealed at 50 ^{o}C for 8, 24, 72, and 154 hours. In contrast to our results, the permeabilities decreased as the annealing duration increased until 72 hours of annealing; after 72 hours of annealing period, permeabilities remained almost constant with further annealing. These results may indicate that the type of the solvent and polymer used has a considerable influence on gas transport properties of the membranes.

Table 4.5 Effect of annealing conditions on pure PES membrane gas separation performance (Permeate Side Initial Pressure: 0.9 atm, Feed Side Pressure: 3.7 atm)

Membrane Number	Annealing Period and Temperature	Permeability		Selectivity
		H_2	CO_2	H_2/CO_2
M1	1 day, 110 ^oC	5.04	2.52	2.00
M2	3 days , 130 ^oC	6.40	2.88	2.22
M3	3 days, 160 ^oC	9.25	3.63	2.55
M4	3 days, 190 ^oC	12.19	4.69	2.60
M5*	8 hours, 225 ^oC	14.28	5.32	2.68

Annealing the membrane above T_g of PES)

The solvent used in this study, dimethyl sulfoxide, has a relatively high boiling point of 189 ^oC and a relatively higher molar volume of 71 cm^3/mol. The increase in permeability values might be explained with not only the physical properties of the solvent, DMSO, but also the effects of the residual solvent in the membrane on the fluctuation and flexibility of the polymer segments and the free volume. At higher amounts of residual solvent in the membrane, the competition between the penetrant gas molecules and the residual solvent molecules can be anticipated. Depending on the increasing permeabilities with decrease in residual solvent, the extraction of solvent would enlarge the free volume in the membranes, thus provide more suitable sites for gas sorption. Even though the residual solvent in the membrane may facilitate the movements of polymer segments, the increasing permeabilities with a reduction in residual solvent amount can be attributed to the released free volume occupied by the solvent molecules by means of annealing the membranes at higher temperatures for longer durations. In addition, DMSO might leave imprints on the membrane matrix due to its high molar volume and high boiling point. These observations agree well with the literature results [68, 76].

Aforementioned studies imply that the state of the polymer in the membrane strongly depends on the type and amount of the solvent remained in membrane matrix. Since annealing period and temperature is directly related to the solvent removal, the periods and temperatures of annealing was increased step by step. In accordance with the gas permeation experiments, thermal gravimetric analyses (TGA) were performed to observe the remained amount of the solvent in the membrane. The weight loss that stems

from the solvent removal is estimated by TGA. Figure 4.3 represents the TGA graph of membranes annealed at different conditions.

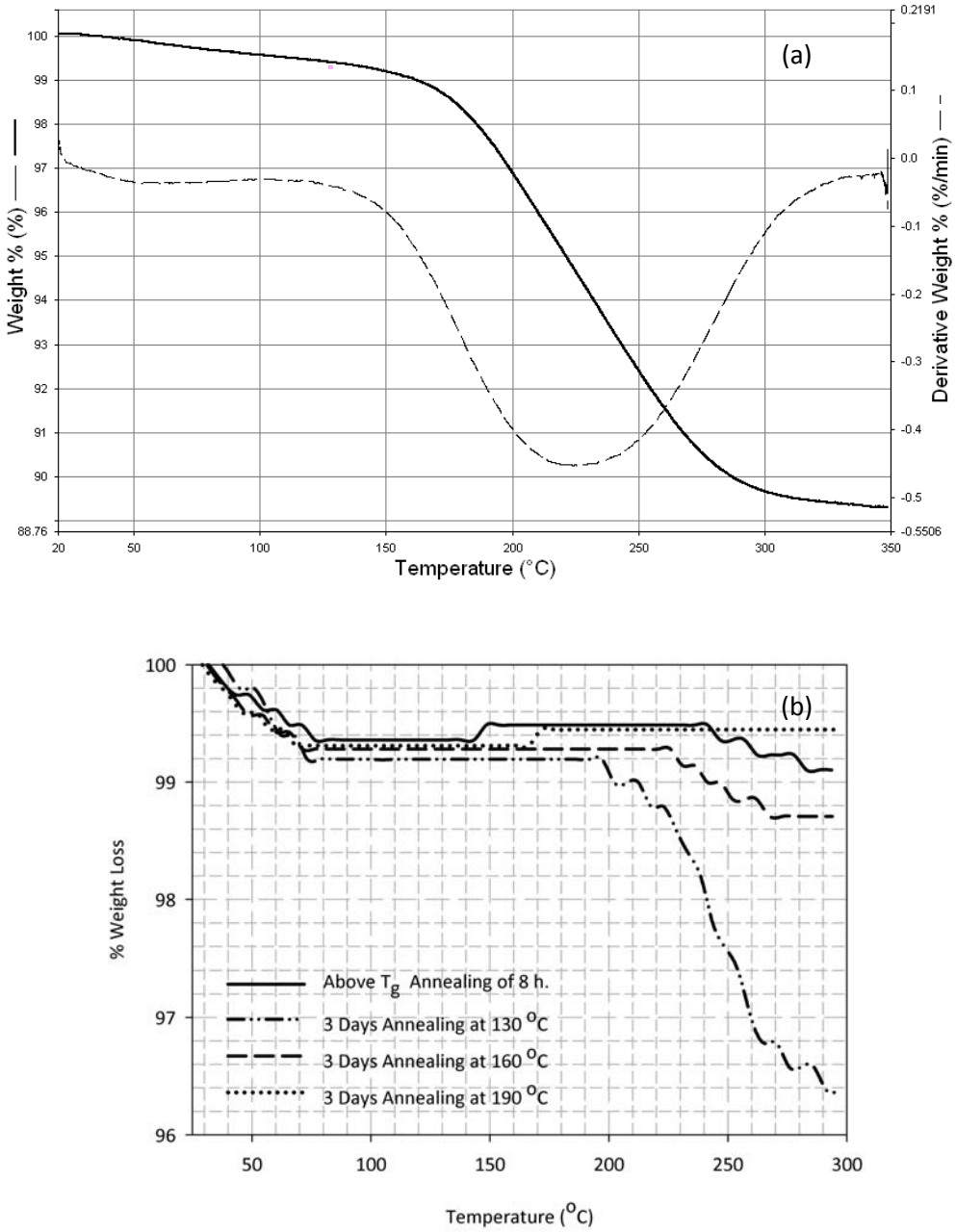

Figure 4.3 TGA graph of membranes (a) annealed at 110 °C for 24 hour (b) annealed at 130 °C, 160 °C, 190 °C for 3 days, 225 °C for 8 hours, respectively.

The weight loss is more than 10 % for the membranes annealed at 110 °C for 24 hours, and this weight loss is mainly attributed to solvent loss. Figure 4.3 further indicates that solvent loss starts nearly from 150 °C and continues till 300 °C. This temperature range includes the boiling point of the solvent used, 189 °C. Therefore, the annealing temperature was increased to 160 °C, and annealing period was extended to three days for removal of

residual solvent. The weight loss of the membranes prepared with the just mentioned annealing conditions was found to be around 2 % with TGA analysis. Annealing temperature was further increased to 190 ^{o}C, which is almost the same with the boiling point of the solvent, DMSO. The TGA analysis of these membranes revealed nearly 1 % weight loss.

The effect of residual solvent on the performance of dense membranes has been studied by several authors, often in relation to the membrane preparation conditions. Depending on many studies [60, 68-72], one can conclude that knowledge of the amount of residual solvent in as-cast membranes, of its effect on the membrane performance and of possible methods to realize its complete removal is very important. The absolute value usually depends on the membrane preparation procedure [60] and on the solvent type, but even for low-volatile solvents it generally does not exceed a few percent [68]. Since the scope of this work is not examining the effects of residual solvent, only methods for complete removal of residual solvent is searched.

Complete solvent removal by increasing the annealing period and temperature, may not be achieved [60, 72]. In addition, as speculated elsewhere [60, 68-72] specific interactions like hydrogen bonding may occur between the solvent molecules and the membrane matrix, and imprints left in the polymer chain structure formation throughout the preparation period, affecting the transport properties severely.

Annealing above the glass transition temperature of the polymer is recommended as an effective way to destroy the imprints of the structure, and erase the thermal history of the membrane [60, 70-72]. Based on our results and literature discussions, annealing conditions were decided to be changed to 225 ^{o}C and 8 hours. Table 4.5 shows the single gas permeation results of H_2 and CO_2 gases for the membrane prepared at the mentioned conditions. As Table 4.5 reveals that annealing the neat PES membranes above the glass transition temperature of PES resulted in higher single gas permeabilities and in slight increase of the H_2/CO_2 selectivity. This might be attributed to the molecular rearrangement of polymer chains by residual solvent before the membrane was annealed above T_g, favoring the motion of gas molecules.

Although annealing above the glass transition temperature is recommended to erase the thermal history, and to avoid the uncontrolled free volume modifications, there is a very few number of studies systematically investigated the effects of above or below T_g

annealing on neat polymeric membranes. Even though a clear conclusion cannot be withdrawn for the effect of annealing above T_g on the gas permeation performance of the membranes from these studies, these studies are all in agreement that this method erases thermal history of the membranes [70-72].

Alentiev et al. [70] reported that the above T_g annealed pure PEI films showed increased O_2/N_2 selectivities with a loss in O_2 permeability. However, Kostina et al. [71] from the same research group reported both reduced permeabilities and selectivities for the pure PEI membranes annealed above T_g. In addition to these two studies both employing the same polymer and same procedures, Macchione et al. [72] studied the influence of residual solvent on dense Hyflon AD60X membranes by using two solvents; Galden HT (boiling point 55 ^{0}C) and HFE 7100 (boiling point 60 ^{o}C). They reported increased permeabilities for small molecules such as H_2 whereas decreased permeabilities for bulkier molecules such as CO_2.

The considered studies imply that the effect of annealing above the glass transition temperature of the polymer on the gas permeation properties of neat polymer requires further investigation with a systematic approach, since the data presented in literature might be contradictory. However, this is not the goal of this study rather an appropriate membrane preparation procedure is a concern resulting in solvent free, reproducible stable membranes. As discussed in section 4.2.2, reproducible membranes can be produced when the annealing is held at 225 ^{o}C for 8 hours. Annealing above T_g is favored not only from the view point of removal of solvent and erasing the imprints of structure stems from the casting and evaporation steps, but also from the viewpoint of being a frequently proposed and used strategy in improving the polymer/zeolite interface morphology in mixed matrix membranes and hence improving the overall performance of MMMs. Due to these reasons, all of the membranes annealed above T_g in this study.

4.3 PES/LMWA Blend Membranes

4.3.1 Effect of Low Molecular Weight Additive Type on PES/LMWA Blend Membranes

Membranes containing the selected low molecular weight additives were prepared from membrane casting solutions including 20 w/v % PES. The LMWA concentration in the membrane casting solution was kept constant at 4 w/w %, in order to

investigate the effect of type of the additive and hence the effect of chemical structure. Homogeneous, reproducible PES membranes blended with the LMWAs; para-nitroaniline (pNA), 2-hydroxy 5-methyl aniline (HMA), 4-amino 3-nitro phenol (ANP), 2, 4, 6-Triaminopyrimidine (TAP), 2-Amino-4-hydroxy-6-methylpyrimidine (AHMP), 2-Amino-4-methylpyrimidine (AMP), 2-Methyldimidazole (Mia), and Melamine (MEL) were prepared and excluding PES/TAP, PES/MEL, all of the mentioned membranes' single gas permeabilities of H_2 and CO_2 gases were measured.

The LMWAs TAP, AHMP, and MEL dispersed unevenly and formed visible small agglomerates throughout the membrane matrix probably due to the limited solubility of them in DMSO and their limited miscibility with PES. These possible reasons can be accompanied with the possibility of exceeding the precipitation limit of these three LMWAs during the solvent evaporation from the pre-mature unsolidified membrane. Figure 4.4 shows the inhomogeneous morphology of PES/AHMP membrane from both the top and cross section view. The island-like agglomerations of AHMP can be clearly seen in SEM images shown in Figure 4.4. In spite of the non-homogeneous structure of these membranes, the single gas permeability measurements were performed for PES/AHMP membranes. As expected, these membranes were not reproducible and reliable. The results of PES/AHMP membranes are tabulated in Appendix B. Based on the non-reliable results of non-homogeneous PES/AHMP membranes, the single gas permeability experiments of PES/TAP and PES/MEL membranes were not performed, even though these membranes were prepared.

Permeability and selectivity results of PES membranes casted with pNA, HMA, ANP, Mia, and AMP are reported in Table 4.6. Their reproducibility results were given in Appendix B. During the single gas permeation experiments performed for screening the LMWA type effect, only H_2 and CO_2 gases were employed. Since CH_4 experiments are very long compared to H_2 and CO_2, performed in 3-7 days depending on the membrane formulation, CH_4 gas permeation experiments were not done. The operating conditions of the permeation were 3.7 bar of feed side pressure and ~0.9 bar of permeate initial pressure was used for the same reason, since these conditions reveal faster permeations compared to 2 bar feed side pressure and permeate initially at vacuum conditions.

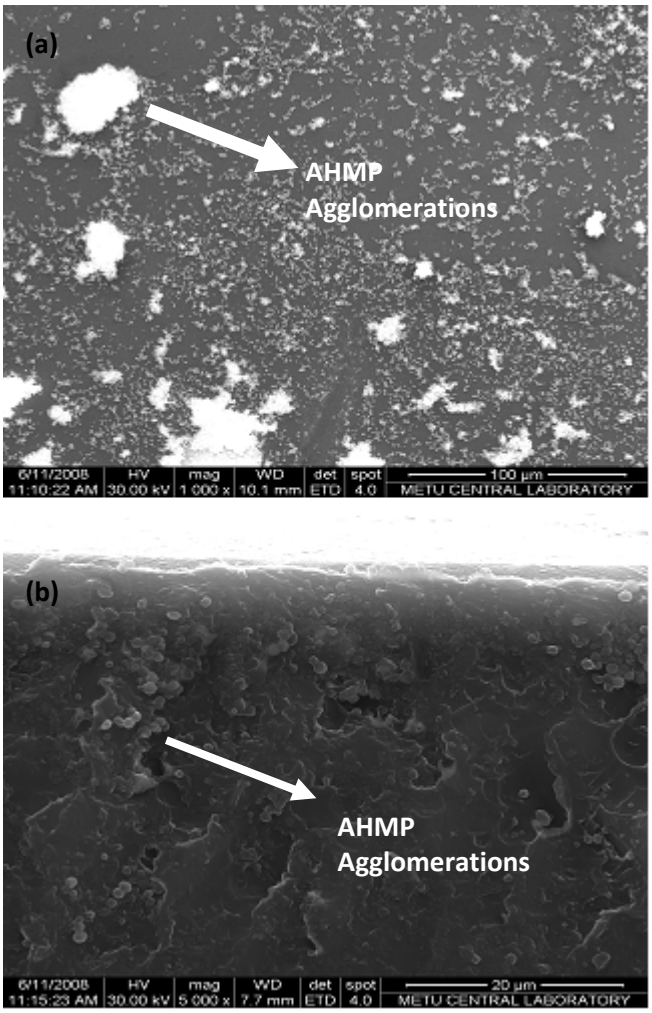

Figure 4.4 SEM images of PES/AHMP, indicating the AHMP agglomerations (a) Top view (b) Cross-sectional (AHMP/PES= 4 w/w %, PES/DMSO= 20 w/v %)

Table 4.6 Permeability and selectivity results* for PES/LMWA membranes (LMWA /PES in the casting solution= 4 w/w %)

Membrane	Additive	Permeability (Barrer)		Selectivity
		H_2	CO_2	H_2/CO_2
Pure PES	NA	14.28	5.32	2.68
PES / pNA	pNA	10.42	2.71	3.85
PES / HMA	HMA	11.01	2.82	3.91
PES / ANP	ANP	11.12	2.76	4.02
PES / AMP	AMP	13.85	4.34	3.19
PES / Mia	Mia	13.65	4.53	3.02

*Results were obtained at 3.7 bar of feed side pressure and ~0.9 bar of permeate initial pressure.

The effect of blending of additives on neat polymer membranes were not only examined based on gas permeation properties but also investigated using change in the glass transition temperatures of the polymer/additive membranes. DSC analyses of the membranes, prepared by blending PES with different type of low molecular weight additives, were performed and the glass transition temperatures of them were determined. Table 4.7 shows the effect of the LMWAs used in this study including pNA, HMA, ANP, AMP, and Mia on the glass transition temperature of pure PES membranes. The DSC thermograms of these membranes are given in Appendix C.

Table 4.7 T_g of PES membranes prepared with different LMWAs (LMWA /PES = 4 w/w %)

Membrane	Additive	T_g
Pure PES	NA	220
PES / pNA	pNA	206
PES / HMA	HMA	206
PES / ANP	ANP	196
PES / AMP	AMP	213
PES / Mia	Mia	210

Although chemical structures of low molecular weight additives were different, effect of these LMWAs on the gas permeation performance and glass transition temperatures of pure PES membranes were similar. All LMWAs decreased the H_2 and CO_2 permeabilities and increased the H_2/CO_2 ideal selectivity; also they all decreased the glass transition temperatures of the membranes. The most significant decrease in permeability and most remarkable T_g reduction was seen in PES/pNA, PES/HMA, and PES/ANP blend membranes. Single gas permeabilities and glass transition temperatures of the membranes decreased in the order of pure PES > AMP ≈ Mia > HMA ≈ ANP ≈pNA.

Apart from the order of impact of different LMWAs on gas permeation properties of PES membranes, one another remark may be on the effect of these LMWAs on the permeability of different gases. As Table 4.6 indicates, H_2 molecules were less affected from the structural changes in membrane owing to the small size of them. The order of the LMWAs for the reduction of CO_2 permeability was the same with the order encountered for

H_2. The reduction in CO_2 permeability is greater compared to the reduction in H_2 permeabilities regardless of the additive type which in turn led to increase in H_2/CO_2 selectivities in the order of pure PES < AMP ≈ Mia < HMA ≈ ANP ≈pNA. The kinetic diameter of the employed gases in this study is tabulated in Table 4.8.

Table 4.8 Kinetic diameters of studied gases [2]

Gas	H_2	CO_2	CH_4
Kinetic Diameter (nm)	0.289	0.33	0.38

The decrease in permeabilities with increase in selectivities accompanied by a modest reduction in glass transition temperature is a behavior usually encountered with the incorporation of additives to neat polymer membrane formulation [20, 21, 29-34, 36]. These researchers were well agreed on that the additives were affecting the free volume of the polymer and acting as anti-plasticizers. Antiplasticization is defined as increasing stiffening of polymers with the addition of a low molecular weight compound due to reduced rates of segmental motions in the polymer chain and hence reduced the free volume in the polymer [29-31].

Anti-plasticization effect of additives was studied with different polymer/additive systems by many researchers [30-34, 36]. Ruiz-Trevino and Paul [32] observed that the extent of shift from the T_g of neat polymers is believed to depend on the T_g of the pure additive, that is larger shifts were observed for additives having lower glass transition temperatures. The decrease in glass transition temperature was explained by the diluent effect of additives. Similarly, Larocca and Pessan [33] reported smaller shifts for membranes prepared with additives having higher glass transition temperatures. These researchers suggested that it is the degree of interaction between LMWA and polymer that determines the extent of the shift from the T_g of pure polymer membrane. Based on these literature discussions and our results tabulated in Tables 4.6 and 4.7, we may claim that the LMWAs used in this study acted as anti-plasticizers.

Three of the low molecular weight additives used in this study, pNA, HMA, and ANP were also used by Şen et al. [36] in polycarbonate based membranes. Their results showed that all of the LMWAs or so called compatibilizers, acted as anti-plasticizers decreasing permeability and glass transition temperature of the neat polycarbonate

membrane and increasing the selectivities. They reported that the most effective LMWA which provided the highest selectivity and lowest permeability in PC membranes was pNA, and the least effective one was cathecol. However the results presented in Table 4.6 and Table 4.7 shows that pNA, HMA, and ANP have very similar effects for gas permeation properties of membranes based on polyethersulfone polymer.

Based on the results discussed, HMA, pNA, and ANP are the most effective anti-plasticizers. The incorporation of additives AMP and Mia resulted in smaller decrease in permeabilities compared to the PES/pNA, PES/HMA, PES/ANP membranes, indicating lower antiplasticization effect of AMP, and Mia. Similarly, one can observe from Table 4.7 that the LMWA type is also affecting the extent of the shift from the T_g of pure PES membrane. HMA, pNA, and ANP resulted in greater extents of shifts from T_g of neat polymer compared to AMP and Mia, which can be explained with the larger interaction possibility of HMA, pNA, and ANP with PES. As the aforementioned studies [30-34, 36] reveal that the larger extents of shifts the larger degree of interaction between the polymer and LMWA. This order in affecting the gas permeation properties and T_g of the PES membranes should be related to the structural properties of these additives. These results could be expected since both AMP and Mia have one functional group, and multifunctionality of the LMWA is anticipated in modifying the polymer chain structure by physical incorporation of additives [20, 36]. The possession of amine, nitro, and hydroxyl groups are favorable in LMWAs since these functional groups are directive and activating groups extending the hydrogen bonding capability of LMWAs with polymer [36]. The most effective LMWAs; pNA, HMA and ANP possess amine, nitro, and hydroxyl functional groups. Nevertheless, no certain conclusion can be drawn for the importance of ortho, para, meta positions of these functional groups.

Solubility parameter based approach is a frequently used method not only in selection of membrane materials but also in estimation of the level of interaction between the polymer and the additives [34, 73, 74]. This approach was also used to evaluate the effect of LMWA type. However three components Hansen solubility parameters for most of the additives could not be found, hence a group contribution method, Hoy's method, was used to calculate these parameters. Three component solubility parameters of the LMWAs, PES, and the differences in solubility parameters of the LMWAs with respect to PES are represented in Table 4.9. Only the PES and pNA parameters were taken from tabulated data by Hansen [57], since their solubility parameters were incalculable due to missing

fragment values of the aromatic nitro functional group (-NO_2) and the sulfone group (-SO_2) for this method. The parameters for ANP are not tabulated since they could be neither found from literature nor calculated since it includes nitro group. The details of this method and the calculation steps are reported in Appendix D.

The difference in solubility parameters of the additives with respect to PES gives an estimation on the order of additives possibly interact with PES. Small differences in the values of δ parameter (< or ≈ 5 J/cm^3) indicate high interaction between polymer and additive (solubility). As expected, differences in solubility parameters of AHMP, TAP, and MEL are highly larger than 5 J/cm^3. The membranes including these additives were not homogeneous as mentioned, this observation agrees very well with situation encountered by Vidotti and Pessan [34]. They investigated the effects of two additives, HFBPA and PNA, on properties of PES films. The difference between solubility parameters (Δδ) was found to be 4.20 J/cm^3 for PES–PNA membranes, 14.77 J/cm^3 for PES/HFBPA membranes; they concluded that these values indicate a higher interaction between PES and PNA additive than PES and HFBPA. They observed phase separation during the preparation of membranes including HFBPA having a solubility difference of 14.77 J/cm^3. In addition, the gas permeation experiments, DSC analysis together with solubility parameter approach reveal that AMP and Mia are the least effective additives.

Table 4.9 Solubility Parameters Values of Polyethersulfone and Additives

	δ_t (J/cm^3)	δ_p (J/cm^3)	δ_h (J/cm^3)	δ_d (J/cm^3)	Δδ (J/cm^3)
PES*	24.20	10.80	9.20	19.60	-
HMA	22.70	14.57	7.63	15.65	5.69
pNA*	30.09	18.7	10.3	21.2	8.14
mia	24.56	16.57	12.64	12.99	9.42
AMP	25.25	17.73	13.50	11.87	11.24
AHMP	26.48	19.29	13.57	12.02	12.19
TAP	28.70	20.53	17.51	9.78	16.13
MEL	30.30	21.84	19.29	8.32	18.73

* Solubility parameters of PES and pNA were taken from the reference [57]

Eight different LMWAs were incorporated to pure PES membranes; incorporation of five of them resulted in homogeneous blends of PES/additive membranes. Despite their

different chemical structure, they all anti-plasticized the structure which caused stiffening in membrane and leading to lower permeabilities and higher selectivity with respect to pure PES membrane. The order of impact of these additives was found similar in all analyses including single gas permeation tests and DSC analysis; pNA, HMA, and ANP were the most effective anti-plasticizers. For the parametric study of effect of LMWA loading on PES/LMWA membranes, one of those three LMWAs would be selected.

PES/pNA, PES/HMA, PES/ANP membranes were all homogeneous in physical appearance, but physical properties, even like color is important at the stage of selection one of them for the loading study. HMA turns the color of PES membrane to brownish yellow, pNA to amber, ANP to blackish red at 4 wt/wt % LMWA/PES ratio in the casting solution. These observations enabled the elimination of ANP, since ANP might not be an appropriate additive for the loading study. At higher loadings like 25 wt/wt % LMWA/PES ratio, the homogeneity of PES/ANP could not be observed due to its dark color.

Gas permeation experiments, DSC analysis, solubility parameter approach together with other concerns such as experimentally found solubilities in DMSO, physical properties even like color, made HMA a candidate to investigate the effect of additive concentration on PES/HMA membranes.

4.3.2 Effect of Low Molecular Weight Additive Loading on PES/LMWA Blend Membranes

2-hydroxy 5-methyl aniline (HMA) incorporated PES membranes were prepared keeping the PES concentration in the casting solution constant at 20 w/v %. All of the PES/HMA membranes prepared were homogeneous and reproducible. Single gas permeability experiments of these membranes were performed with H_2, CO_2, CH_4 gases at constant 35 ^{o}C with initially vacuum at the permeate side and a feed pressure of 2 bar.

In this study, membranes were prepared from membrane casting solutions at the HMA/PES ratios of 2, 4, 7, 10, 15, and 25 w/w %. The HMA content of the membranes were increased to high loadings like 15 and 25 w/w % determine the solubility limit of HMA in PES. Şen et al [36] observed a solubility limit of pNA in polycarbonate at 10 w/w %. Their SEM images of pNA/PC membranes at this pNA concentration reveal the non-homogeneity of these membranes. They also observed sharp decrease in CO_2/N_2 and O_2/N_2 selectivities at 10 w/w % of pNA. They explained this behavior with the limited solubility of pNA in DCM

and its limited miscibility with PC. But this case was not seen even at 25 w/w % HMA loading. In our case, we obtained homogeneous, workable and reproducible membranes with decreasing permeabilities and increasing selectivities with the increasing concentration of HMA even at 25 w/w %. These results imply that HMA is an appropriate LMWA to observe the effect of concentration in PES-DMSO system.

Figures 4.5 to 4.7 show the change in permeability with the change in HMA/PES ratio in the membrane casting solution for H_2, CO_2, and CH_4 gases respectively. The results are also tabulated in Appendix B. The permeabilities of all gases decreased with increasing HMA loading. The decreasing permeabilities of all gases imply that HMA affected the chain packing of PES and reduced the free volume. As these figures indicate, the reduction of permeabilities was sharpest with the addition of 2 w/w % of HMA. Then, between 2-10 w/w % concentration range of HMA in the casting solution, the decrease in permeabilities of all gases, especially CO_2, CH_4, are nearly linear and still strong. After 10 w/w % of HMA, permeabilities decreased much slowly with increasing HMA amount.

Effect of additives and additive concentrations in polymeric membranes on gas permeation properties was mainly observed with compounds having high molar mass [29-34] in literature except Yong et al. [20] and Şen et al. [36]. Şen et al. [36] used para nitroaniline (pNA) to anti-plasticize the polycarbonate (PC) matrix. They observed the effect of pNA concentration in the range of 0.5-10 w/w % in PC membrane. They reported that pNA affected the permeation characteristics of PC membranes sharply up to 2 w/w % of pNA. But after this concentration, the rate of decrease in permeabilities and increase in selectivities was slower with increasing pNA concentration. These observations agree well with the results represented in Figures 4.5-4.7.

Also in this study low molecular weight additives were employed, and these additives were effective at very low concentrations. Permeability decrease with the addition of HMA can be explained by anti-plasticization effect stiffening the membrane structure since it is known that anti-plasticizers decrease the gas permeabilities through glassy polymers [29-31].

The impact of increasing HMA/PES ratio in the membrane casting solution on each gas was different; the largest reduction in permeability was observed for CH_4, the

smallest was on H_2. The decreasing order of permeabilities parallel to increasing order of kinetic diameter of gases implies that HMA enhanced the size selectivity of the membranes.

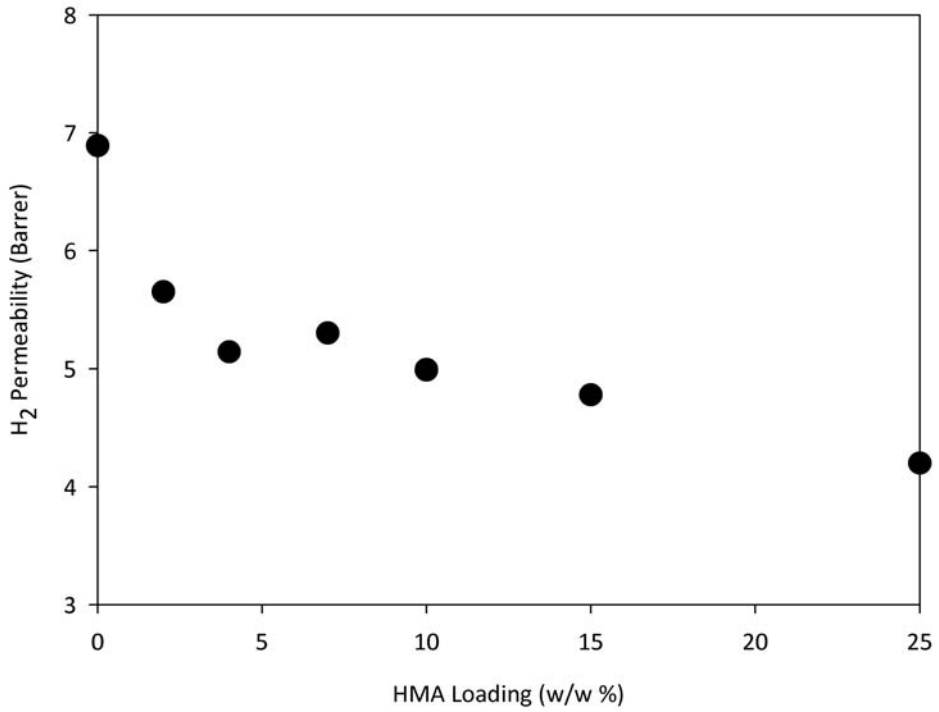

Figure 4.5 Reduction in H_2 permeability with increasing HMA/PES ratio in the membrane casting solution.

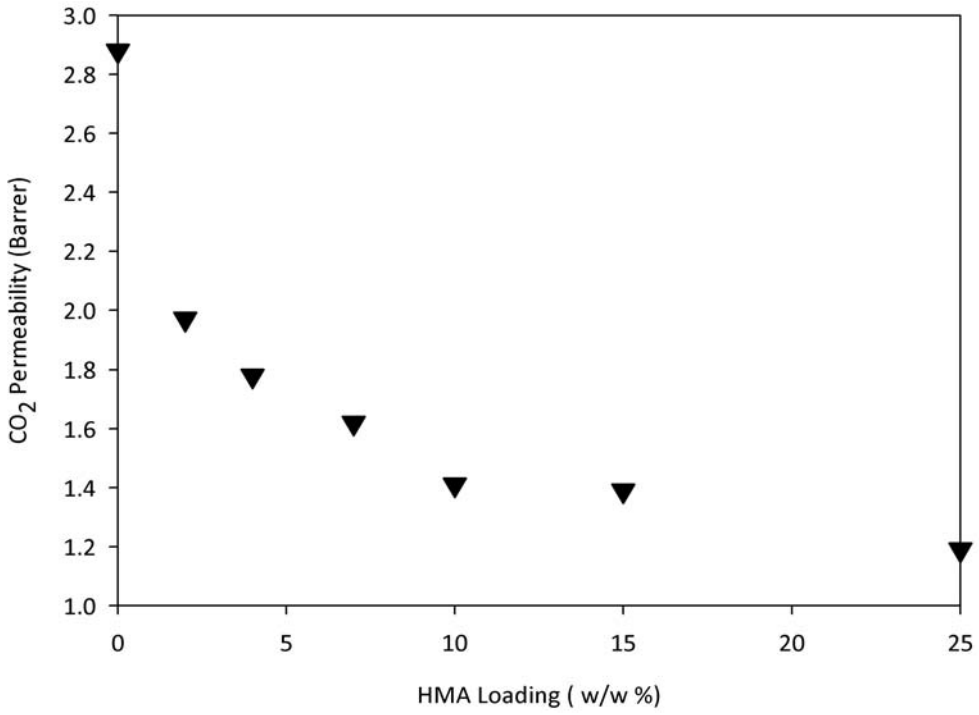

Figure 4.6 Reduction in CO_2 permeability with increasing HMA/PES ratio in the membrane casting solution.

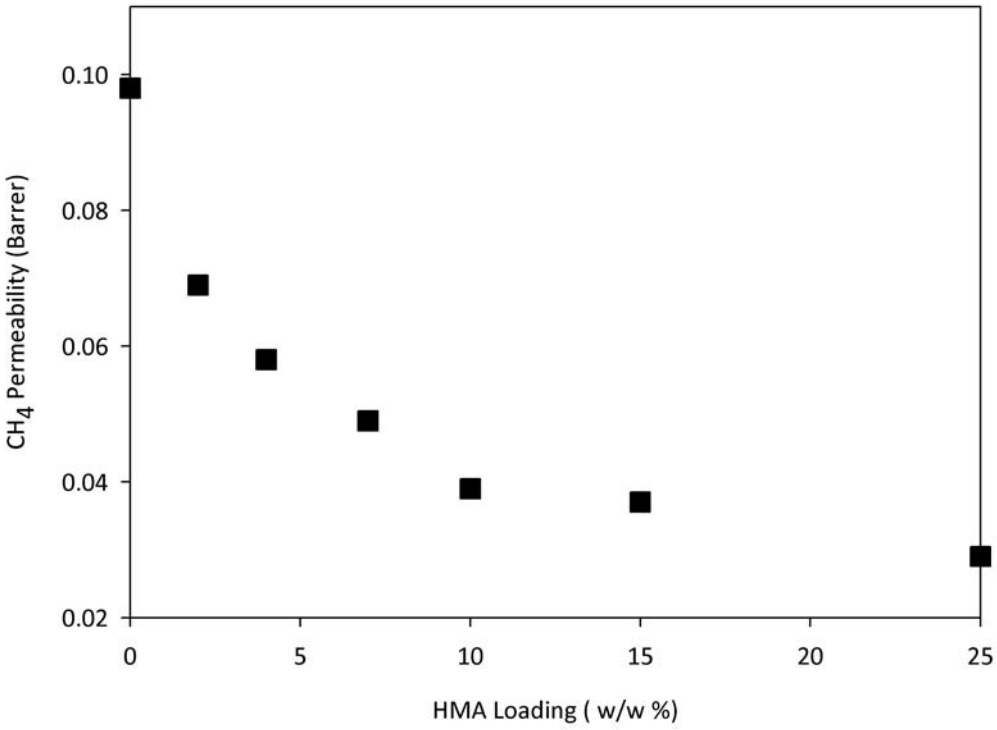

Figure 4.7 Reduction in CH_4 permeability with increasing HMA/PES ratio in the membrane casting solution.

When the ideal gas selectivities were calculated for H_2/CO_2, CO_2/CH_4, and H_2/CH_4, which are industrially important gas pairs [2-5], considerable improvements were observed with increasing concentration of HMA in the membrane casting solution. Figures 4.8-4.10 show the selectivities of H_2/CO_2, CO_2/CH_4, and H_2/CH_4 with increasing HMA/PES ratio in the membrane casting solution. The results are also tabulated in Appendix B.

The pure PES H_2/CH_4 ideal selectivity of 70.34 was increased to 127.95 with the addition of 10 w/w % of HMA. Similarly, CO_2/CH_4 gas pair selectivity increased from 29.34 to 36.15, and H_2/CO_2 gas pair selectivity was increased from 2.40 to 3.54. As stated previously, the decreasing order of permeabilities are parallel to increasing order of kinetic diameter of gases, and hence this behavior resulted in increase in selectivities especially for gas pairs having large differences in their kinetic diameter. The percent increases in selectivities for PES/HMA membranes with 25 w/w % HMA content are found to be approximately 103, 48, and 38 % for H_2/CH_4, H_2/CO_2, and CO_2/CH_4 gas pairs respectively compared to neat PES membranes.

Based on the results represented in Figures 4.8-4.10, incorporation of HMA at increasing concentrations enhanced the size discrimination of the permeating gases. The

effect of HMA on gas pairs having larger differences between the kinetic diameters of the gases such as; H_2/CH_4, and H_2/CO_2 are more remarkable compared to the improvement for CO_2/CH_4 gas pair. Hence, it may claim that addition of HMA mainly enhanced the diffusion selectivity of PES membranes. This also verifies that antiplasticizing (i.e. chain stiffening and free volume reduction) effect of HMA.

The addition of different type of LMWAs and increasing the concentration of HMA pushed the performance of pure PES membrane up only to a small extent, accompanied by permeability loss. However, the enhancement in permeability is also critical since both high productive and selective membranes are attractive industrially. As discussed in the earlier chapters, polymeric gas separation membranes suffer from a trade-off between their productivity, or permeability, and separation efficiency, or selectivity [4, 5]. Similarly, PES/LMWA membranes produced in this study encountered this trade-off.

After a substantial research effort has been directed to overcome the limit imposed by the upper bound by modifying the pure polymeric membranes, the researchers leaded their way to the concept of mixed matrix membranes having the potential of revealing both high permeability and selectivity and hence the potential of overcoming the trade-off limit [11].

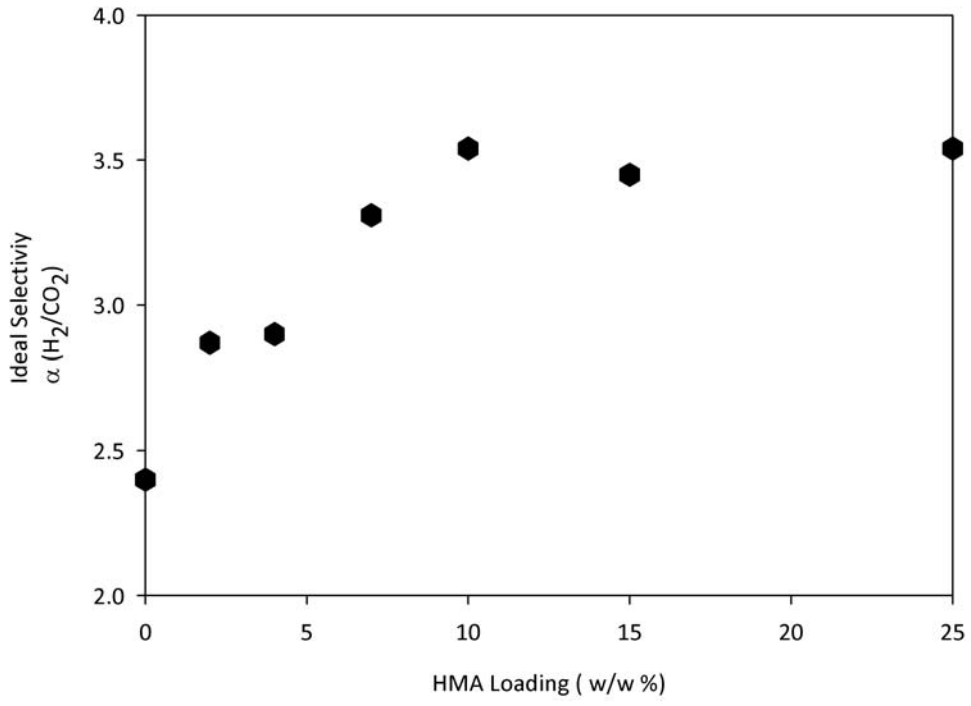

Figure 4.8 Effect of increasing HMA/PES ratio in the casting membrane solution on H_2/CO_2 ideal selectivity

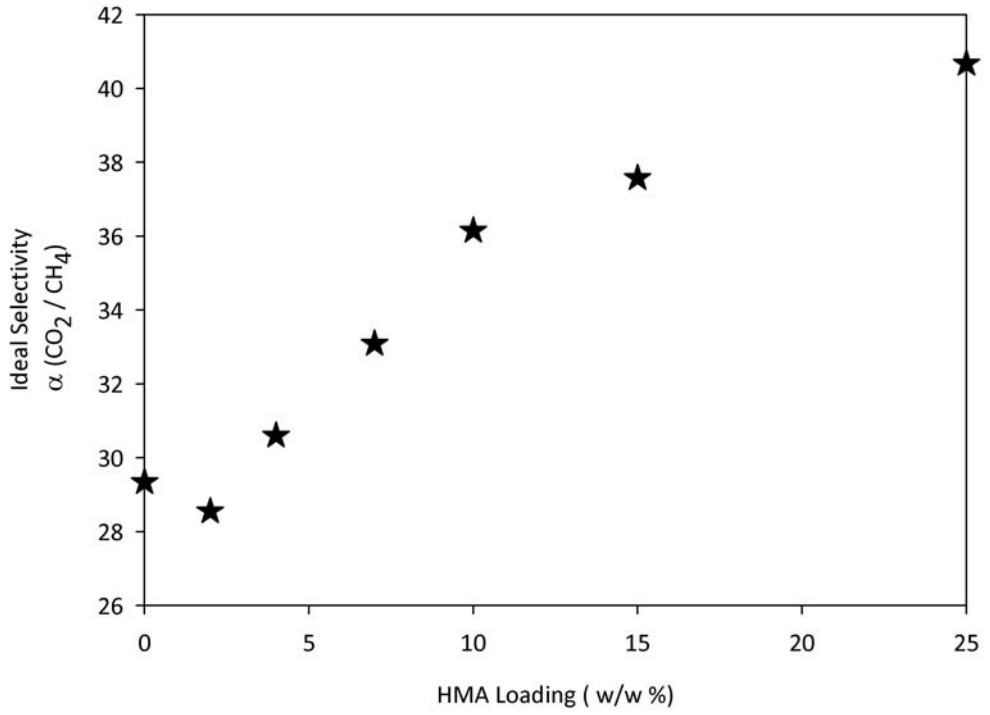

Figure 4.9 Effect of increasing HMA/PES ratio in the casting membrane solution on CO_2/CH_4 ideal selectivity

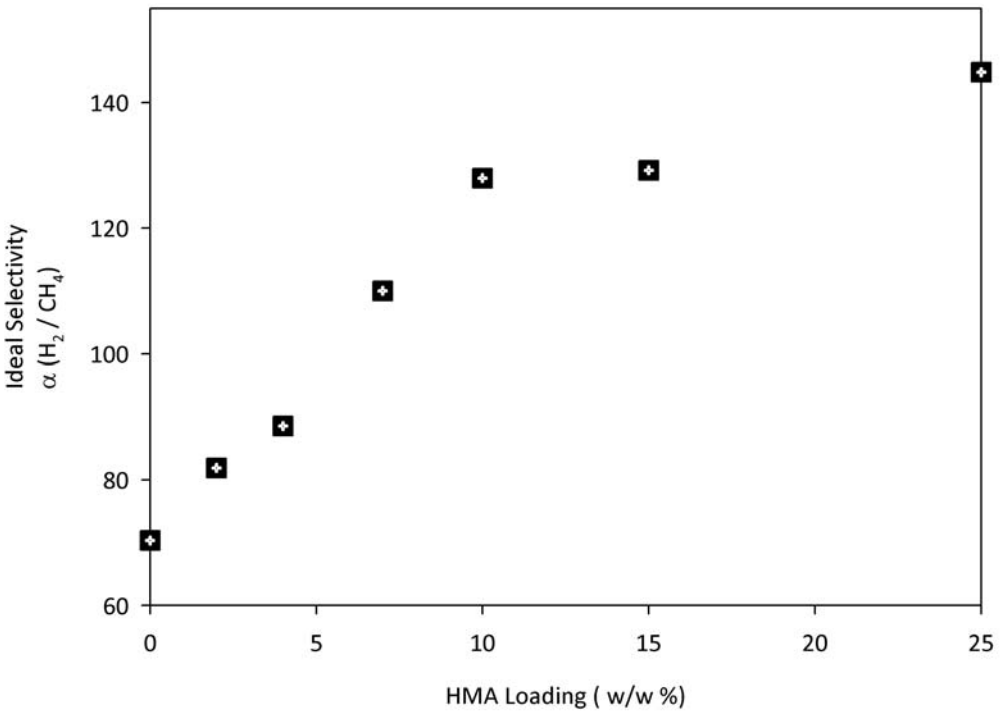

Figure 4.10 Effect of increasing HMA/PES ratio in the casting membrane solution on H_2/CH_4 ideal selectivity

Owing to these considerations, in the rest of this study, we aim to prepare SAPO-34 filled polyethersulfone mixed matrix membranes, and observe the effects of several preparation parameters including the incorporation of low molecular weight additive HMA.

4.4 Development of SAPO-34 Filled Mixed Matrix Membranes

4.4.1 PES/SAPO-34 Mixed Matrix Membranes

SAPO-34 is incorporated to the neat PES membrane as the inorganic phase. Although the effect of zeolite loading is reported as strongly affecting the structure and properties of mixed matrix membranes [21, 41], the SAPO-34 loading was kept constant at 20 w/w % in this study. Low zeolite loading (< 10 w/w %) may not obviously affect membrane properties, while at high zeolite loadings (> 30 w/w %) the membranes may not be mechanically strong enough. The single gas permeabilities and ideal selectivities of PES/SAPO-34 MMMs were presented in Table 4.10.

Table 4.10 Permeabilities and ideal selectivities of PES/SAPO-34 mixed matrix membranes including 20 w/w % SAPO-34.

SAPO-34 Loading (w/w %)	Permeability (Barrer)			Ideal Selectivity		
	H_2	CO_2	CH_4	$\alpha(H_2/CO_2)$	$\alpha(CO_2/CH_4)$	$\alpha(H_2/CH_4)$
0	6.90	2.88	0.098	2.40	29.39	71.31
20	12.57	5.12	0.206	2.45	24.88	61.02

Incorporation of SAPO-34 zeolite improved the performance of membranes. PES/SAPO-34 membranes had permeabilities nearly 2 times higher than neat PES membranes with slight losses in selectivities. As Table 4.10 indicates, the CH_4 permeability was enhanced 2.1 times whereas the H_2 and CO_2 permeabilities were enhanced 1.8 and 1.77 times with respect to neat PES membranes. Enhancement of permeabilities with the addition of SAPO-34 to membrane matrix accompanied with a slight increase in H_2/CO_2 selectivity, and nearly 15 % loss in CO_2/CH_4 and H_2/CH_4 selectivities. The trend of increase in permeabilities with decrease in selectivities was reported also for various polymer/ zeolite systems, many researchers related this behavior to the polymer zeolite incompatibility, creating interfacial voids around zeolite [20, 41, 43].

These results suggest that the polymeric membrane structure changes after SAPO-34 zeolite particles were embedded. The results may be explained with different mechanistic speculations. One reason for the increased permeabilities might be the porous structure of SAPO-34 having a pore size of 0.38 nm which is larger than the kinetic diameter of H_2 and CO_2, and being same with that of CH_4.

Incorporation of SAPO-34 particles might form microcavities resulting in a loosened structure of PES/SAPO-34 membranes. This could be due to partial incompatibility of polymer chains and zeolite particles. The interfacial voids around the zeolites may connect and provide alternate path for gas molecules, and this may lead to increases in the permeation rates of gas molecules.

As stated previously, annealing the membranes above the glass transition temperature is one of the proposed and used strategies for better polymer-sieve contact [12, 13, 19, 42, 43]. Although PES/SAPO-34 membranes were annealed above the glass transition temperature of PES, prepared PES/SAPO-34 membranes revealed increased permeabilities with slight decrease in selectivities compared to neat PES membranes. This observation suggested further modification such as the incorporation of low molecular weight additives to above T_g annealed PES/SAPO-34 membranes could lead to elimination of formation of voids and consequently contributed to a better membrane performance.

4.4.2 PES/HMA/SAPO-34 Mixed Matrix Membranes

PES/HMA/SAPO-34 membranes were prepared keeping the PES concentration at 20 w/v %, and SAPO-34 concentration at 20 w/w %. PES/HMA/SAPO-34 membranes were prepared from membrane casting solutions at the HMA/PES ratios of 4, 7, and 10 wt/wt %. The permeabilities of H_2, CO_2, and CH_4 gases through PES / SAPO-34 / HMA mixed matrix membranes are presented in Table 4.11. Likewise to the effect of HMA on PES/HMA membranes, HMA also stiffens the structure of PES/SAPO-34/HMA membranes. Similarly, the decreasing order of permeabilities with the addition of increasing concentrations of HMA is parallel to increasing order of kinetic diameter of gases.

Similar to PES/HMA binary membranes, increasing concentrations of HMA in the mixed matrix membrane solution HMA resulted in decreasing H_2, CO_2, and CH_4

permeabilities, while H_2 and CO_2 permeabilities were still above those of the virgin PES membranes. Figure 4.11 represents the effect of HMA loading on the permeabilities of H_2, CO_2, and CH_4 gases for PES/HMA/SAPO-34 mixed matrix membranes.

Table 4.11 Single gas permeabilities through PES/SAPO-34/HMA MMMs

PES / SAPO-34 (y %) / HMA (x %)		Permeability (Barrer)		
x	y	H_2	CO_2	CH_4
0	0	6.90	2.88	0.098
0	20	12.57	5.12	0.206
4	20	11.24	3.58	0.121
7	20	9.35	2.38	0.074
10	20	7.06	1.53	0.041

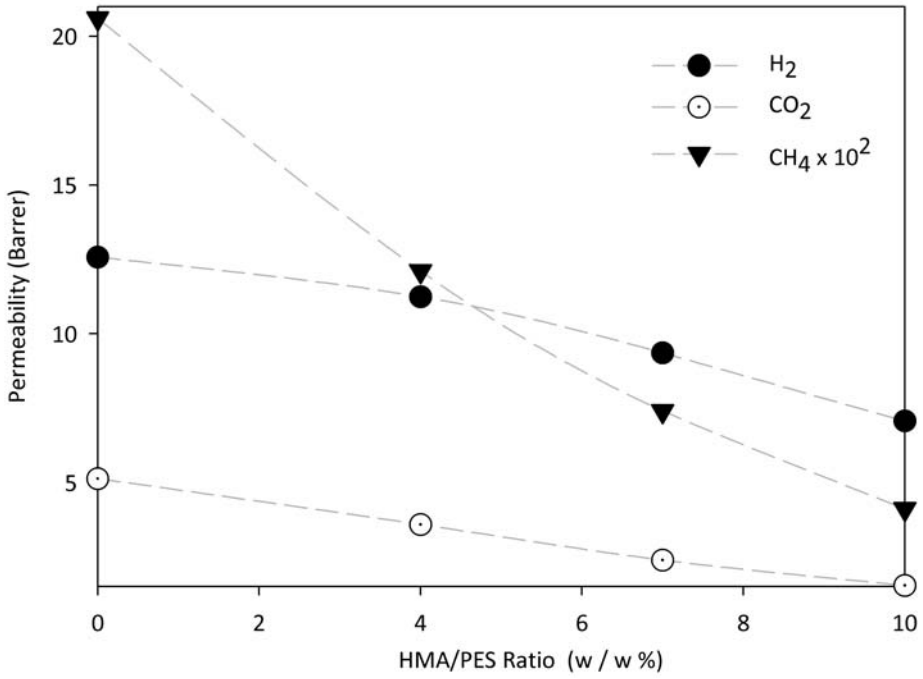

Figure 4.11 Effect of HMA loading on the gas permeabilities of H_2, CO_2, and CH_4. The permeability values of CH_4 are expanded by 100.

When the ideal gas selectivities were calculated for H_2/CO_2, CO_2/CH_4, and H_2/CH_4, which are industrially important gas pairs [2-5], considerable improvements were observed with increasing concentration of HMA in the membrane casting solution of PES/HMA/SAPO-34 membranes. Table 4.12 shows the selectivities of H_2/CO_2, CO_2/CH_4, and H_2/CH_4 with increasing HMA/PES ratio in the membrane casting solution.

Table 4.12 Ideal Selectivity values of PES/SAPO-34/HMA MMMs

(PES / SAPO-34 (y %) / HMA (x %)		Ideal Selectivity		
x	y	H_2/CO_2	CO_2/CH_4	H_2/CH_4
0	0	2.40	29.39	71.31
0	20	2.45	24.88	61.02
4	20	3.15	29.83	93.71
7	20	3.93	33.07	127.53
10	20	4.64	37.44	175.79

The results represented in Tables 4.11-12 indicate that both permeabilities and ideal selectivities of PES/SAPO-34/HMA were improved for all gas pairs when compared to neat PES membranes, which shows the success of our membrane development strategy. At all HMA/PES ratios, H_2 permeability of PES/HMA/SAPO-34 membranes was improved. CO_2 and CH_4 permeabilities of HMA incorporated MMM were increased at 4 wt/wt % HMA/PES ratio, with a slight loss the other HMA loadings. The percent increases in selectivities for PES/HMA/SAPO-34 membranes with 10 wt/wt % HMA content are found to be approximately 146, 93, and 27 % for H_2/CH_4, H_2/CO_2, and CO_2/CH_4 gas pairs respectively compared to neat PES membranes. Incorporation of HMA increased the selectivities of gas pairs having larger size difference between the gases. Likewise to HMA effect on binary PES/HMA membranes, HMA enhanced the diffusion selectivity of the ternary PES/HMA/SAPO-34 membranes.

Figure 4.12 (a) and (b) represent the similar trends for H_2 permeability and H_2/CH_4 ideal selectivity values for PES/HMA and PES/SAPO-34/HMA membranes with increasing HMA/PES ratio in the membrane casting solutions. The permeability and selectivity values of pure PES and PES/SAPO-34 membranes are also given in Figure 4.12 for comparison purposes. As Figure 4.12 (a) represents, for the PES/SAPO-34/ HMA membranes at all HMA/ratios, the reduction in permeabilities for PES / HMA membranes were recovered for

the H_2 gas with the addition of SAPO-34 to HMA containing PES membranes, indicating the importance of combined usage LMWA and zeolite. As Figure 4.12 (b) indicates, the H_2/CH_4 selectivity of PES/SAPO-34 (20%)/HMA (10 %) membrane is 175.79 which is 2.5 times higher than that of pure PES membrane and 2.9 times higher that of PES/SAPO-34 (20%) membrane with high enough permeabilities.

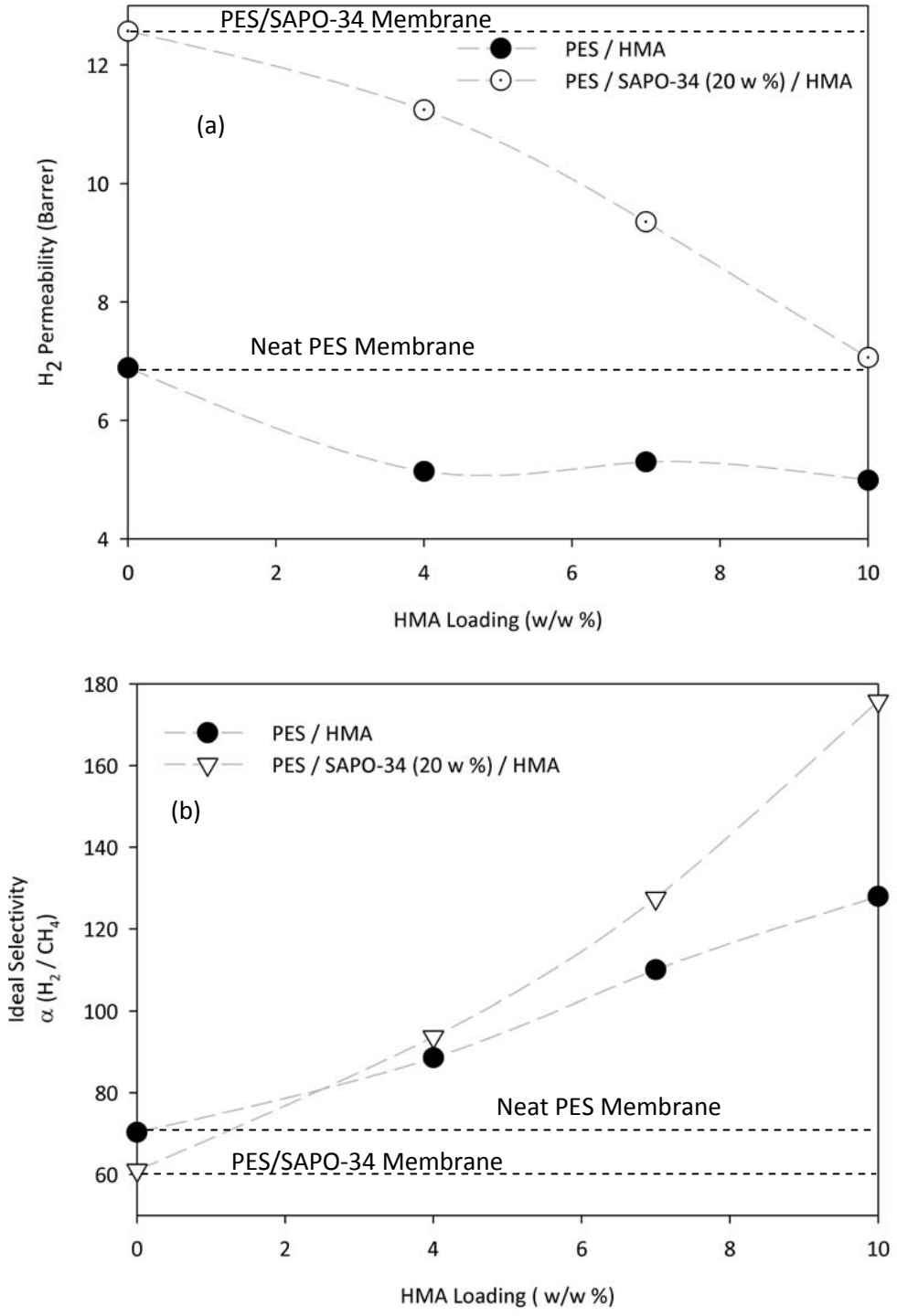

Figure 4.12 Comparison of increasing HMA/PES ratio (w/w %) on (a) H_2 permeability (b) H_2/CH_4 ideal selectivity between PES/HMA and PES/SAPO-34 (20%)/HMA membranes

Figures 4.13-4.14 show the increasing H_2/CO_2 and CO_2/CH_4 ideal selectivities with increasing HMA/PES ratio in the membrane solution for PES/SAPO-34/HMA and PES/HMA membranes, respectively. The selectivity values of pure PES and PES/SAPO-34 membranes are also indicated in Figures 4.13-4.14.

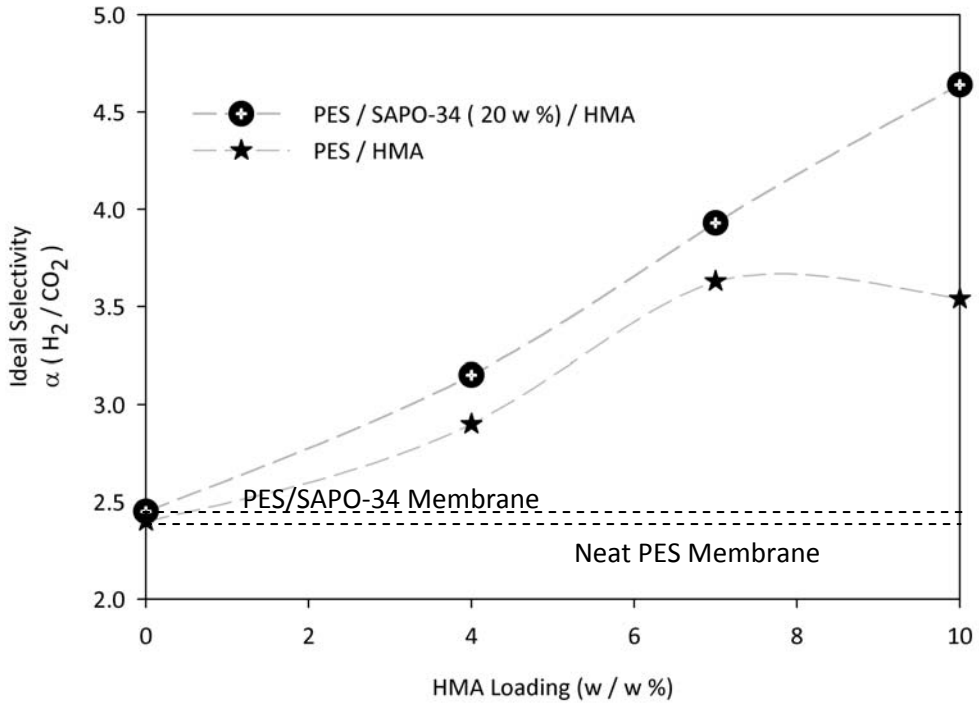

Figure 4.13 Effect of increasing HMA/PES ratio (w/w %) on H_2/CO_2 ideal selectivity for PES/SAPO-34 (20%)/HMA and PES/HMA membranes

As Figures 4.13 and 4.14 indicate, similar trends for H_2/CO_2 and CO_2/CH_4 ideal selectivity values for PES/HMA and PES/SAPO-34/HMA membranes with increasing HMA/PES ratio in the membrane casting solutions were observed, respectively. As can be seen in Figure 4.13, the H_2/CO_2 selectivity of PES/SAPO-34 (20 wt %)/ HMA (10 w/w %) membrane is 4.64 which is nearly 2 times greater than pure PES and PES/SAPO-34 (20 wt %) membranes, respectively. Approximately 30 % enhancement in H_2/CO_2 selectivity for 10 wt/wt % HMA containing ternary membrane is achieved compared to PES/HMA (10 wt/wt %) binary membrane.

Similar to H_2/CH_4 and H_2/CO_2 gas pairs, for CO_2/CH_4 gas pair also, improvement in gas permeation properties of mixed matrix membranes with the addition of HMA was observed. As can be seen in Figure 4.14, the CO_2/CH_4 is 37.44 which is 1.3 times and 1.5 times greater than pure PES and PES/SAPO-34 (20 wt %) membranes, respectively.

However, unlike to H_2/CH_4 and H_2/CO_2 gas pairs, the performance of PES/HMA binary membranes and PES/SAPO-34 (20 wt %) /HMA ternary membranes remained more or less the same for CO_2/CH_4 gas pair.

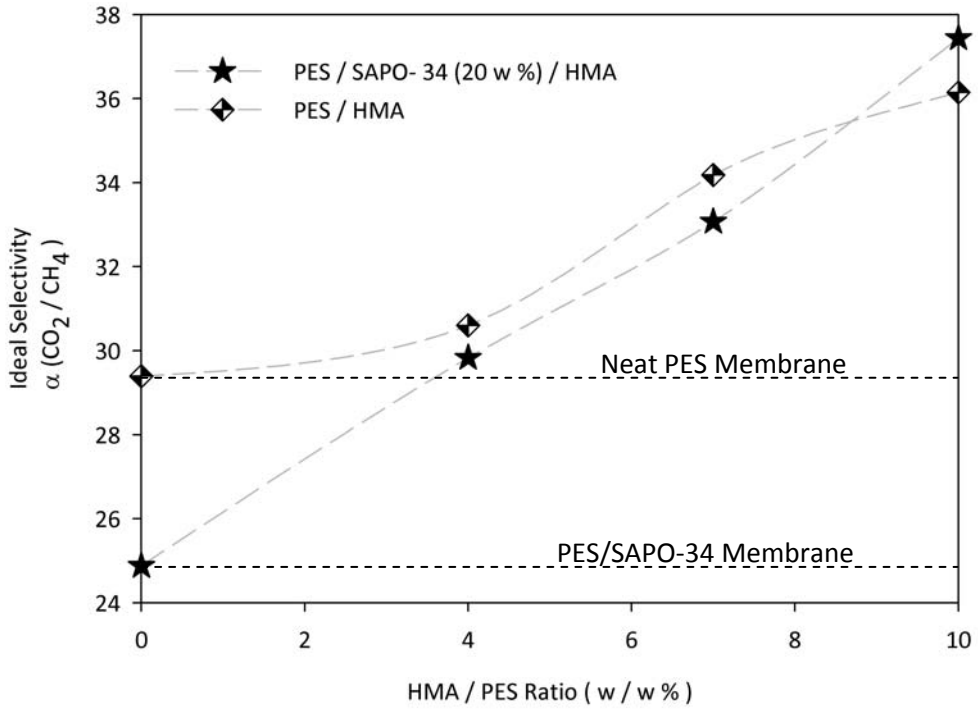

Figure 4.14 Effect of increasing HMA/PES ratio (w/w %) on CO_2/CH_4 ideal selectivity for PES/SAPO-34 (20%)/HMA membranes

Based on the results represented in Figures 4.12 (b), 13, and 14; remarkable improvements were obtained for all gas pairs, but the order of impact of HMA on gas pairs decreases as the size differences of the gases decrease. Approximately 40 % increase in H_2/CH_4 selectivity was followed by 30 % increase in H_2/CO_2 selectivity for PES/SAPO-34 (20 %)/HMA (10 %) membranes compared to PES/HMA (10 %). The slight improvement in CO_2/CH_4 selectivity which is 3.5 % for PES/SAPO-34 (20 %)/HMA (10 %) compared to PES/HMA (10 %) seem to reveal size dominated mechanism of resultant HMA incorporated MMMs. These results might be an indication of that addition of HMA and SAPO-34 enhanced the diffusion selectivity more than the sorption selectivity of the resultant ternary membranes.

The comparison of permeabilities and selectivities of pure PES, PES/HMA, PES/SAPO-34 and PES/SAPO-34/HMA membranes indicates the strong effect of HMA on the membrane matrix, and suggests that the use of SAPO-34 and HMA together in the PES

membrane has more contribution to the membrane performance than their individual use in the membranes. Either PES/HMA or PES/SAPO-34 membranes could not overcome the trade-off imposed. Binary PES/HMA membranes possessed increased selectivities, but the loss in permeabilities revealed that these membranes could not overcome the trade-off. PES/SAPO-34 membranes revealed enhanced permeabilities with slight decrease in selectivities. The increasing trend of permeabilities and decreasing trend of selectivities with the addition of zeolites into glassy polymer matrices has been similarly reported in many studies [20, 41, 43] which is explained by the formation of interfacial unselective voids. However the addition of HMA to PES/SAPO-34 membranes not only recovered the permeability loss encountered in PES/HMA membranes but also considerably increased the ideal selectivities. Hence the resultant PES/SAPO-34/HMA MMMs have both higher selectivities and permeabilities compared to PES/HMA membranes.

Interestingly, for PES/SAPO-34 (20 %)/HMA(10 %) membranes the enhancement in H_2 permeability was 41.5 %, CO_2 permeability was 8.5 %, CH_4 permeability was 5 % that is the highest permeability enhancement was for the smallest molecule H_2 and smallest permeability enhancement was for the largest molecule CH_4. However this trend was just the opposite for PES/SAPO-34 membranes favoring the permeability of the largest molecule CH_4. These results may indicate the loosened structure of PES/SAPO-34 membranes resulting in lowered resistance to the permeation of CH_4 molecules. The reversed trend with the addition of HMA can be explained by different hypotheses.

Yong et al. [20] prepared PI, PI/TAP, PI/ zeolite 13 X, and PI/zeolite 13 X/ TAP membranes. Similar to the results in this study, the permeabilities were increased and selectivities were decreased with the addition of zeolite 13 X and vice versa with the addition of low molecular weight additive, 2,4, 6-triaminopyrimidine, to neat PI membranes. However the addition of TAP and zeolite 13 X to PI membrane resulted in increased selectivities and permeabilities with respect to PI/TAP membranes. They concluded that; TAP acted as a compatibilizer between PI and zeolite 13 X, interacted simultaneously with both of them owing to the amine functional groups in the TAP structure and filled the space between the polymer and zeolite which is referred as interfacial void. The permeabilities of CO_2 and CH_4 through PI/TAP/zeolite 4A membranes were lower but the selectivity for CO_2 over CH_4 was higher than pure PI membrane.

Depending on the above mentioned single gas permeability results together with the literature discussions, it may be proposed that HMA might be modifying the membrane morphology by acting as a compatibilizer between SAPO-34 and PES, and enabling the gas molecules pass through the "windows" of the zeolite SAPO-34. However as Süer et al. [41] noted that the complex heterogeneous micromorphology of the MMMs might be the major factor in the improvements of gas separation performance of the membranes. The complex micro morphological structure of the PES/ SAPO-34/HMA MMMs, which is expected to have different characteristics than PES and PES/SAPO-34 membranes, may be the reason for improved performance.

A similar study employing the incorporation of LMWAs into MMM was performed by Şen et al. [36]. They prepared PC/pNA (5w/w %)/ zeolite 4A (20 w/w %) membranes. CO_2/CH_4 and O_2/N_2 selectivities were considerably improved compared to neat PC membranes whereas the permeabilities of all gases were below the virgin PC membrane. As our results indicate, with the incorporation of HMA at each concentration to the above T_g annealed PES/SAPO-34 membranes, both permeabilities and selectivities were improved compared to neat PES membranes. These results might stem from the combined effect of incorporation of HMA and annealing the membranes above the glass transition temperature of PES.

4.4.2.1 Effect of Zeolite Loading on PES/SAPO-34/HMA Mixed Matrix Membranes

Effect of zeolite loading on the performance of PES/HMA/SAPO-34 mixed matrix membranes were investigated by preparing membranes with varying zeolite amounts between 10 and 40 w/w %. HMA incorporated MMMs were self-supporting pinhole free permselective membranes at each SAPO-34 concentration. HMA/PES ratio in the membrane casting solution was kept constant at 10 w/w %. The single gas permeabilities and ideal selectivities of PES/HMA/SAPO-34 MMMs are presented in Tables 4.13 and 4.14, respectively.

As can be seen in Table 4.13, the permeabilities through PES/HMA/SAPO-34 MMMs remained nearly the same with the addition of 10 w/w % SAPO-34, whereas permeabilities noticeably increased with 20 w/w % SAPO-34 incorporation. After 20 w/w % SAPO-34 loading, the permeabilities showed an additional slight increase. The most noticeable increase was in the permeability of CH_4.

Table 4.13 Effect of zeolite loading on the gas permeabilities for PES/SAPO-34/HMA MMMs

(PES / SAPO-34 (y %) / HMA (10 wt/wt %)	Permeability (Barrer)		
y	H_2	CO_2	CH_4
0	4.99	1.41	0.039
10	4.48	1.12	0.034
20	7.06	1.53	0.041
30	6.94	1.55	0.046
40	7.19	1.61	0.056

The increasing trend of permeabilities with the addition of zeolites into glassy polymer matrices has been similarly reported in many studies [1, 4, 5, 8, 12, 13, 39, 77]. Suer et al. [41], who prepared zeolite 4A filled polyethersulfone (PES) mixed matrix membranes, reported an increase in permeabilities above 33.3 % (w/w) zeolite 4A loading which was continued up to 50 % (w/w) zeolite 4A loading. They claimed that as the percentage of zeolite in the matrix increases, the interfacial voids around the zeolites may connect and provide alternate path for gas molecules, and this may lead to increases in the permeation rates of gas molecules.

In addition to permeabilities, selectivities of PES/HMA (10 w/w %)/SAPO-34 MMMs for H_2/CO_2, CO_2/CH_4, and H_2/CH_4 gas pairs are represented in Table 4.14. With the addition of 10 w/w % SAPO-34, ideal selectivities remained nearly the same for all gas pairs. However, incorporation of 20 w/w % SAPO-34 resulted in noticeable increase in selectivities.

The improvement in the selectivities with the addition of zeolites into the glassy polymer membranes had also been previously reported [1, 16, 45]. In these studies, the zeolite loading was usually 20 % or 30 %. Similarly, our membranes showed a significant improvement in the selectivities by adding 20 % (w/w) SAPO-34 into the membrane formulation. However, increasing zeolite amount in the PES/HMA/SAPO-34 membranes beyond 20 w/w % resulted in decreasing selectivities. Similar observation was also experienced by other researchers [39, 77]. Duval et al. [39] and Ismail et al. [75] both concluded that with increasing zeolite amount, the free voids between the polymer chains

and zeolite particles were likely to govern the direction of the gas molecules to pass through the membrane instead of absorb through the open pore of zeolite particles.

Table 4.14 Effect of zeolite loading on the ideal selectivities for PES/SAPO-34/HMA MMMs

(PES / SAPO-34 (y %) / HMA (10 wt/wt %)	Ideal Selectivity		
y	H_2/CO_2	CO_2/CH_4	H_2/CH_4
0	3.54	36.15	127.95
10	4.00	33.14	132.55
20	4.64	37.44	175.79
30	4.52	33.92	153.94
40	4.48	28.75	128.39

Gas permeation results apparently showed that the addition of 20 % (w/w) SAPO-34 has lead to a significant enhancement in both selectivity and permeability for PES/HMA/SAPO-34 MMMs compared to the PES/HMA blend polymeric membranes. MMMs with 20 % (w/w) zeolite loading demonstrated a higher value of selectivity compared to the others. In contrast, the selectivity trend changed for MMM at 30 and 40 w/w % zeolite loading. The down turn of the selectivities when the zeolite loading exceeding 20 w/w % might be due to the incresed void volume resulting from poor adhesion of polymer chains and SAPO-34 particles. Similar observation was also experienced by Duval et al. [39] and Ismail et al [75]. Both researchers observed a similar down turn when the zeolite loading exceeding 30% and concluded that beyond this amount, the free voids were likely to govern the direction of the gas molecules to pass through the membrane.

4.5 Characterization of Membranes

4.5.1 TGA Experiments

The thermograms of pure PES membrane and PES/LMWA membranes reported in Figure in 4.15 reveals that the weight loss is below than 1%, which shows that our samples can be considered as solvent free. The TGA thermograms of the other membranes are given in Appendix E.

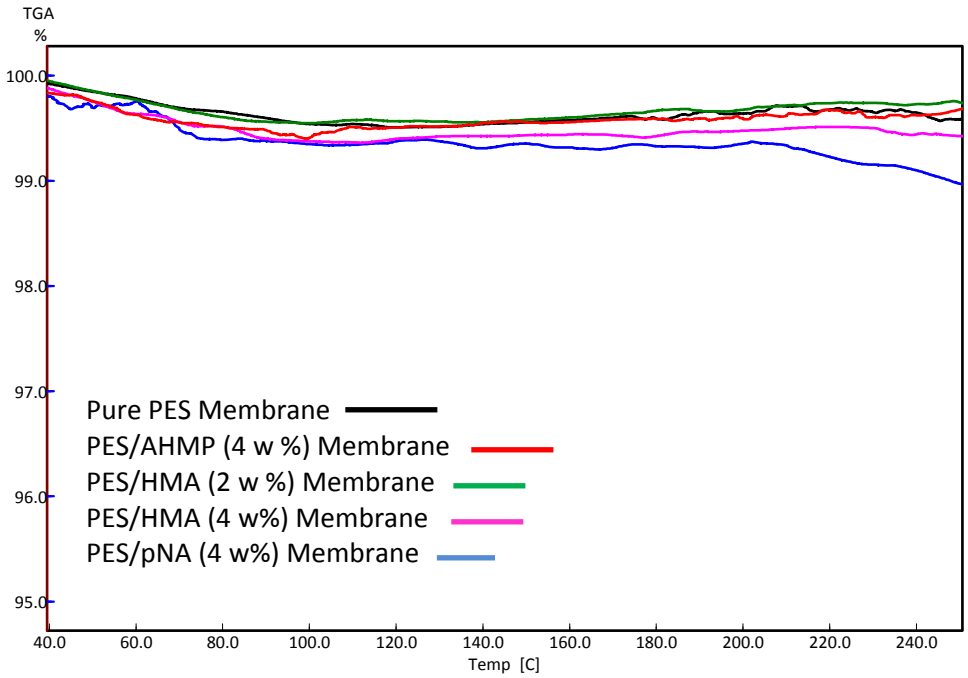

Figure 4.15 Comparison of TGA graphs of pure PES and various PES/LMWA membranes annealed at 225 ^{o}C for 8 hours

Thermogravimetric analysis was also used to check the SAPO-34 content of MMMs. PES/SAPO-34 membranes with zeolite loading of 20 w/w % were heated from room temperature up to 850 ^{o}C with a 5 ^{o}C/min rate. Figure 4.16 shows the thermogram of PES/SAPO-34 membrane performed in air atmosphere with 80.47 % weight loss. This result is interpreted as the polymer burns and starts to leave around 450 ^{o}C and disappear around 850 ^{o}C. Hence, TGA results give the SAPO content is 19.53 w/w%. However the sample weight in TGA analysis is very low, no more than a few milligrams. Therefore to check the accuracy, another part of the PES/SAPO-34 membrane with weight of 0.3 gram was placed in a crucible, which was dried at 110 ^{o}C for a day, heated from room temperature to 900 ^{o}C, and kept at this temperature for 5 hours in ash oven. The weight of the sample was found immediately after this process, and the weight loss was found to be 78.07 (w/w) % which implies that the SAPO-34 content of the membrane is 21.93 (w/w) %.

Thermogravimetric analyses performed for different parts of the PES/SAPO-34 membrane and the analysis performed with ash oven for another section of the PES/SAPO-34 membrane revealed SAPO-34 content of the membranes around 20 w/w %. These results support the finding of the homogeneous distribution of SAPO-34 in the membranes.

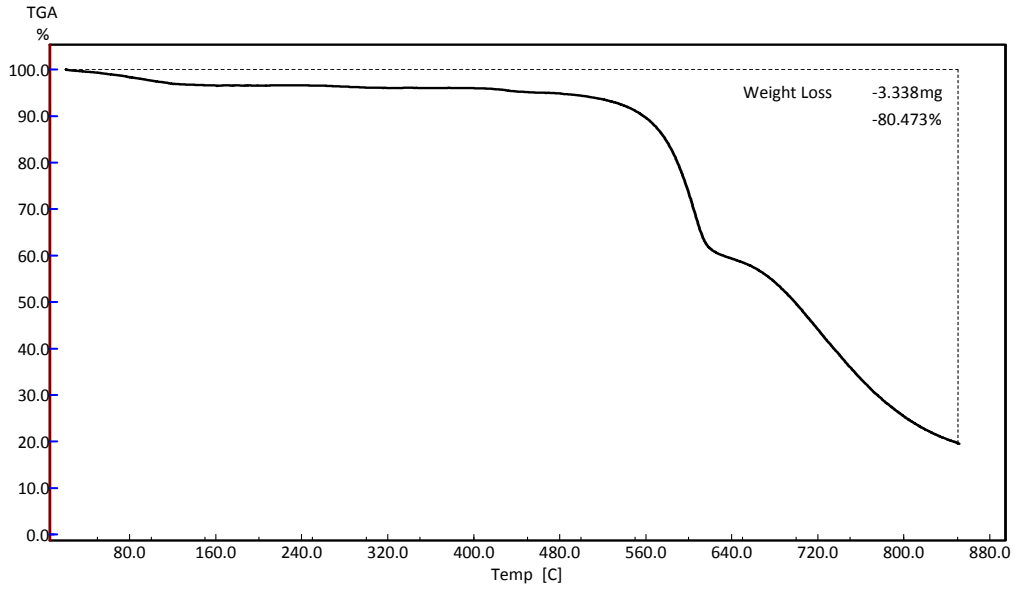

Figure 4.16 Thermogravimetric analysis of PES/SAPO-34 membrane performed between room temperature and 850 ^{o}C.

4.5.2 DSC Experiments

Glass transition temperature is one of the most important properties of polymers and it is the temperature below which free rotations cease because of the intra-molecular energy barriers. Hence, glass transition temperature can give an insight about the flexibility of polymers at room temperature. Many researchers indicated the importance of flexibility of polymer chains noting that favorable polymer/zeolite interface morphology can be obtained by this way [4, 11, 16, 21]. Therefore, DSC analysis is very useful to compare the effect of LMWA type and loading on polymer chain rigidity for PES/LMWA and PES/SAPO-34/LMWA mixed matrix membranes.

In this study, pure PES, PES/LMWA dense homogenous membranes and PES/SAPO-34, PES/HMA/SAPO-34 MMMs were prepared, and the glass transition temperatures of them were determined from the second scan DSC thermograms of the membranes.

As discussed in section 4.3.1, eight different types of low molecular weight additive were incorporated to neat PES matrix at 4 w/w %. Excluding AHMP, TAP, and MEL, homogenous membranes were obtained with the addition of different type LMWAs. As shown in Table 4.7, all LMWAs decreased the glass transition temperature of PES meaning that they increased the degree of flexibility of PES membranes, even at low concentrations,

unlike many blend membranes reported in literature, in which similar effects were observed with additive concentrations of greater than 10 % (w/w) [29-34]. In parallel to the gas permeation results of these membranes, pNA, HMA, and ANP were more effective in lowering the T_g of PES probably due to their diluent effect and interaction capability with PES.

The effect of HMA loading in PES membranes was also analyzed by DSC experiments. Glass transition temperature drops with increasing content of HMA. Table 4.15 shows the increasing extent of shift from glass transition temperature of PES with increasing HMA content in membrane casting solution.

Table 4.16 shows the effects of HMA and SAPO-34 contents on the T_g of the ternary membranes. No change on the T_g was seen with the incorporation of SAPO-34 in the absence of HMA, suggesting that there is no significant interaction between PES and SAPO-34 particles. Battal et al. [55] reported also unchanged glass transition temperature with the addition of zeolite 4A particles to PES membranes.

On the other hand, several researchers [52, 53, 66] reported an increase in T_g of the membranes with the addition of zeolite particles. This observation was explained as the restricted segmental motion of the polymer chain because of polymer-zeolite interactions. Apparently, the increase in T_g was speculated to be the result of rigidified polymer chains around zeolite particles, signaling the favorable interaction between two phases.

Table 4.15 Effect of HMA/PES ratio on the glass transition temperatures of PES/HMA blend membranes

HMA Content (w / w %)	Glass Transition Temperature (^oC)
0	220
2	209
4	206
7	205
10	197
15	194
25	188

On the contrary, PES/SAPO-34 membranes showed increased permeabilities with some selectivity losses, and their glass transition temperatures were the same with neat PES membranes. However incorporation of HMA to MMMs resulted in lower glass transition temperatures with respect to PES/SAPO-34 membranes but higher glass transition temperatures with respect to PES/HMA membranes. As can be seen in Table 4.16, 4 w/w % addition of HMA to the PES/SAPO-34 (20 w %) membrane resulted in nearly 10 ^{o}C reduction in the T_g of PES/SAPO-34 membrane. Similarly, addition of SAPO-34 to PES/HMA (4 w%) blend membrane resulted in nearly 4 ^{o}C increase in the T_g of the resultant ternary component membranes. The considerable increase in T_g with respect to PES/HMA membrane can be explained in terms of polymer chain rigidification around SAPO-34 particles in accordance with the literature data. Chain rigidification might be one of the causes of reduced permeabilities of PES/SAPO-34/HMA membranes compared to PES/SAPO-34 membranes.

Şen et al. [21] reported also similar results for polycarbonate-zeolite 4A and pNA system. They reported pure PC and PC/zeolite 4A membranes T_g to be 146 ^{o}C, whereas addition 5 w% pNA to PC/zeolite 4A membranes resulted in a T_g value of 127 ^{o}C. They concluded that pNA provided the interaction between polymer and the zeolite. Therefore, likewise to the above mentioned study, we may also claim that HMA acted as a mediating agent to provide the interaction and is essential in order SAPO-34 to affect the PES matrix.

Apart from these results, for all type of membranes, whether PES/LMWA or mixed matrix membrane a distinctive single T_g was observed, indicating the existence of a single homogeneous polymer phase in the membranes [2]. The second scan DSC thermograms of some of the membranes were given in Appendix C.

4.5.3 Morphological Characterization

The SEM images of pure PES membrane and some of the PES/LMWA blend membranes are shown in Figure 4.17. The membranes have dense and homogenous structures, and no defects were observed at these magnifications. All of the additives formed homogenous compatible blends with PES polymer matrix at a concentration of 4 w/w %, except AHMP, TAP, and MEL. At this concentration phase separation of AHMP, TAP, and MEL took place, which was also observed visually due to limited solubility during the solvent evaporation, as discussed in section 4.3.1.

Table 4.16 Comparison of glass transition temperatures of mixed matrix membranes with pure PES and PES/HMA blend membranes

Membrane	PES / SAPO-34 (y %) / HMA (x %)		$T_g \pm 2\ ^oC$
	x	y	
Pure PES	0	0	220
PES/SAPO-34	0	20	219
PES/HMA	4	0	206
PES/SAPO-34/HMA		20	210
PES/HMA	7	0	205
PES/SAPO-34/HMA		20	210
PES/HMA	10	0	197
PES/SAPO-34/HMA		10	195
PES/SAPO-34/HMA		20	200
PES/SAPO-34/HMA		30	198
PES/SAPO-34/HMA		40	201

In some micrographs in the figures below, the channel-like structures were observed; this may due to the surface damage of the samples when they were broken in the liquid nitrogen. The elongation of polymer resulting in channel like structures during the sample preparation could not be avoided.

In contrast to the case encountered for AHMP, HMA was soluble at each concentration used in this study. In order to see the upper limit concentration of HMA at which no longer homogeneous PES/HMA membranes cannot be prepared, membranes having a HMA/PES ratio of 25 w % was produced. However, HMA yields homogeneous PES/HMA membrane morphology even at this high loading. This result shows that HMA is an appropriate low molecular weight additive for preparing PES/LMWA membranes, and for investigating the effect of loading of LMWA on blend membranes. Figure 4.18 shows the SEM image of PES/HMA membrane having a HMA/PES ratio of 25 w % in the membrane casting solution.

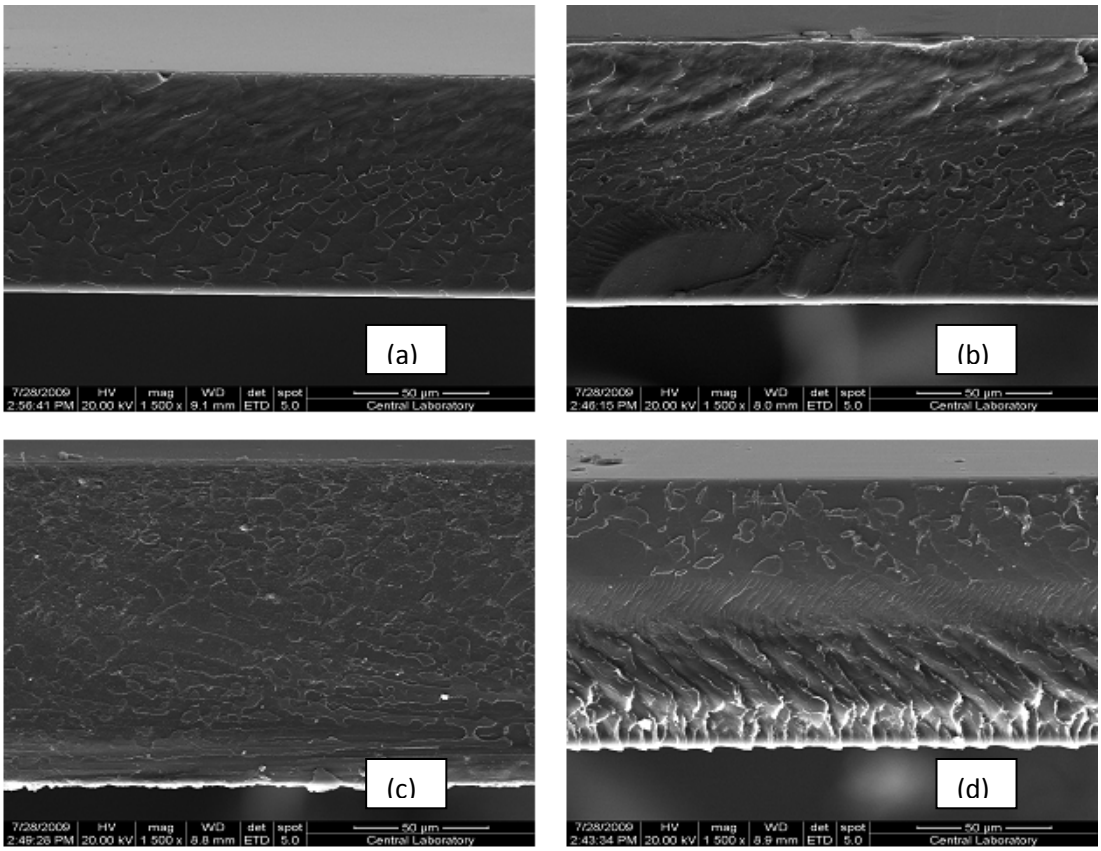

Figure 4.17 Cross-sectional SEM images of (a) pure PES, (b) PES/pNA, (c) PES/HMA and (d) PES/ANP membranes. (LMWA/PES= 4 w/w %, PES/DMSO= 20 w/v %),(1500 magnification).

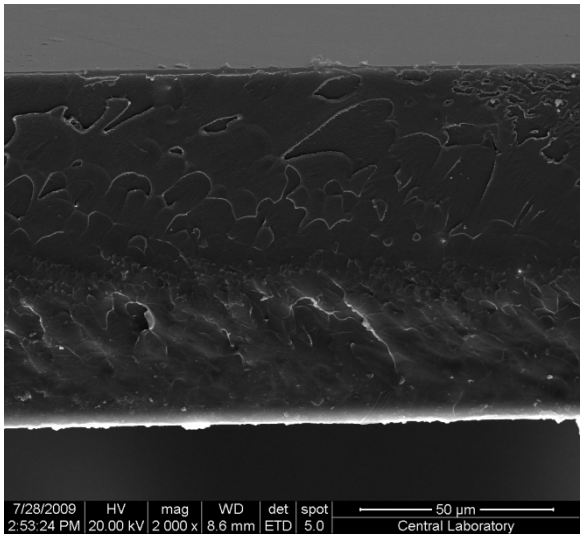

Figure 4.18 Cross sectional SEM image of PES/HMA membrane (HMA/PES ratio = 25 w/w %)

SEM analysis was also performed for PES/SAPO-34, PES/SAPO-34/HMA mixed matrix membranes. In contrast to the pure PES and PES/LMWA membranes, MMMs have heterogeneous structures, where the cubic particles are SAPO-34 crystals, and the continuous phase is PES. Figure 4.19 shows SEM images of PES/SAPO-34, and PES/SAPO-34/HMA membranes including 4, 7, and 10 w % HMA and a 20 w % SAPO-34.

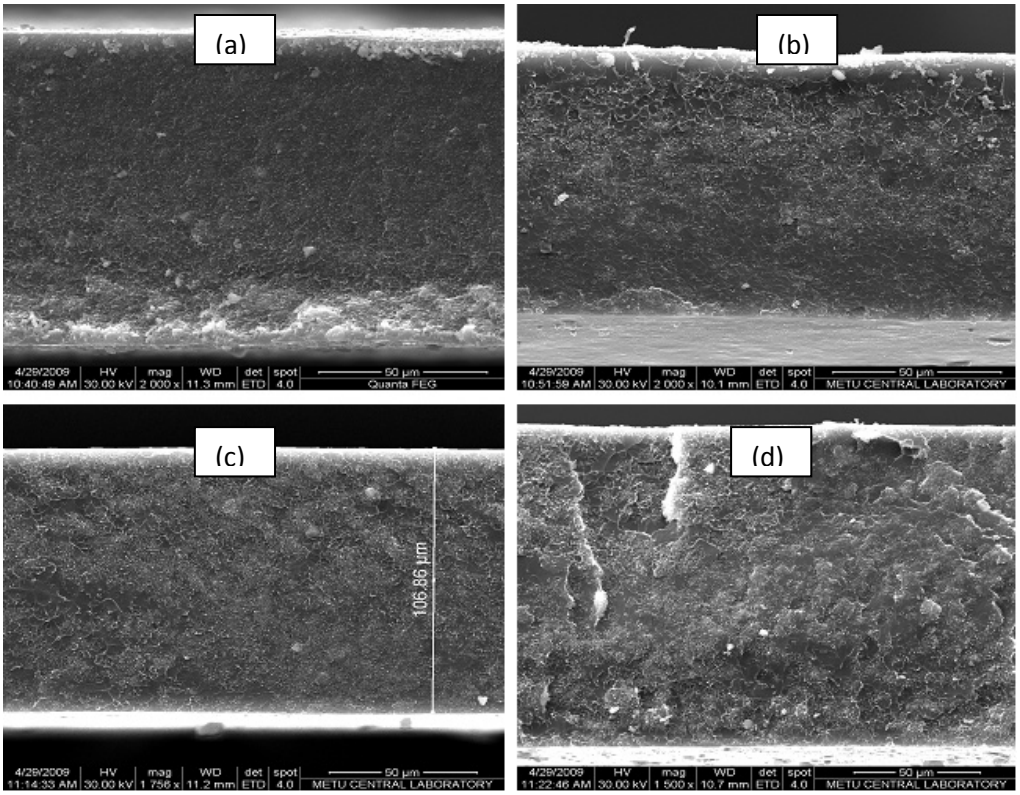

Figure 4.19 Cross sectional SEM images of PES/SAPO-34 (a), PES/SAPO-34/HMA membranes at a HMA/PES ratio of 4 w/w % (b), 7 w/w % (c), 10 w/w % (d).
(SAPO-34 content = 20 w/w %)

Figure 4.20 shows SEM images of PES/SAPO-34/HMA membranes including 30, and 40 wt % SAPO-34 and 10 wt % HMA. SEM images in Figures 4.19-20 reveal the well dispersion of SAPO-34 particles. In addition, there is no sedimentation or large agglomeration of SAPO-34 particles.

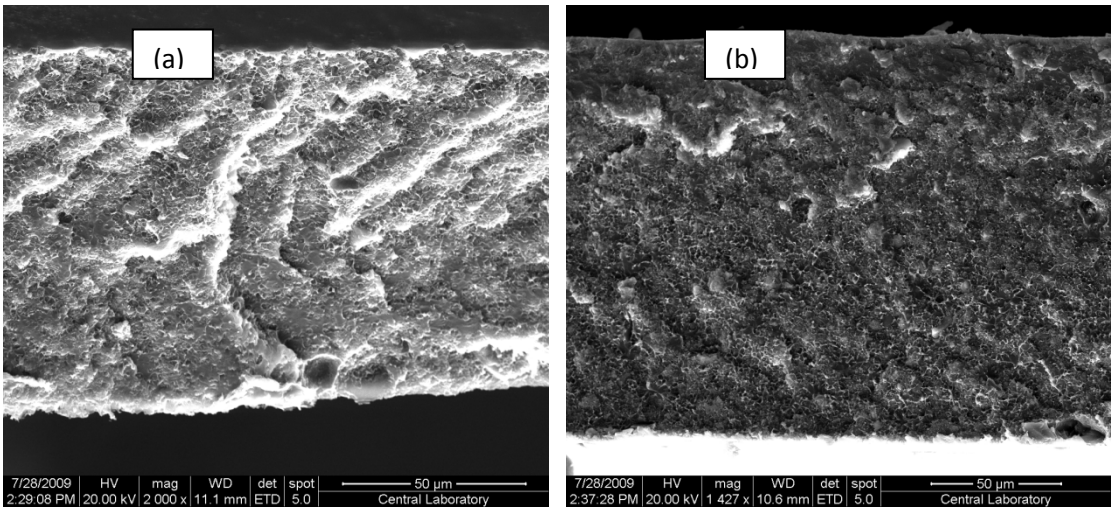

Figure 4.20 Cross sectional SEM images of PES/SAPO-34 (30 wt %) /HMA (a), PES/SAPO-34 (40 wt %) /HMA (b) membranes at a HMA/PES ratio of 10 w/w %.

SEM images are also used frequently to observe the interfacial region between polymer and zeolite, the dark area between the zeolite crystals and polymer matrix is considered usually as an empty space (interfacial void) in numerous studies [4, 5, 16, 19, 44, 53]. Though the microcavities possibly forming at this interface and considered as voids cannot be clearly seen in SEM images, however a comparison of membranes prepared at different conditions can be made. Figure 4.21 reveals the cross sectional SEM images of PES/SAPO-34 and PES/SAPO-34/HMA membranes at a higher magnification.

SEM image in Figure 4.21 (a) reflect that the interfacial region around some SAPO-34 particles appears to form a loose structure or is even a void, plausibly resulting in a gaseous bypass between the glassy polymer chains and embedded SAPO-34 particles, and hence PES/SAPO-34 MMMs resulted in increased permeabilities with severe selectivity losses. The incorporation of HMA helped some SAPO-34 particles to be wetted and surrounded better with PES chains.

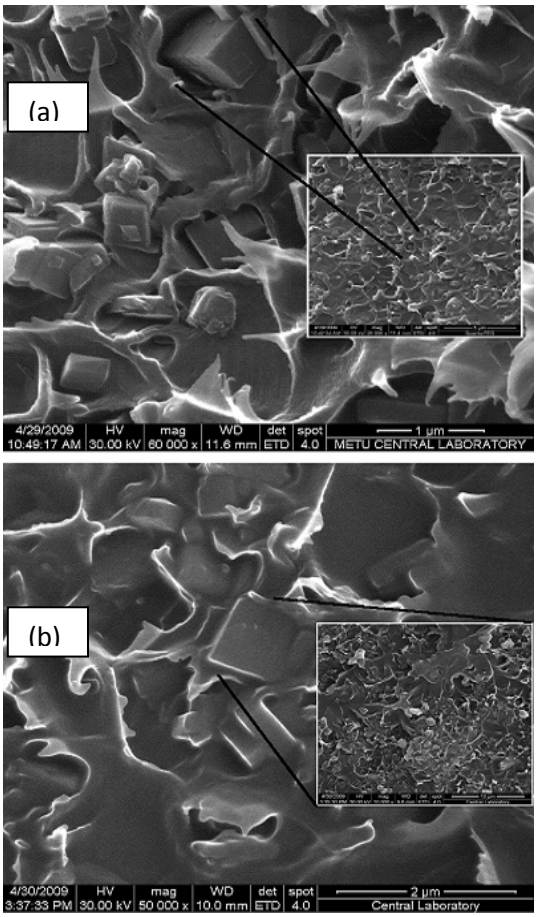

Figure 4.21 Cross-sectional SEM images of PES/SAPO-34 MMMs at higher magnifications x50.000 (a) PES/SAPO-34 (20%) MMM and (b) PES/SAPO-34 (20%)/HMA (10 %) MMM

SEM image in Figure 4.21 (b) reflect the improved interface morphology with the addition of 10 w % HMA to PES/SAPO-34 membrane. Similar morphologies were observed for all of the HMA incorporated MMMs at different HMA/PES ratios.

4.5.4 Characterization of Membranes by Carbon-Nitrogen-Sulphur Elemental Analysis

PES/HMA blend polymeric membranes were prepared from membrane casting solutions at the HMA/PES ratios of 2, 4, 7, 10, 15, and 25 w/w %. Carbon-nitrogen-sulphur (CNS) elemental analysis was performed in order to test the existence of HMA in the membranes. Carbon, hydrogen, nitrogen, and sulphur elements are detected simultaneously in homogeneous, small samples (~ 2 mg) with elemental analysis instrument. Table 4.17 represents the results of elemental analysis performed for pure PES, PES/HMA (4 w/w %), PES/HMA (7 w/w %), PES/HMA (10 w/w %), PES/HMA (25 w/w %) and PES/HMA (25 w/w %) film only solvent evaporated without annealing. The results tabulated are the average of three measurements, and they are given in terms of weight percentages.

The results of each run of elemental analysis are also tabulated in Appendix F. Table 4.17 also represents the weight percentages of the carbon, nitrogen and sulphur elements calculated theoretically using the chemical structures of the components of the membranes. Detailed calculations regarding the weight percentages of elements in the membranes are given in Appendix F.

Table 4.17 Weight percentages of carbon, nitrogen, and sulphur elements in the PES/HMA membranes obtained by CNS elemental analysis and calculated theoretically*

Membrane	**% C_{exp}**	**% N_{exp}**	**% S_{exp}**	**% C_{theo}**	**% N_{theo}**	**% S_{theo}**
neat PES	60.35	-	13.95	63.96	-	12.18
PES/HMA (4 w/w %)	61.96	0.21	13.59	64.12	0.44	11.71
PES/HMA (7 w/w %)	58.29	0.25	13.45	64.24	0.74	11.39
PES/HMA (10 w/w %)	63.61	0.32	13.38	64.35	1.03	11.08
PES/HMA (25 w/w %)	64.70	0.37	13.02	64.81	2.27	9.75
not annealed PES/HMA (25 w/w %)	57.79	1.86	13.57	64.81	2.27	9.75

*subscripts exp., and theo. stand for values from CNS analysis and theoretical calculation respectively. (Balance is oxygen and hydrogen.)

HMA is the only molecule including nitrogen element in the PES/HMA membranes. For this reason, the detected nitrogen amount can be attributed to the HMA in the membrane. As expected, the amount of nitrogen detected by elemental analysis increases with increasing HMA/PES ratio in the membrane casting solution.

As stated before, membranes are prepared by solvent evaporation method in this study. Membranes are further annealed at 225 ^{o}C which is above the glass transition temperature of PES, and also above the melting point of HMA. Therefore, elemental analysis was also performed for not-annealed PES/HMA membrane prepared from 25 w/w % HMA containing casting solution. Interestingly, the nitrogen amount detected for un-annealed film was greater than the nitrogen amount detected for annealed film.

Based on the nitrogen element weight percentages detected in the 2 mg samples, which are tabulated in Table 4.17, HMA content of the PES/HMA membranes were estimated. Table 4.18 represents the estimations of HMA contents of PES/HMA membranes

based on the amount of nitrogen element detected by CNS elemental analysis. Detailed calculations regarding the conversion of weight percentages of nitrogen obtained from elemental analysis to the weight percentages of HMA in the membrane are given in Appendix F.

Table 4.18 Estimations of HMA contents of PES/HMA membranes based on the amount of nitrogen element detected by CNS elemental analysis

Membrane	HMA/PES (w/w) ratio estimate in the membrane
neat PES	-
PES/HMA (4 w/w %)	1.89
PES/HMA (7 w/w %)	2.25
PES/HMA (10 w/w %)	2.90
PES/HMA (25 w/w %)	3.37

Based on CNS elemental analysis nitrogen element results, the predictions of HMA/PES ratios which are represented in Table 4.18 may imply that some portion of HMA added to the membrane casting solution might be escaping from the membrane matrix during the solvent evaporation and annealing procedures. However, the actual HMA/PES ratio in the membranes cannot be found exactly by depending solely on the amount of nitrogen element detected by CNS analysis, since there is the possibility of material loss during the elemental analysis employing 2 mg of sample. In addition to nitrogen element, we expect increasing amounts of carbon element with increasing HMA/PES ratio in the casting solution. However, as Table 4.17 reveals the carbon amount detected is less than the expected for the PES/HMA (7 w/w %) and un-annealed PES/HMA (25 w/w %) samples. In addition the percentages of all elements detected by CNS analysis are lower than the expected values obtained from theoretical calculations. Due to these observations regarding the inefficiency of this method to predict the actual HMA concentrations, the HMA/PES ratios in the casting membrane solutions were taken as nominal and reported throughout this study.

CHAPTER 5

CONCLUSIONS

In this study, the effect of low molecular weight additive type and loading on pure PES membrane was investigated. One of the selected additives, HMA, was incorporated to PES/SAPO-34 mixed matrix membranes at different concentrations. The gas permeation properties and morphologies of PES/SAPO-34 (20 w/w %)/HMA (4-10 w/w %) and PES/SAPO-34 (10-40 w/w %)/HMA (10 w/w %) membranes were compared with pure PES, PES/HMA, PES/SAPO-34 membranes.

Following conclusions were encountered;

1. Developed membrane preparation methodology yielded reproducible, solvent free, defect free dense homogeneous pure PES, PES/LMWA and PES/SAPO-34, PES/SAPO-34/LMWA mixed matrix gas separation membranes.

2. Incorporation of low molecular weight additives into the membrane formulation reduced the permeabilities of all gases, reduced glass transition temperatures of the membranes, and increased the ideal selectivities compared to pure PES membranes even at a low concentration like 4 w/w %. Despite their different chemical structures, they revealed similar anti-plasticization effects and changed the performance and structure of PES membranes.

3. PES/HMA blend membranes were produced in the range of 2-25 w/w %. The sharpest effect of HMA on gas permeation properties and glass transition temperature of neat PES membrane was observed at 2 w/w % HMA loading. However, even at 25 w/w % concentration of HMA in casting solution, homogeneous and reproducible PES/HMA membrane was obtained and the anti-plasticization effect of this LMWA was observed

at this loading also. The increasing concentration of HMA in the membrane casting solution led to increasing extents of shifts of both permeabilities of all gases, ideal selectivities and glass transition temperatures with respect to the pure PES membrane properties, respectively.

4. The addition of HMA to PES/SAPO-34 membranes effectively increased the permselective properties of PES/SAPO-34 MMMs at all concentrations of HMA. Single gas permeability experiments of the membranes demonstrated that by the addition of HMA and SAPO-34 to the membrane matrix together overcome the limit imposed by trade-off encountered for polymeric membranes, and both permeability and selectivity of the membranes were improved compared to pure PES, PES/HMA, and PES/SAPO-34 membranes. Addition of HMA to PES/SAPO-34 membranes resulted in increased ideal selectivities very well above the ideal selectivities of pure PES, PES/SAPO-34, and PES/HMA membranes, while keeping the permeabilities of all the gases above the permeabilities of both pure PES and PES/HMA membranes.

5. DSC analysis of the membranes showed that the addition of HMA to neat PES membrane decreased the glass transition temperature of PES membrane, increased the flexibility of the polymer. The addition of SAPO-34 to neat PES membrane did not affect the glass transition temperature of PES membrane. Whereas, the addition of even a small concentration of HMA changed the T_g of PES/SAPO-34/HMA, implying that HMA acted as a facilitator and HMA is a necessary agent enhancing the interaction PES chains and SAPO-34 particles.

6. SEM images of all PES/LMWA membranes reveal homogeneous morphology except AHMP, MEL, and TAP additives. SEM images of all MMMs demonstrate the well dispersion of SAPO-34 particles without agglomerations or sedimentation of these particles. In addition, SEM images at higher magnifications show better interface morphologies, partly elimination of voids seen in the PES/SAPO-34 membranes with the incorporation of HMA to the MMMs.

REFERENCES

[1] Li, Y., Chung, T.S., and Kulprathipanja, S., "Novel Ag-Zeolite/polymer mixed matrix membranes with a high CO_2/CH_4 selectivity", American Institute of Chemical Engineers Journal No:3, 53, 2007, p. 610-616.

[2] Mulder, M., "Basic Principles of Membrane Technology", Kluwer Academic Publishers, Second edition, 1997, Dordrecht.

[3] Nunes, S.P., Peinemann, K.V., "Membrane Technology in the Chemical Industry", Wiley-VCH, First edition, 2001, Weinheim.

[4] Liu, C., Kulprathipanja, S., Hillock, A. M. W., Husain, S., Koros W. J., "Advanced Membrane Technology and Applications Chapter 30: Recent Progress in Mixed Matrix Membranes", 2008, Wiley Interscience.

[5] Moore, T.T., "Effects of Materials, Processing, And Operating Conditions On The Morphology And Gas Transport Properties Of Mixed Matrix Membranes", PhD Thesis, The University of Texas, December 2004.

[6] Robeson, L.M., "Correlation of separation factor versus permeability for polymeric membranes", Journal of Membrane Science, 62, 1991, p. 165-185.

[7] Robeson, L. M., "The Upper Bound Revisited", Journal of Membrane Science, 320, 2008, p. 390-400.

[8] Koros, W.J., Fleming, G.K., "Membrane based gas separation", Journal of Membrane Science, 83, 1993, p. 1-80.

[9] P. Pandey, R.S. Chauhan, R. S., "Membranes for gas separation", Progress in Polymer Science, 26, 2001, p. 853-893

[10] Powell, C.E., Qiao, G.G., "Polymeric CO_2/N_2 gas separation membranes for the capture of carbon dioxide from power plant flue gases", Journal of Membrane Science, 279, 2006, p. 1–49

[11] Chung, T. S., Jiang, L. Y., Lia, Y., Kulprathipanja, S., “Mixed matrix membranes (MMMs) comprising organic polymers with dispersed inorganic fillers for gas separation”, Progress in Polymer Science, 32, 2007, p. 483–507

[12] Duval, J. M., “Adsorbent filled polymeric membranes”, PhD thesis, The University of Twente, 1995.

[13] Boom, J. P., “Transport through zeolite filled polymeric membranes”, Ph. D. Thesis, The University of Twente, 1994.

[14] Jia, M., Peinemann, K. V., Behling, R. D. “Preparation and characterization of thin-film zeolite–PDMS composite membranes”, Journal of Membrane Science, 73, 1992, p. 119–28.

[15] Pechar, T. W., Kim, S., Vaughan, B., Marand, E., Baranauskas, V., Riffle, J., “Preparation and characterization of a Poly(imide siloxane) and zeolite L mixed matrix membrane”, Journal of Membrane Science, 277, 2006, p. 210–218.

[16] Mahajan, R., Burns, R., Schaeffer, M., Koros, W. J., “Challenges in forming successful mixed matrix membranes with rigid polymeric materials”, Journal of Applied Polymer Science, 86, 2002, 881–890.

[17] Shu, S., Husain, S., Koros, W. J., “Formation of nano scale morphology on zeolite surface for enhanced interfacial interaction in mixed matrix membranes”, North American Membrane Society, Chicago IL, 2006.

[18] Guiver, M. D., Robertson, G. P., Dai, Y., Bilodeau, F., Kang, Y. S., Lee, K. J., “Structural characterization and gas-transport properties of brominated matrimid polyimide”, Journal of Polymer Science: Polymer Chemistry, 40, 2003, p. 4193–4204.

[19] Mahajan, R., “Formation, characterization and modeling of mixed matrix membrane materials”, PhD thesis, The University of Texas at Austin, 2000.

[20] Yong, H.H., Park, N.C., Kang, Y.S., Won, J., Kim, W.N., “Zeolite filled polyimide membrane containing 2,4,6-triaminopyrimidine”, Journal of Membrane Science, 188, 2001,p. 151–163.

[21] Sen, D., Yilmaz, L., Kalipcilar, H., “Development of polycarbonate based zeolite 4A filled mixed matrix gas separation membranes”, Journal of Membrane Science, 303, 2007, p. 194-203.

[22] Ismail, A.F., Norida, R., Sunarti, A.R., “Latest development on the membrane formation for gas separation” Journal of Science Technology, 24, 2002, p. 1025-1043.

[23] Freeman, B. D., “Basis of permeability/selectivity tradeoff relations in polymeric gas separation membranes”, Macromolecules, 32, 1999, p. 375-380.

[24] Matteucci, S., Yampolskii, Y., Freeman, B. D., Pinnau, I. “Materials Science of membranes for Gas and Vapor Separation, Chapter 1: Transport of Gases and Vapors in Glassy and Rubbery Polymers”, 2006, John Wiley and Science.

[25] Stern, S. A., “Polymers for gas separations: The next decade”, Journal of Membrane Science, 94, 1994, p. 1-65.

[26] Ebner, A. D., Ritter, J. A., “State-of-the-Art Adsorption and Membrane Separation Processes for Carbon Dioxide Production from Carbon Dioxide Emitting Industries”, Separation Science and Technology, 44, 2009, p. 1273 – 1421.

[27] Kapantaidakis, G. C., Koops, G. H., “High Flux polyethersulfone-polyimide blend hollow fiber membranes for gas separation.” Journal of Membrane Science, 204, 2002, p. 153-171

[28] Sridhar, S., Smitha, B., Ramakrishna, M., Aminabhavi, T.M., “Modified poly(phenylene oxide) membranes for the separation of carbon dioxide from methane”, Journal of Membrane Science, 280, 2006, p. 202-209.

[29] Robeson, L.M., “The effect of antiplasticization on secondary loss transitions and permeability of polymers”, Polymer Engineering and Science, 9, 1969, p. 277-281.

[30] Maeda, Y., Paul, D.R., “Effect of antiplasticization on gas sorption and transport. I. Polysulfone”, Journal of Polymer Science: Part B: Polymer Physics, 25, 1987, p. 957-980.

[31] Maeda, Y., Paul, D.R., “Effect of antiplasticization on gas sorption andtransport. II. Poly(phenylene Oxide)”, Journal of Polymer Science: Part B: Polymer Physics, 25, 1987, p. 981-1003.

[32] Ruiz-Treviño, F.A., Paul, D.R., “Modification of polysulfone gas separation membranes by additives”, Journal of Applied Polymer Science, 66, 1997, p. 1925-1941.

[33] Larocca, N.M., Pessan, L.A., “Effect of antiplasticization on the volumetric, gas sorption and transport properties of polyetherimide”, Journal of Membrane Science, 218, 2003, p. 69-92.

[34] Vidotti, S. E., Chinellato, A. C., Pessan, L. A., “Effects of Antiplasticization on the Thermal, Volumetric, and Transport Properties of Polyethersulfone” Journal of Applied Polymer Science, 103, 2007, p. 2627–2633

[35] Van Krevelen, D. W., “Properties of Polymers—Correlation with Chemical Structure”, 1990, Elsevier.

[36] Şen, D., Kalıpçılar, H., Yılmaz, L., “Gas Separation Performance of Polycarbonate Membranes Modified with Multifunctional Low- Molecular Weight Additives”, Separation Science and Technology, 41, 2006, p. 1813-1828

[37] Paul, D. R., Kemp, D. R., “The diffusion time lag in polymer membranes containing adsorptive fillers”, Journal of Polymer Science: Polymer Physics, 41, 1973, p. 79–93.

[38] Jia, M., Peinemann, K.V., Behling, R.D., “Molecular sieving effect of the zeolite-filled silicone rubber membranes in gas permeation”, Journal of Membrane Science, 57, 1991, p. 289-300.

[39] Duval, J.M., Folkers, B., Mulder, M.H.V, Desgrandchamps, G., Smolders, C.A., “Adsorbent filled membranes for gas separation, part 1: Improvement of the gas separation properties of polymeric membranes by incorporation of microporous adsorbents”, Journal of Membrane Science, 80, 1993, p. 189-201.

[40] Tantekin-Ersolmaz, B., Atalay-Oral, Ç., Tatlıer, M., Erdem-Şenatalar, A., Schoeman, B., Sterte, J., “Effect of zeolite particle size on the performance of polymer-zeolite mixed matrix membranes”, Journal of Membrane Science, 175, 2000, p. 285-288.

[41] Suer, M.G., Bac, N., Yilmaz, L., “Gas permeation characteristics of polymer-zeolite mixed matrix membranes”, Journal of Membrane Science, 91, 1994, p. 77-86.

[42] Huang, Z., Li, Y., Wen, R., Teoh, M. M., Kulprathipanja, S., “Enhanced gas separation properties by using nano-structured PES-Zeolite 4A mixed matrix membranes", Journal of Applied Polymer Science, 101, 2006, p. 3800-3805

[43] Huang, Z., Su, J., Su, X., Guo, Y., Teng, L., Yang, C. M., “Preparation and permeation characterization of β-Zeolite incorporated composite membranes”, Journal of Applied Polymer Science, 112, 2009, p. 9-18

[44] Sen, D., “Polycarbonate based Zeolite 4A filled mixed matrix membranes: Preparation, Characterization and gas separation performances”, PhD thesis, Middle East Technical University, 2008.

[45] Mahajan, R., Koros, W.J., “Mixed matrix membrane materials with glassy polymers. Part I”, Polymer Engineering and Science, 42, 2002, p. 1420-1431.

[46] Vu, D. Q., Koros, W. J., Miller, S. J., "Mixed matrix membranes using carbon molecular sieves I. Preparation and experimental results" Journal of Membrane Science 211, 2003, p. 311–334.

[47] Choi, S., Coronas, J., Lai, Z., Yust, D., Onorato, F., Tsapatsis, M., "Fabrication and gas separation properties of polybenzimidazole (PBI)/nanoporous silicates hybrid membranes", Journal of Membrane Science, 316, 2008, p. 145–152.

[48] Perez, E. V., Balkus, K. J., Ferraris, J. P., Musselman, I. H., "Mixed-matrix membranes containing MOF-5 for gas separations" Journal of Membrane Science, 328, 2009, p. 165–173

[49] Jha, P., Way, J. D., "Carbon dioxide selective mixed-matrix membranes formulation and characterization using rubbery substituted polyphosphazene", Journal of Membrane Science, 324, 2008, p. 151–161.

[50] Zimmerman, C.M., Singh, A., Koros, W.J., "Tailoring mixed matrix composite membranes for gas separation", Journal of Membrane Science, 137, 1997, p. 145-154.

[51] Barrer, R. M., James, S. D., "Electrochemistry of crystal-polymer membranes, I. Resistance measurements", Journal of Physical Chemistry, 64, 1960, p. 417–421.

[52] Li, Y., Chung, T., Cao, C., Kulprathipanja, S., "The effects of polymer chain rigidification, zeolite pore size and pore blockage on polyethersulfone (PES)-zeolite 4A mixed matrix membranes", Journal of Membrane Science, 260, 2005, p. 45-55.

[53] Moore, T. T., Koros, W. J., "Non-ideal effects in organic-inorganic materials for gas separation membranes", Journal of Molecular Structure, 739, 2005, p. 87–98.

[54] Zhang, Y., Balkus, K. J., Musselman, I. H., Ferraris, J. P., "Mixed-matrix membranes composed of matrimid and mesoporous ZSM-5 nanoparticles", Journal of Membrane Science, 325, 2008, p. 28–39.

[55] Battal, T., Baç, N., Yilmaz, L., "Effect of feed composition on the performance of polymer-zeolite mixed matrix gas separation membranes", Separation Science and Technology, 30, 1995, p. 2365-2384.

[56] Billmeyer, F.W., "Textbook of Polymer Science", John Wiley and Sons, 1962.

[57] Hansen, C. M., "Hansen solubility parameters: A User's Handbook", CRC Press, 2007.

[58] Weast, R.C., "CRC Handbook of Chemistry and Physics", The Chemical Rubber Company, 53rd Edition, 1972.

[59] Szostak, R., “Molecular Sieves, principles of synthesis and identification.”, van Nostrand, 1989.

[60] Hacarlioglu, P., Toppare, L., Yilmaz, L., “Effect of preparation parameters on performance of dense homogenous polycarbonate gas separation membranes”, Journal of Applied Polymer Science, 90, 2002, p. 776-785.

[61] Hacarlioglu, P., Toppare, L., Yilmaz, L., “Polycarbonate-polypyrrole mixed matrix gas separation membranes”, Journal of Membrane Science, 225, 2003, p. 51-62.

[62] Li, Y., Chunga, T. S., Huang, Z., Kulprathipanja, S., "Dual-layer polyethersulfone (PES)/BTDA-TDI/MDI co-polyimide (P84) hollow fiber membranes with a submicron PES–zeolite beta mixed matrix dense-selective layer for gas separation", Journal of Membrane Science, 277, 2006, p. 28–37.

[63] Wang, D. L., Li, K., Teo, W. K., "Effects of temperature and pressure on gas permselection properties in asymmetric membranes", Journal of Membrane Science, 105, 1995, p. 89–115.

[64] Sanders E. S., "Penetrant induced plasticization and gas permeation in glassy polymers", Journal of Membrane Science, 63, 1988, p. 63-80.

[65] Haraya, K., Hwang, S. T., "Permeation of oxygen, argon and nitrogen through polymer membranes ", Journal of Membrane Science, 71, 1992, p. 13-27.

[66] Li, Y., Guan, H. M., Chung, T. S., Kulprathipanja, S., " Effects of novel silane modification of zeolite surface on polymer chain rigidification and partial pore blockage in PES-zeolite A mixed matrix membranes", Journal of Membrane Science, 275, 2006, p. 17-28.

[67] Chiou, J. S., Maeda, Y., Paul, D. R., “Gas permeation in polyethersulfone”, Journal of Applied Polymer Science, 33, 1987, p. 1823-1828.

[68] Joly, C., Le Cerf, D., Chappey, C., Langevin, D., Muller, G., “Residual solvent effect on the permeation properties of fluorinated polyimide films”, Separation Science and Purification Technology, 1999, 16 p. 47-54.

[69] Khulbe, K. C., Matsuura, T., Lamarche, G., Kim, J. H., “The morphology characterisation and performance of dense PPO membranes for gas separation”, Journal of Membrane Science, 135, 1997, p. 211-223.

[70] Alentiev, A., Yampolskii, Y., Kostina, J., Bondarenko, G., “New possibilities for increasing the selectivity of polymer gas separating membranes”, Desalination, 199, 2006, p.121-123.

[71] Kostina, J., Bondarenko, G., Alentiev, A., Yampolskii, Y., “The influence of conformation composition of polyheteroarylenes on their transport properties” Desalination, 200, 2006, p.34-36.

[72] Macchione, M., Jansen, J. C., De Luca, G., Tocci, E., Longeri, M., Drioli, E., “Experimental analysis and simulation of the gas transport in dense Hyflon AD60X membranes: Influence of residual solvent”, Journal of Polymer, 48, 2007, p. 2619-2635.

[73] Buckley Smith, M. K., “The Use of solubility parameters to select membrane materials for pervaporation of organic mixtures”, PhD Thesis, University of Waikato, 2006.

[74] Liu, Y., Shi, B., “Hollow fiber supported liquid membrane for extraction of ethylbenzene and nitrobenzene from aqueous solution: A Hansen Solubility Parameter approach”, Separation and Purification Technology, 65, 2009, p. 233–242.

[75] Ismail, A. F., Rahim, R. A., Rahman, W. A., “Characterization of polyethersulfone/matrimid 5218 miscible blend mixed matrix membranes for O_2/N_2 gas separation”, Separation and Purification Technology, 63, 2008, p. 200–206.

[76] Chang, K. S., Hsiung, C. C., Lin, C. C., Tung, K. L., “Residual Solvent Effects on Free Volume and Performance of Fluorinated Polyimide Membranes: A Molecular Simulation Study”, Journal of Physical Chemistry, 113, 2009, p. 10159–10169.

APPENDIX A

AMOUNTS OF MATERIALS IN MEMBRANE PREPARATION

Table A.1 Weights of polymer and additive and volume of the solvent used during pure polymer, and polymer/additive membranes

Membrane Type	PES weight (g)	HMA weight (g)	DMSO (ml)
Pure PES	1.45	0	7.25
PES/HMA (4 % (w/w))	1.45	0.0580	7.25
PES/HMA (7 % (w/w))	1.45	0.1015	7.25
PES/HMA (10 % (w/w))	1.45	0.1450	7.25
PES/HMA (15 % (w/w))	1.45	0.2175	7.25
PES/HMA (25 % (w/w))	1.45	0.3625	7.25

Table A.2 Weights of polymer and zeolite and volume of the solvent used during polymer/zeolite and polymer/zeolite/additive mixed matrix membranes

Membrane Type	PES weight (g)	HMA weight (g)	SAPO-34 weight (g)	DMSO volume (ml)
PES/SAPO-34	1.45	0	0.290	7.25
PES/SAPO-34 (20 %)/HMA (4 %)	1.45	0.0580	0.290	7.25
PES/SAPO-34 (20 %)/HMA (7 %)	1.45	0.1015	0.290	7.25
PES/SAPO-34 (20 %)/HMA (10 %)	1.45	0.1450	0.290	7.25
PES/SAPO-34 (10 %)/HMA (10 %)	1.45	0.1450	0.145	7.25
PES/SAPO-34 (30 %)/HMA (10 %)	1.45	0.1450	0.435	7.25
PES/SAPO-34 (40 %)/HMA (10 %)	1.45	0.1450	0.580	7.25

APPENDIX B

REPRODUCIBILITY EXPERIMENTS FOR SINGLE GAS PERMEABILITY MEASUREMENTS

Results of reproducibility experiments of single gas permeability measurements performed with feed pressure of 2 bar and initially vacuum permeate side are tabulated in Tables B.1 to B.11. Results of reproducibility experiments of single gas permeability measurements performed with feed pressure of 3.7 bar and permeate side of 0.9 bar are tabulated in Tables B.12 to B.18.

Table B.1 Reproducibility data for pure PES membrane.

Membrane Number	Run Number	Permeability (Barrer)			Selectivity		
		H_2	CO_2	CH_4	H_2/CO_2	CO_2/CH_4	H_2/CH_4
M1 (145 µm)	1	6.64	2.61	0.084			
	2	6.63	2.59	-			
	avg.	6.64	2.60	-	2.55	30.95	79.05
M2 (100 µm)	1	6.96	3.05	0.105			
	2	6.89	3.04	-			
	avg.	6.93	3.05	0.105	2.28	29.05	66
M3 (100 µm)	1	7.17	2.97	0.105			
	2	7.06	2.99	-			
	avg.	7.12	2.98	0.105	2.39	28.42	67.81

Table B.2 Reproducibility data for PES/HMA(2 w/w %) membrane.

Membrane Number	Run Number	Permeability (Barrer)			Selectivity		
		H_2	CO_2	CH_4	H_2/CO_2	CO_2/CH_4	H_2/CH_4
M1	1	5.83	2.16	0.074			
(133 µm)	2	5.93	2.04	-			
	avg.	5.86	2.10	0.074	2.79	28.38	79.19
M2	1	5.45	1.83	0.064			
(132 µm)	2	5.43	1.85	-			
	avg.	5.44	1.84	0.064	2.96	28.75	85.00

Table B.3 Reproducibility data for PES/HMA(4 w/w %) membrane.

Membrane Number	Run Number	Permeability (Barrer)			Selectivity		
		H_2	CO_2	CH_4	H_2/CO_2	CO_2/CH_4	H_2/CH_4
M1	1	5.17	1.77	0.057			
(113 µm)	2	5.13	1.70	-			
	avg.	5.15	1.74	0.057	2.96	30.53	90.35
M2	1	4.96	1.83	0.059			
(110 µm)	2	5.27	1.85	-			
	avg.	5.12	1.84	0.059	2.78	31.19	86.78

Table B.4 Reproducibility data for PES/HMA (7 w/w %) membrane.

Membrane Number	Run Number	Permeability (Barrer)			Selectivity		
		H_2	CO_2	CH_4	H_2/CO_2	CO_2/CH_4	H_2/CH_4
M1	1	5.29	1.78	0.055			
(115 µm)	2	5.25	1.74	-			
	avg.	5.27	1.76	0.055	2.99	32.00	95.82
M2	1	5.37	1.51	0.043			
(130 µm)	2	5.31	1.43	-			
	avg.	5.34	1.47	0.043	3.63	34.19	124.19

Table B.5 Reproducibility data for PES/SAPO-34 membrane.

Membrane Number	Run Number	Permeability (Barrer)			Selectivity		
		H_2	CO_2	CH_4	H_2/CO_2	CO_2/CH_4	H_2/CH_4
M1 (140 µm)	1	11.09	4.52	0.184			
	2	11.32	4.55	-			
	avg.	11.21	4.54	0.184	2.47	24.67	60.92
M2 (120 µm)	1	12.25	5.49	0.216			
	2	12.64	5.25	-			
	avg.	12.45	5.37	0.216	2.32	24.86	57.64
M3 (125 µm)	1	12.69	4.93	0.195			
	2	12.39	4.22	-			
	avg.	12.54	4.58	0.195	2.74	23.49	64.31

Table B.6 Reproducibility data for PES/SAPO-34(20 w/w %)/HMA(4 w/w %) membrane.

Membrane Number	Run Number	Permeability (Barrer)			Selectivity		
		H_2	CO_2	CH_4	H_2/CO_2	CO_2/CH_4	H_2/CH_4
M1 (130 µm)	1	10.67	3.47	0.111			
	2	11.34	3.48	-			
	avg.	11.01	3.48	0.111	3.16	31.35	99.19
M2 (125 µm)	1	11.09	3.75	0.130			
	2	11.84	3.61	-			
	avg.	11.47	3.68	0.130	3.12	28.31	88.23

Table B.7 Reproducibility data for PES/SAPO-34(20 w/w %)/HMA(7 w/w %) membrane.

Membrane Number	Run Number	Permeability (Barrer)			Selectivity		
		H_2	CO_2	CH_4	H_2/CO_2	CO_2/CH_4	H_2/CH_4
M1 (125 µm)	1	9.06	2.34	0.071			
	2	8.83	2.30	-			
	avg.	8.95	2.32	0.071	3.86	32.68	126.06
M2 (125 µm)	1	9.53	2.34	0.076			
	2	9.96	2.53	-			
	avg.	9.75	2.44	0.076	3.99	32.11	128.29

Table B.8 Reproducibility data for PES/SAPO-34(20 w/w %)/HMA(10 w/w %) membrane.

Membrane Number	Run Number	Permeability (Barrer)			Selectivity		
		H_2	CO_2	CH_4	H_2/CO_2	CO_2/CH_4	H_2/CH_4
M1 (130 µm)	1	7.12	1.47	0.039			
	2	7.21	1.50	-			
	avg.	7.17	1.49	-	4.81	38.21	183.85
M2 (130 µm)	1	6.78	1.49	-			
	2	7.28	1.60	-			
	avg.	7.04	1.55	-	4.54	-	-
M3 (130 µm)	1	6.53	1.54	0.042			
	2	7.39	1.54	-			
	avg.	6.96	1.54	0.042	4.52	36.67	165.72

Table B.9 Reproducibility data for PES/SAPO-34(10 w/w %)/HMA(10 w/w %) membrane.

Membrane Number	Run Number	Permeability (Barrer)			Selectivity		
		H_2	CO_2	CH_4	H_2/CO_2	CO_2/CH_4	H_2/CH_4
M1 (130 µm)	1	4.42	1.12	0.034			
	2	4.54	1.11	-			
	avg.	4.48	1.12	0.034	4.00	33.14	132.55

Table B.10 Reproducibility data for PES/SAPO-34(30 w/w %)/HMA(10 w/w %) membrane.

Membrane Number	Run Number	Permeability (Barrer)			Selectivity		
		H_2	CO_2	CH_4	H_2/CO_2	CO_2/CH_4	H_2/CH_4
M1 (150 µm)	1	6.41	1.33	0.039			
	2	7.16	1.49	-			
	avg.	6.79	1.41	0.039	4.81	36.15	174.10
M2 (150 µm)	1	6.53	1.68	0.053			
	2	7.64	1.68	-			
	avg.	7.09	1.68	0.053	4.22	31.69	133.77

Table B.11 Reproducibility data for PES/SAPO-34(40 w/w %)/HMA(10 w/w %) membrane.

Membrane Number	Run Number	Permeability (Barrer)			Selectivity		
		H_2	CO_2	CH_4	H_2/CO_2	CO_2/CH_4	H_2/CH_4
M1 (130 µm)	1	6.73	1.60	0.056			
	2	7.65	1.61	-			
	avg.	7.19	1.61	0.056	4.48	28.75	128.39

Table B.12 Data for pure PES membrane, above T_g annealed and gas permeated at feed pressure of 3.7 bar with a initially vacuum permeate side pressure

Membrane Number	Run Number	Permeability (Barrer)		Selectivity
		H_2	CO_2	H_2/CO_2
M1 (130 µm)	1	14.35	5.48	
	2	14.21	5.17	
	avg.	14.28	5.32	2.68

Table B.13 Data for PES/pNA (4 w/w %) membranes.

Membrane Number	Run Number	Permeability (Barrer)		Selectivity
		H_2	CO_2	H_2/CO_2
M1 (155 µm)	1	9.95	2.66	
	2	9.76	2.48	
	avg.	9.86	2.57	3.84
M2 (165 µm)	1	10.85	2.70	
	2	11.11	2.97	
	avg.	10.98	2.84	3.87

Table B.14 Data for PES/ANP (4 w/w %) membranes.

Membrane Number	Run Number	Permeability (Barrer)		Selectivity
		H_2	CO_2	H_2/CO_2
M1 (120 µm)	1	12.19	3.15	
	2	11.85	3.04	
	avg.	12.02	3.10	3.88
M2 (120 µm)	1	10.58	2.52	
	2	9.82	2.34	
	avg.	10.20	2.43	4.19

Table B.15 Data for PES/AMP (4 w/w %) membranes.

Membrane Number	Run Number	Permeability (Barrer)		Selectivity
		H_2	CO_2	H_2/CO_2
M1 (125 µm)	1	14.04	4.35	
	2	13.65	4.34	
	avg.	13.85	4.35	3.18

Table B.16 Data for PES/Mia (4 w/w %) membranes.

Membrane Number	Run Number	Permeability (Barrer)		Selectivity
		H_2	CO_2	H_2/CO_2
M1 (130 µm)	1	13.71	4.49	
	2	13.49	4.58	
	avg.	13.60	4.54	2.99

Table B.17 Data for PES/AHMP (4 w/w %) membranes.

Membrane Number	Run Number	Permeability (Barrer)		Selectivity
		H_2	CO_2	H_2/CO_2
M1 (125 µm)	1	11.55	3.69	
	2	11.60	3.74	
	avg.	11.58	3.72	3.11
M2 (108 µm)	1	12.67	4.71	
	2	12.34	4.84	
	avg.	12.51	4.78	2.62

Table B.18 Data for PES/HMA (4 w/w %) membranes.

Membrane Number	Run Number	Permeability (Barrer)		Selectivity
		H_2	CO_2	H_2/CO_2
M1 (145 µm)	1	11.08	2.77	
	2	10.92	2.79	
	avg.	11.00	2.78	3.96
M2 (120 µm)	1	11.17	2.70	
	2	10.86	2.99	
	avg.	11.02	2.85	3.87

APPENDIX C

SAMPLE DSC THERMOGRAMS OF THE PREPARED MEMBRANES

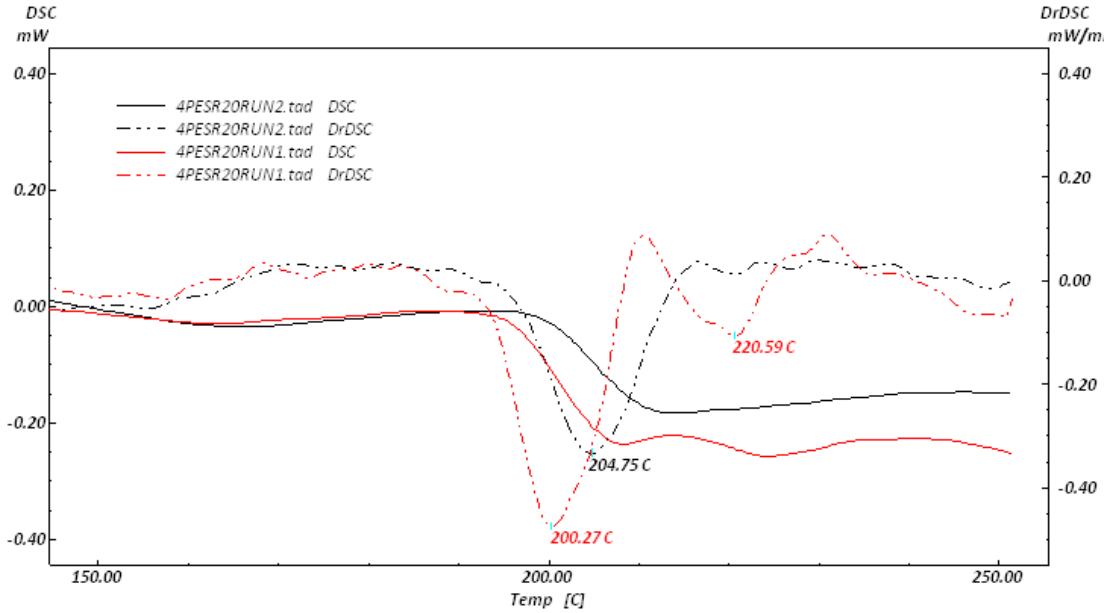

Figure C.1 The DSC graph of pure PES membrane blend (1st and 2nd scan).

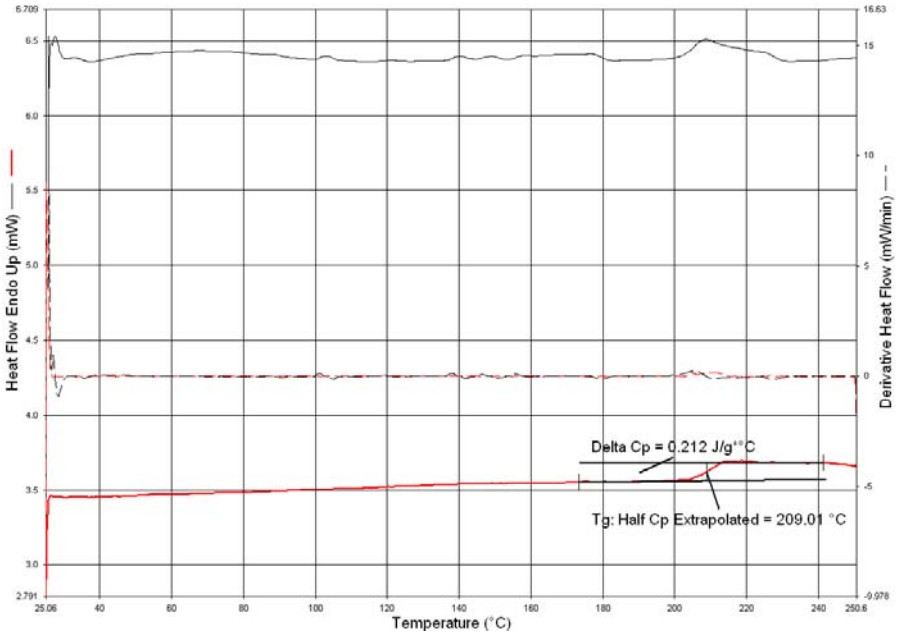

Figure C.2 The DSC graph of PES/HMA (2%) membrane blend (2nd scan).

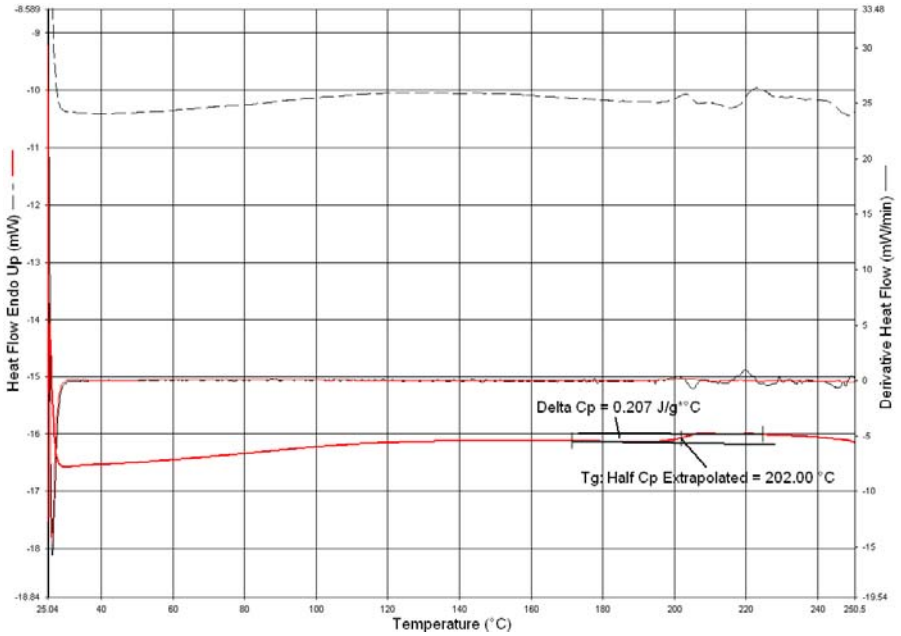

Figure C.3 The DSC graph of PES/HMA (4%) membrane blend (2nd scan).

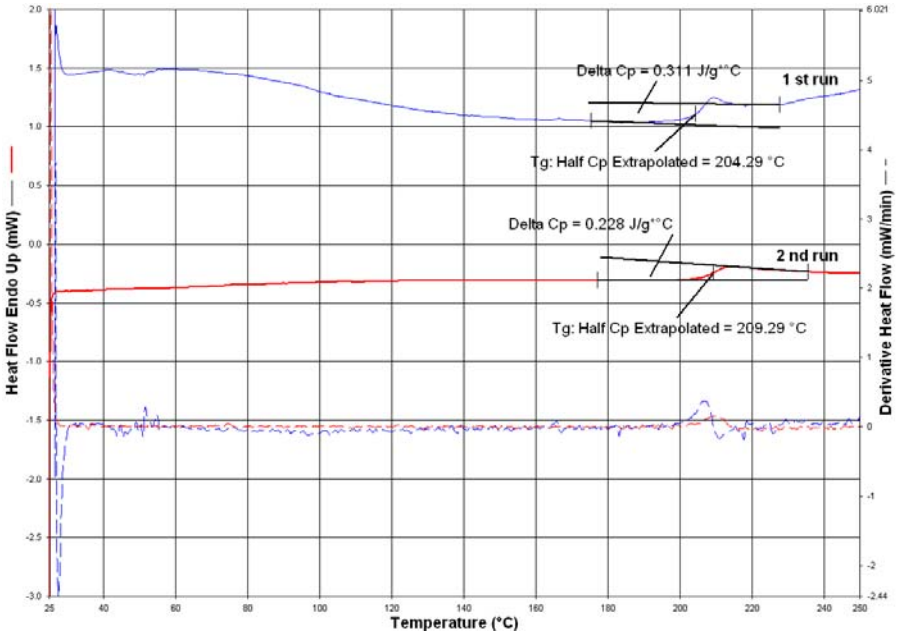

Figure C.4 The DSC graph of PES/HMA (4%) membrane blend (2nd scan).

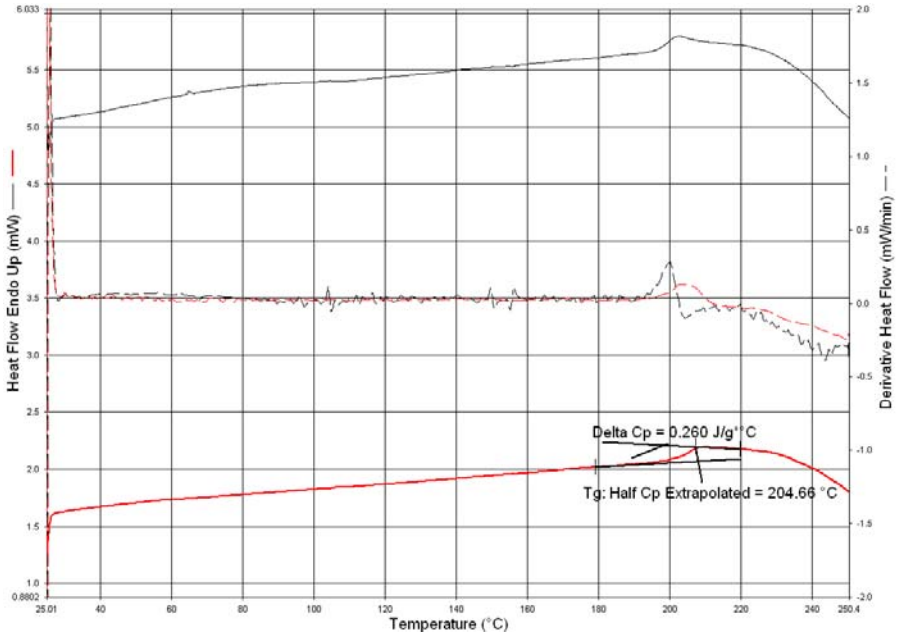

Figure C.5 The DSC graph of PES/HMA (7%) membrane blend (2nd scan).

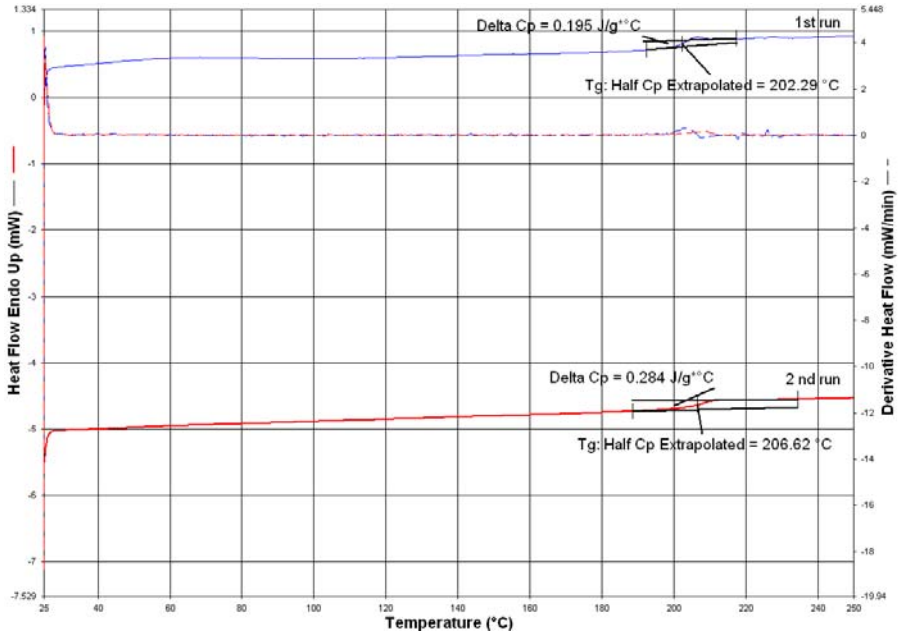

Figure C.6 The DSC graph of PES/HMA (7%) membrane blend (2nd scan).

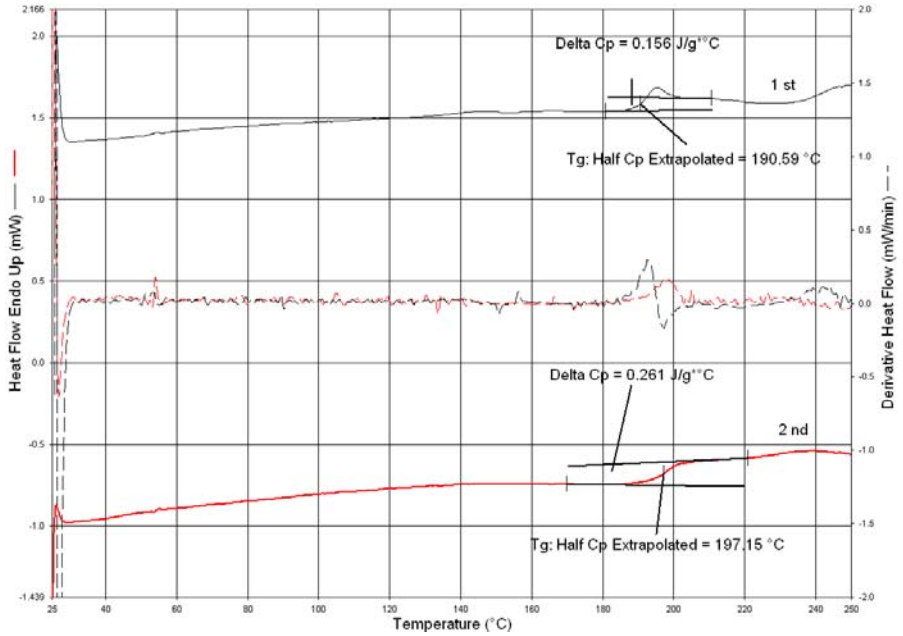

Figure C.7 The DSC graph of PES/HMA (10%) membrane blend (2nd scan).

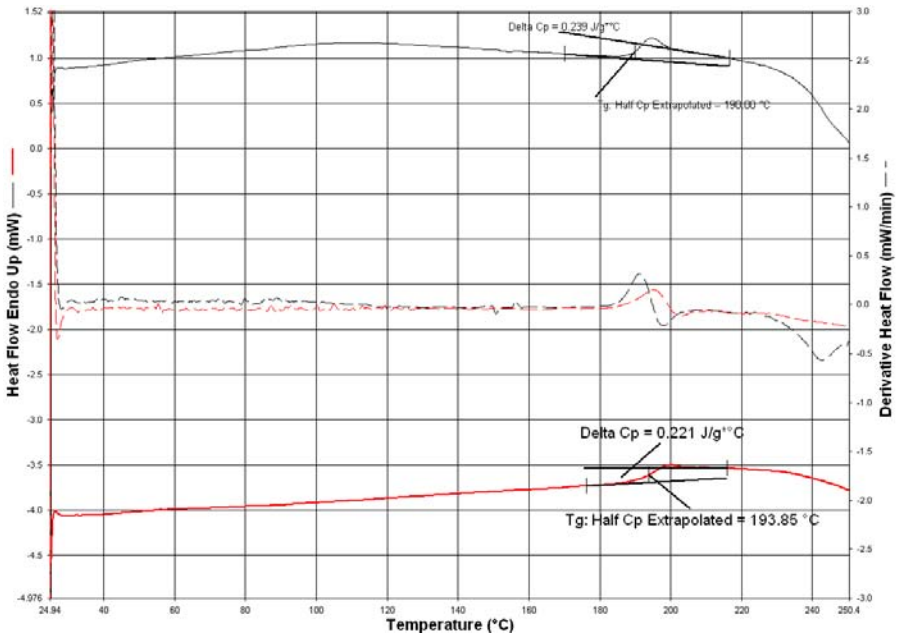

Figure C.8 The DSC graph of PES/HMA (15%) membrane blend (2nd scan).

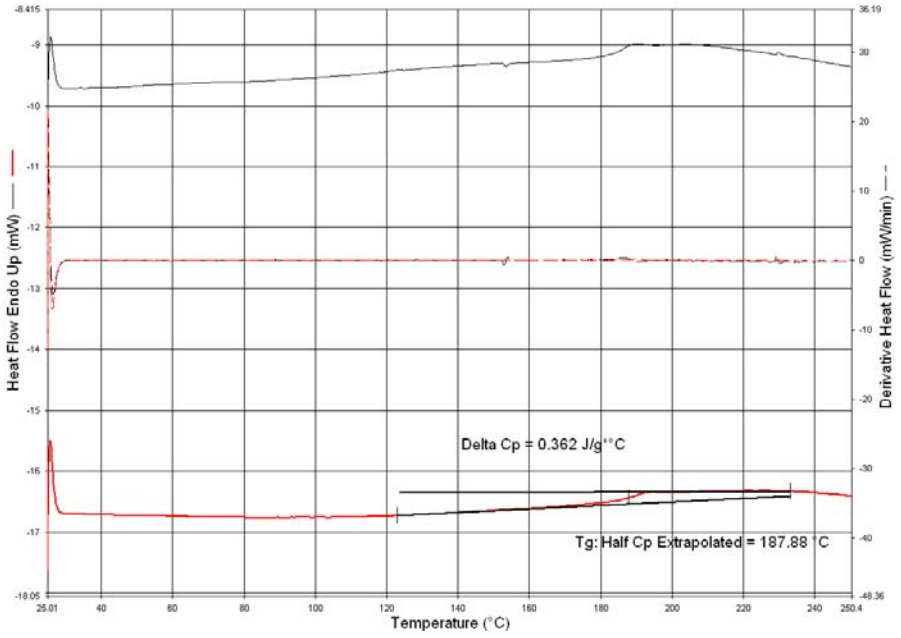

Figure C.9 The DSC graph of PES/HMA (25%) membrane blend (2nd scan).

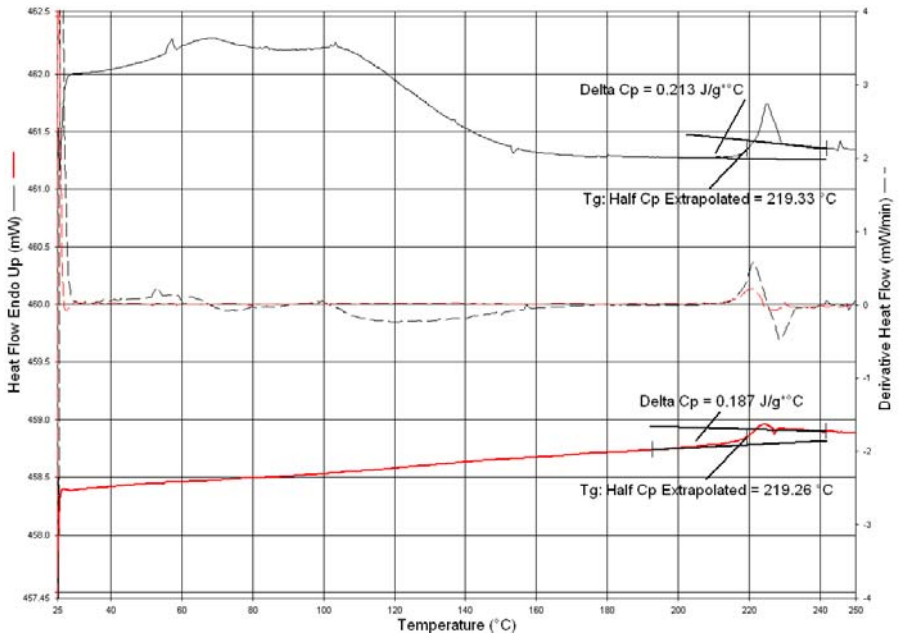

Figure C.10 The DSC graph of PES/SAPO-34 (20%) MMM (2nd scan).

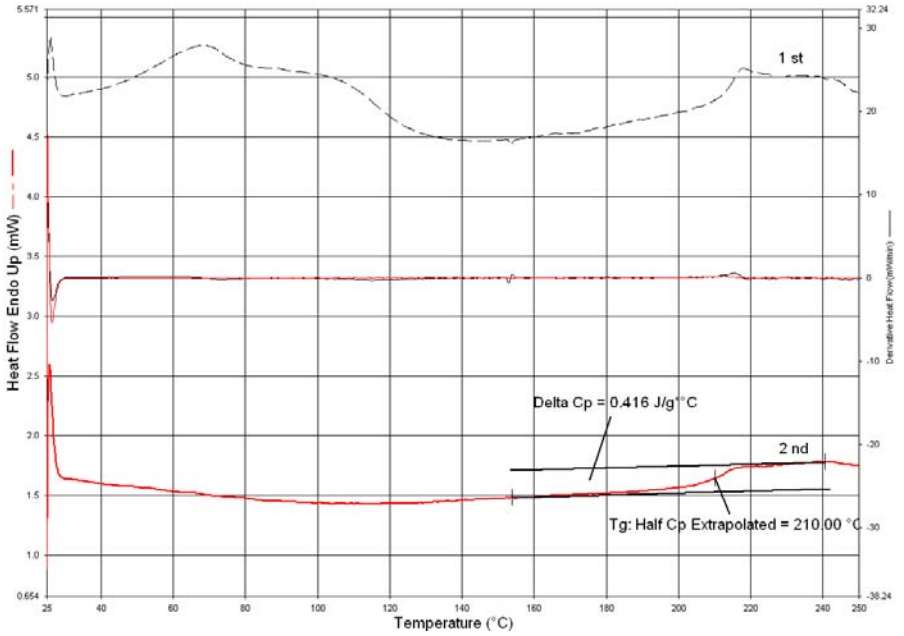

Figure C.11 The DSC graph of PES/SAPO-34 (20%)/HMA (4 %) MMM (2nd scan).

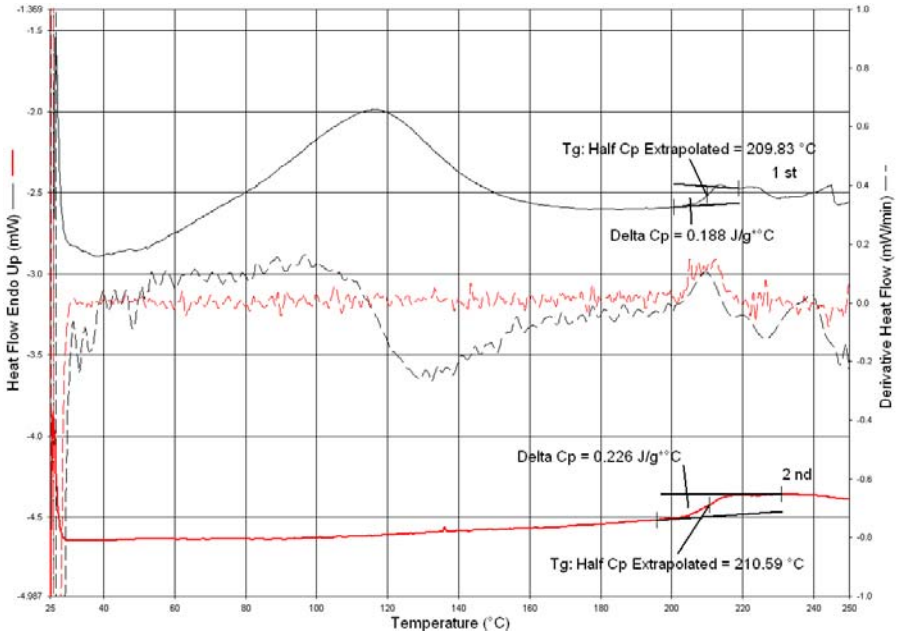

Figure C.12 The DSC graph of PES/SAPO-34 (20%)/HMA (7 %) MMM (2nd scan).

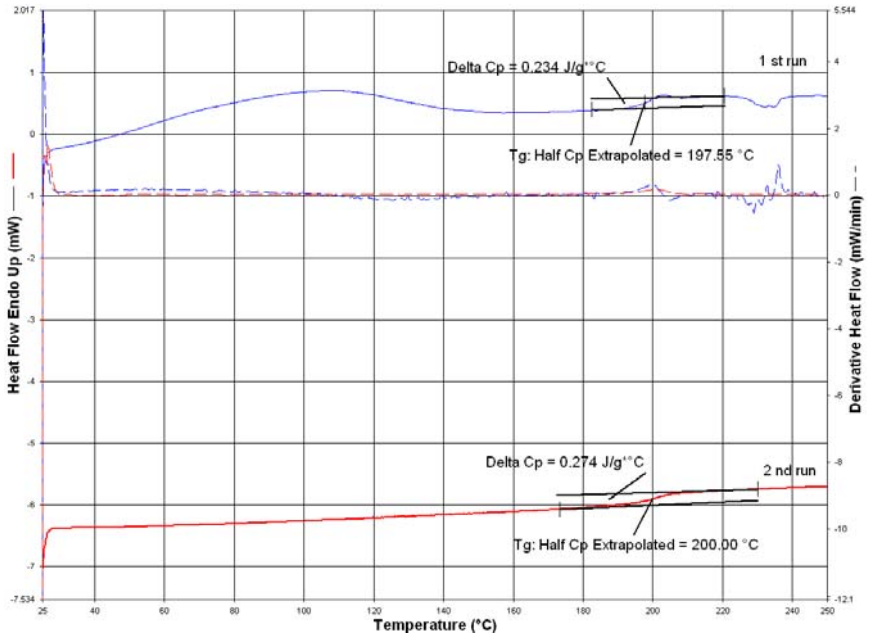

Figure C.13 The DSC graph of PES/SAPO-34 (20%)/HMA (10 %) MMM (2nd scan).

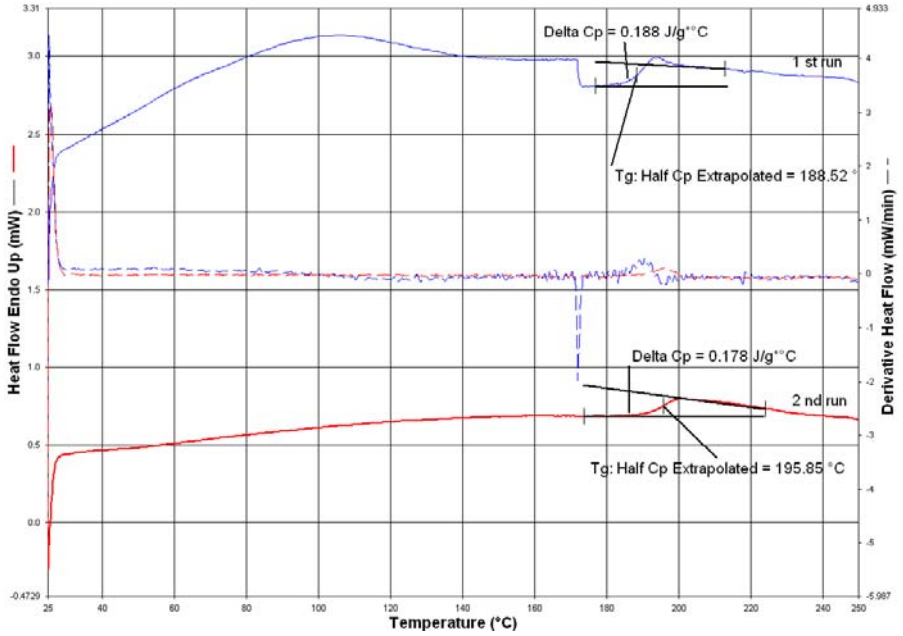

Figure C.14 The DSC graph of PES/SAPO-34 (10%)/HMA (10 %) MMM (2nd scan).

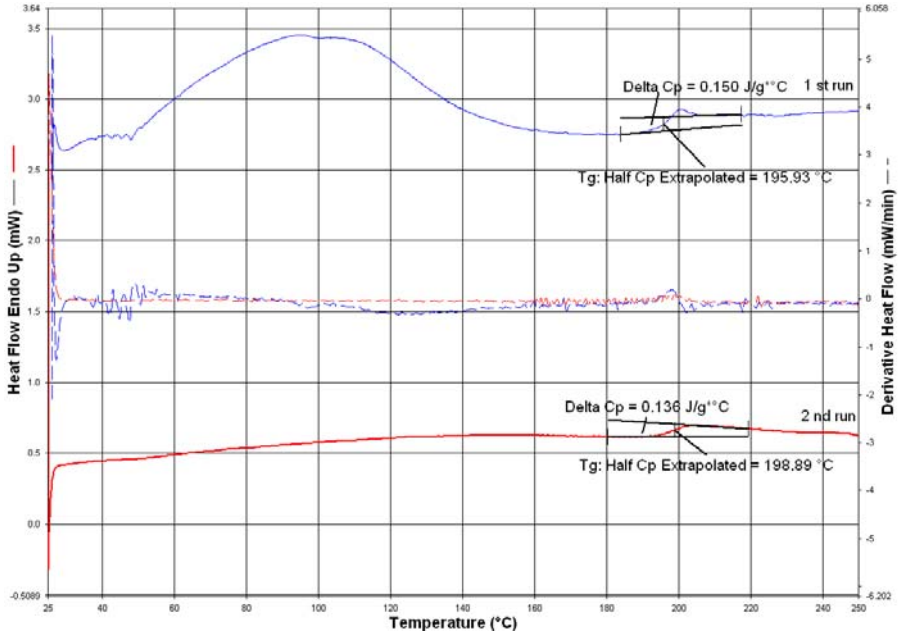

Figure C.15 The DSC graph of PES/SAPO-34 (30%)/HMA (10 %) MMM (2nd scan).

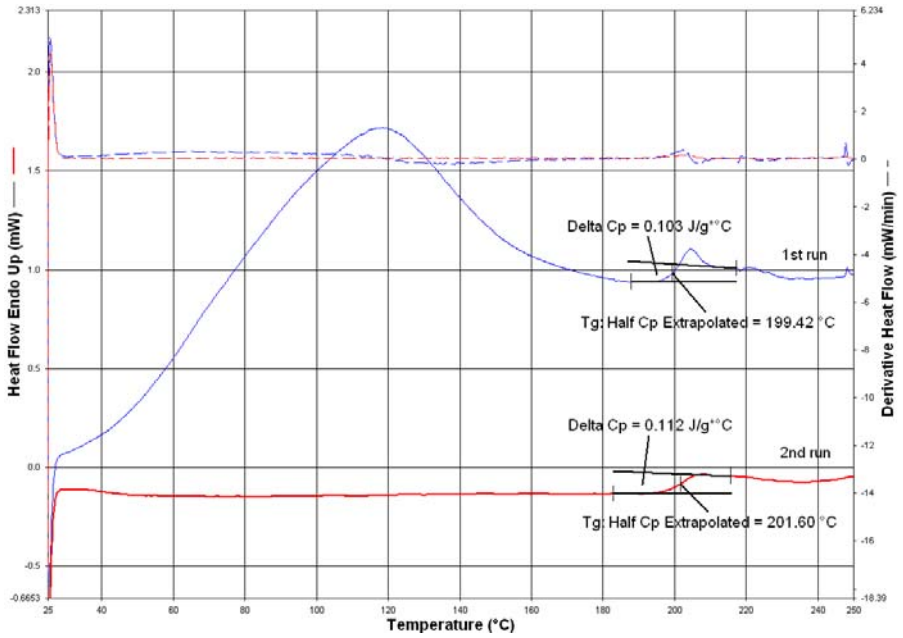

Figure C.16 The DSC graph of PES/SAPO-34 (40%)/HMA (10 %) MMM (2nd scan).

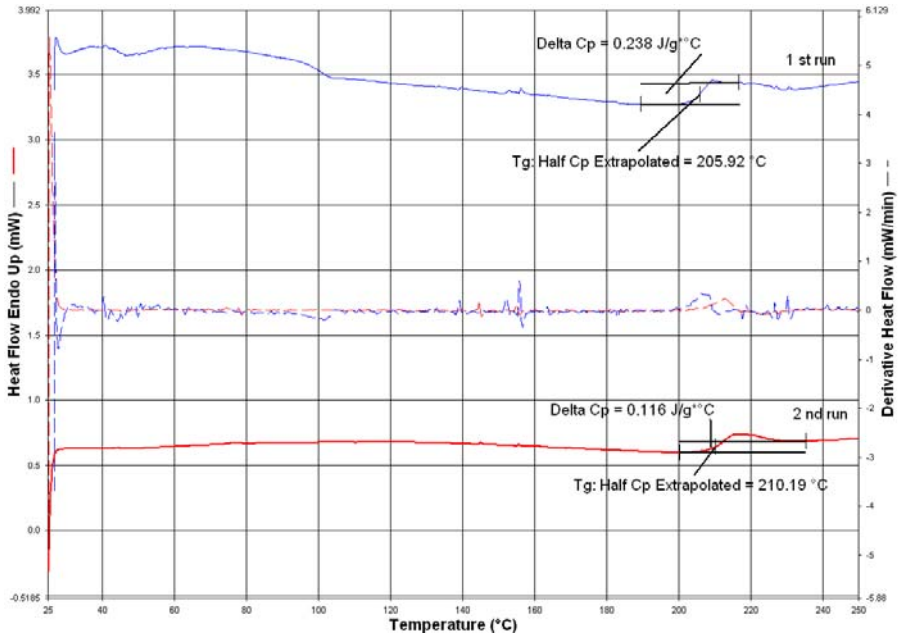

Figure C.17 The DSC graph of PES/Mia (4 %) membrane (2nd scan).

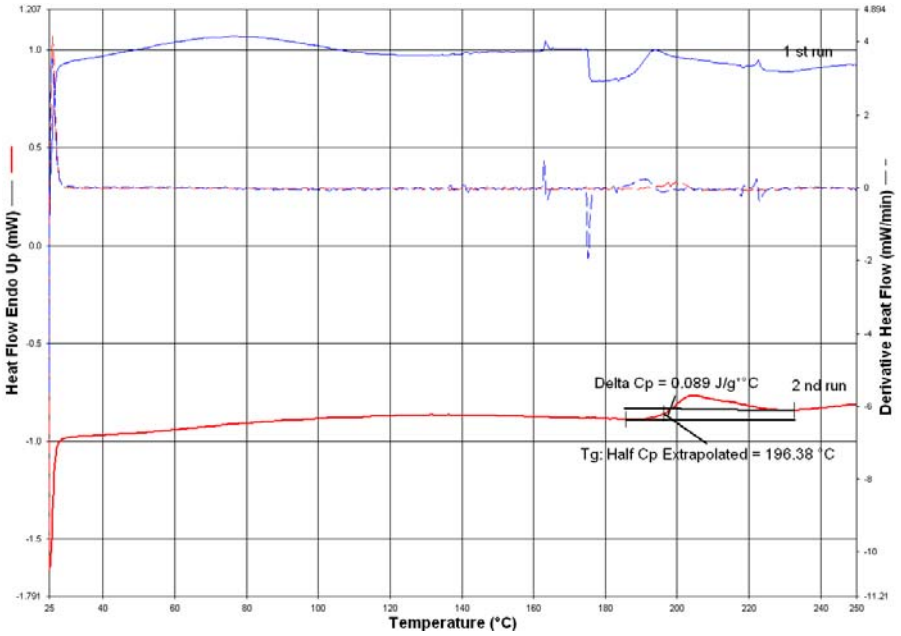

Figure C.18 The DSC graph of PES/ANP (4 %) membrane (2nd scan).

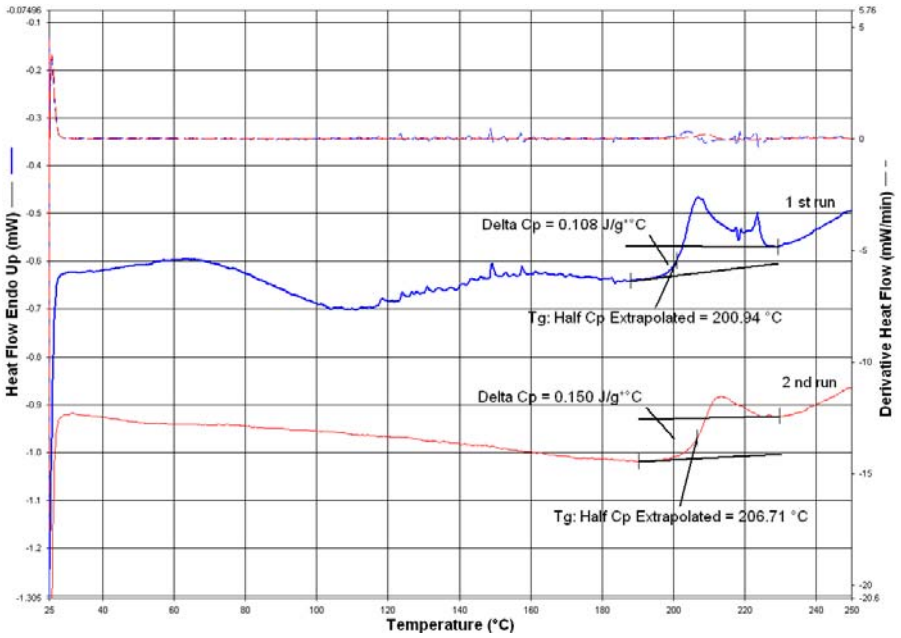

Figure C.19 The DSC graph of PES/pNA (4 %) membrane (2nd scan).

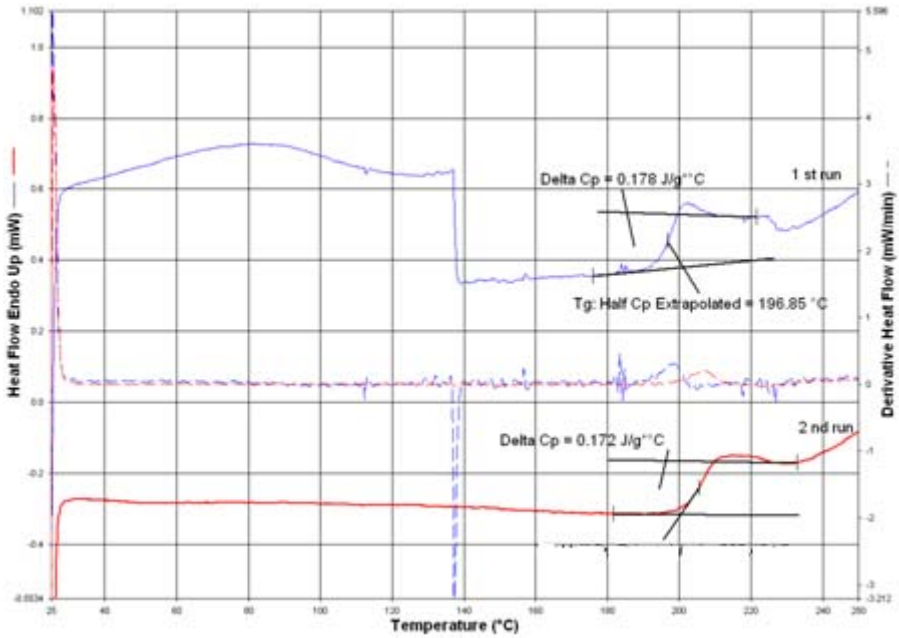

Figure C.20 The DSC graph of PES/AMP (4 %) membrane (2nd scan).

APPENDIX D

DETERMINATION OF SOLUBILITY PARAMETERS BY HOY'S METHOD

The solubility parameter components δ_d, δ_p, δ_h are known for a limited number of species, hence predicting these quantities is valuable. Hoy's method is one of the simplest group contribution methods for estimating solubility parameters. The group contributions of F_t, total molar attraction function, F_p, polar component of total molar attraction function, V, the molar volume of the species, Δ_T, the Lyderson correction for non-ideality can simply be added and used in the auxiliary equations given below. Values of increments in Hoy's system for the molar attraction constants can be found in elsewhere [35].

$$F_t = \sum N_i F_{t,i} \qquad (D.1)$$

$$F_p = \sum N_i F_{p,i} \qquad (D.2)$$

$$V = \sum N_i V_i \qquad (D.3)$$

$$\Delta_T = \sum N_i \Delta_{T,i} \qquad (D.4)$$

$$\alpha^P = \frac{777\Delta_T}{V} \qquad (D.5)$$

$$n = \frac{0.5}{\Delta_T} \qquad (D.6)$$

$$\delta_t = \frac{F_t + B/n}{V} \qquad where\ B = 277 \qquad (D.7)$$

$$\delta_p = \delta_t\left(\frac{1}{\alpha^P}\frac{F_p}{F_t + \frac{B}{n}}\right) \qquad (D.8)$$

$$\delta_h = \delta_t\left(\frac{\alpha^P - 1}{\alpha^P}\right)^{1/2} \qquad (D.9)$$

$$\delta_d = (\delta_t{}^2 - \delta_p{}^2 - \delta_h{}^2)^{1/2} \qquad (D.10)$$

Sample Calculation of Solubility Parameter Estimation by Hoy's Method for 2-Hydroxy 5-Methyl Aniline (HMA)

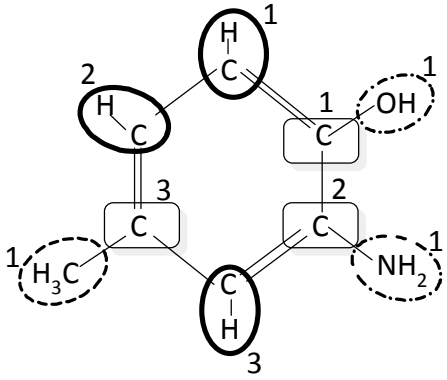

Table D.1 Values of increment of molar functions for Hoy's system

Group	No	Ft	Fp	V	Δ_T
CH(aromatic)	3	239.9	62.2	13.417	0.011
C(aromatic)	3	200.7	64.8	7.422	0.011
OH(phenolic)	1	349.8	349.8	12.457	0.035
NH_2	1	463.5	463.5	17.012	0.031
CH_3	1	303.4	0	21.548	0.02
6 Memb. Ring	1	-48	61	0	0
meta substitution	1	13.5	-24.3	0	0
para substitution	1	82.4	-33.8	0	0
Σ		2486.4	1197.2	113.534	0.152

Table D.2 Estimated solubility parameter components for HMA

α^P	n	δ_t	δ_p	δ_h	δ_d
1.127	3.036	22.703	14.573	7.626	15.6495

APPENDIX E

THERMAL GRAVIMETRY ANALYSIS GRAPHS

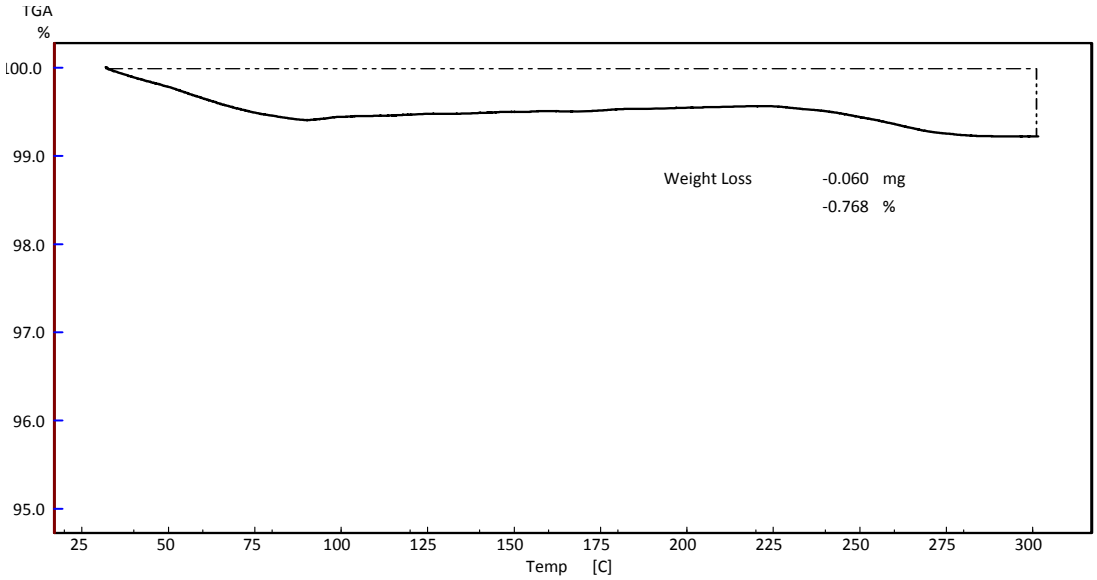

Figure E.1 TGA thermogram of above T_g annealed pure PES membrane (Annealing at 225 ^{o}C for 8 hours)

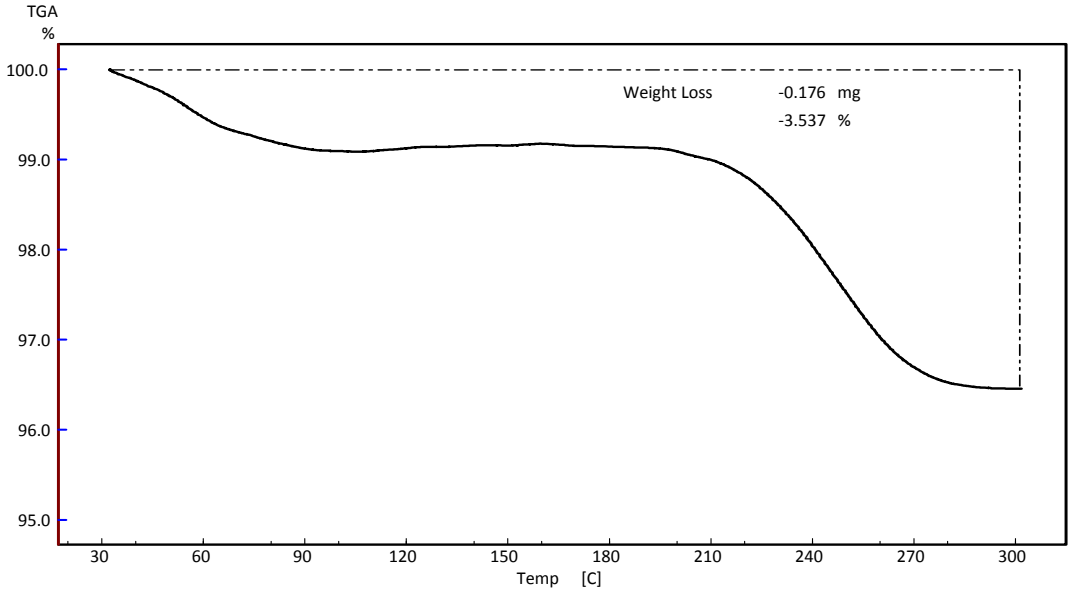

Figure E.2 TGA thermogram of pure PES membrane
(Annealing at 130 ^{o}C for 3 days)

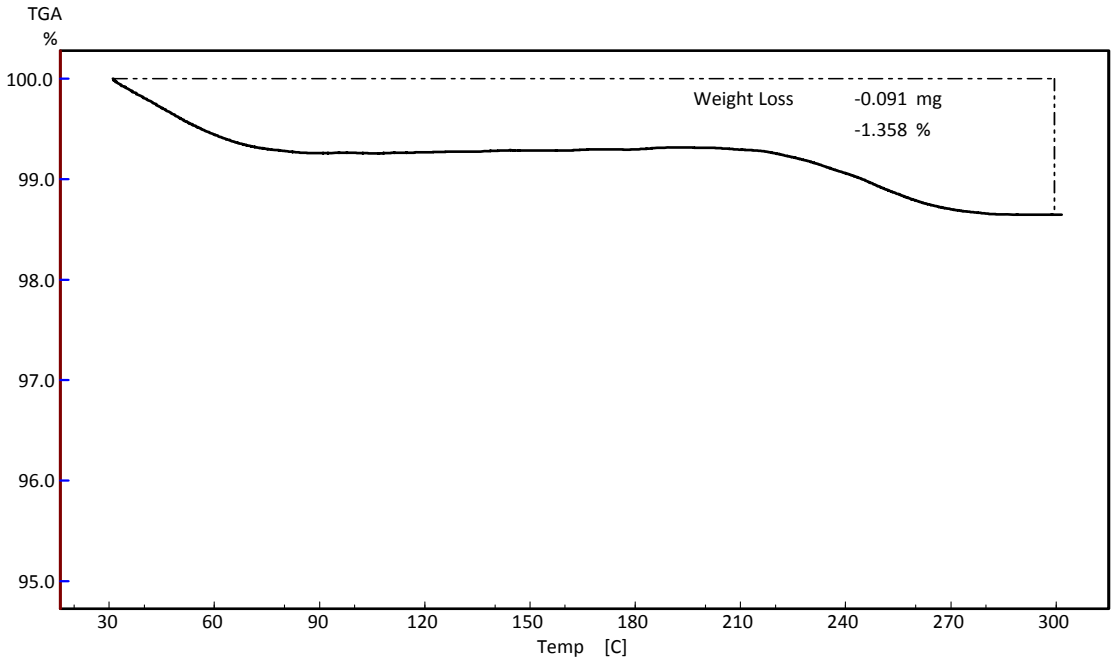

Figure E.3 TGA thermogram of pure PES membrane
(Annealing at 160 ^{o}C for 3 days)

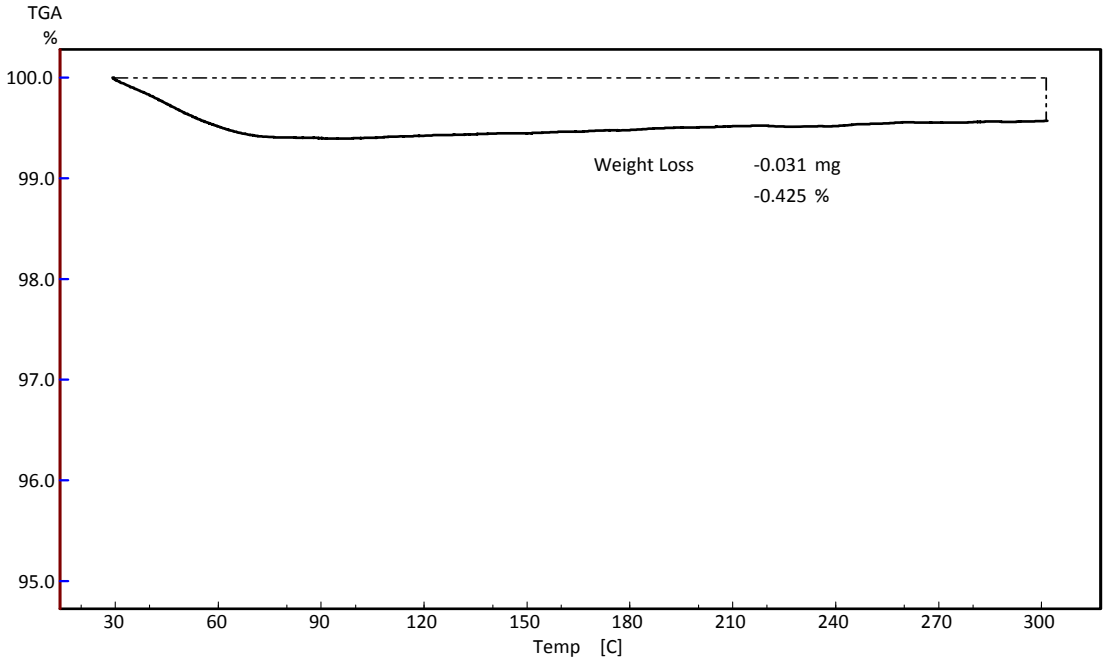

Figure E.4 TGA thermogram of pure PES membrane

(Annealing at 190 ^{o}C for 3 days)

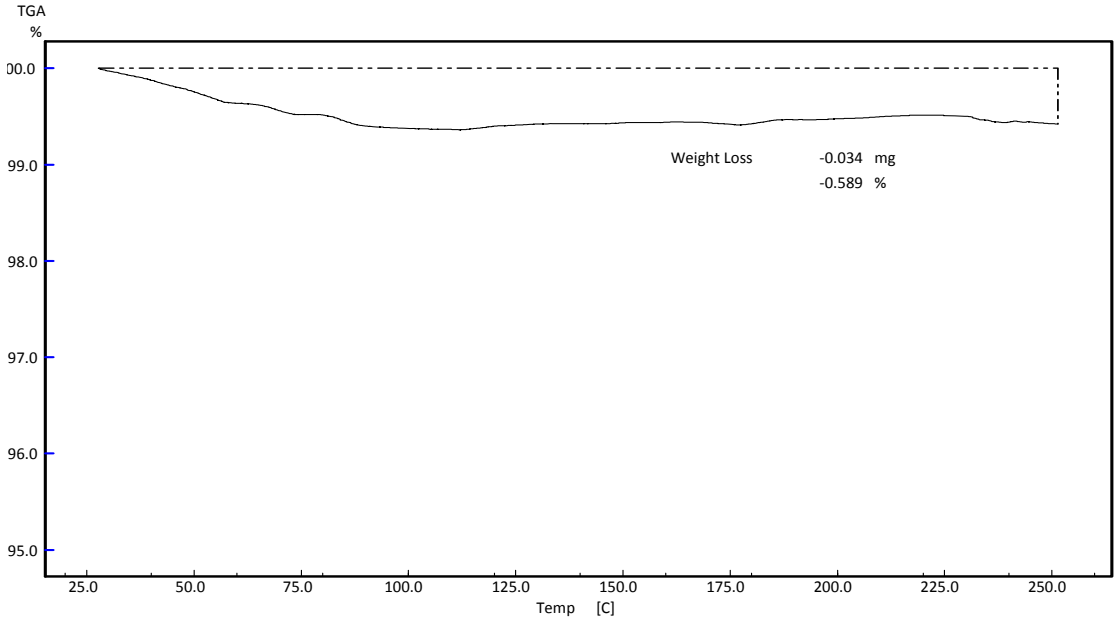

Figure E.5 TGA thermogram of PES/HMA(2 w/w %) membrane

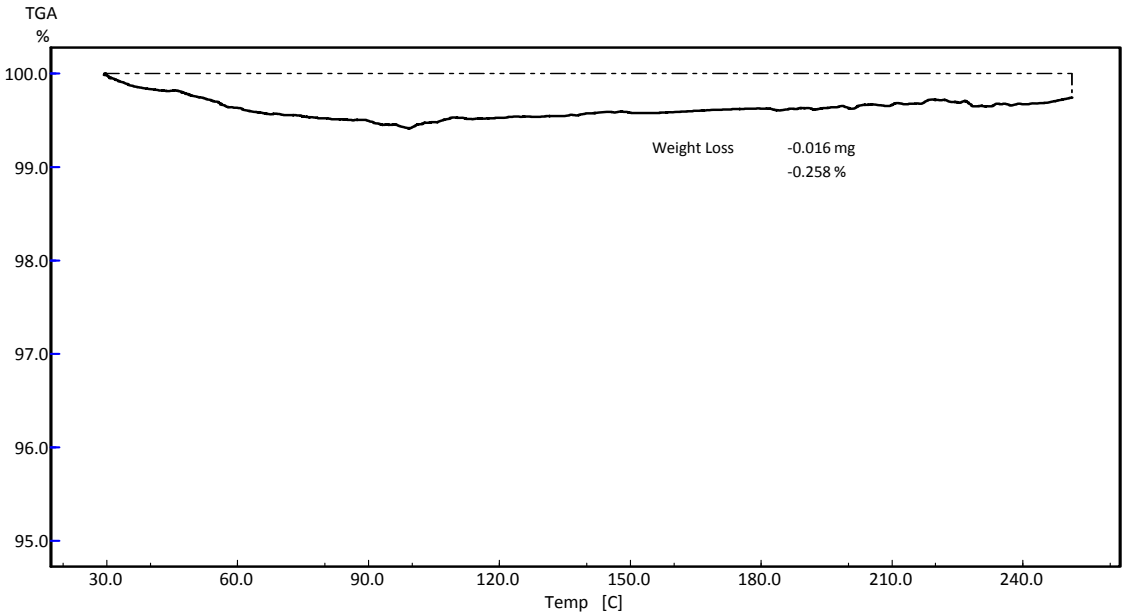

Figure E.6 TGA thermogram of PES/AHMP (4 w/w %) membrane

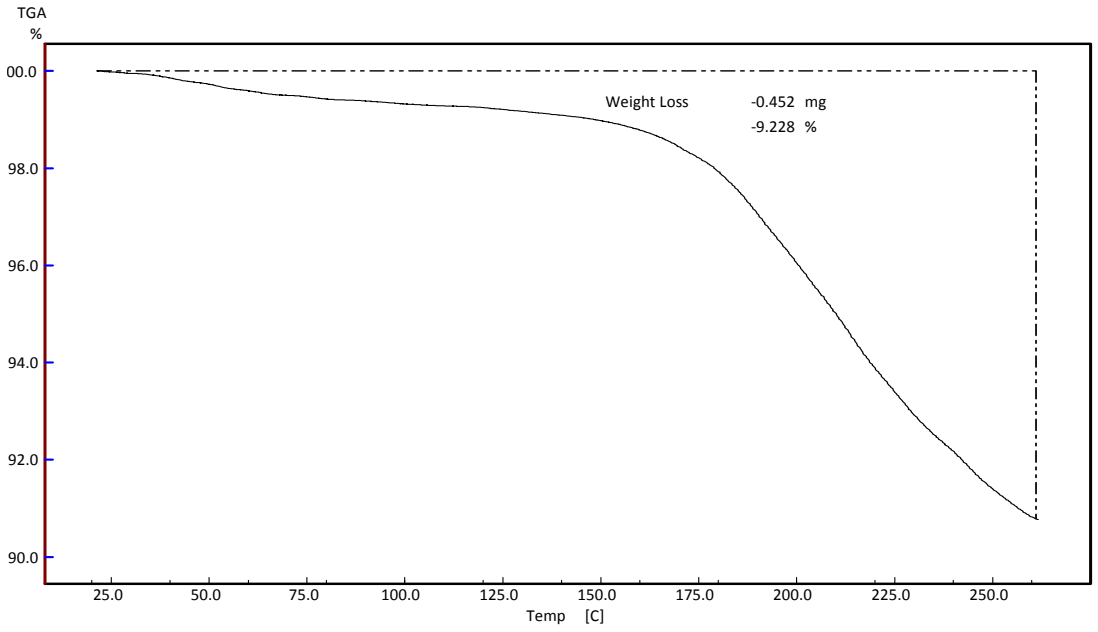

Figure E.7 TGA thermogram of pure PES membrane prepared by only solvent evaporation (without annealing)

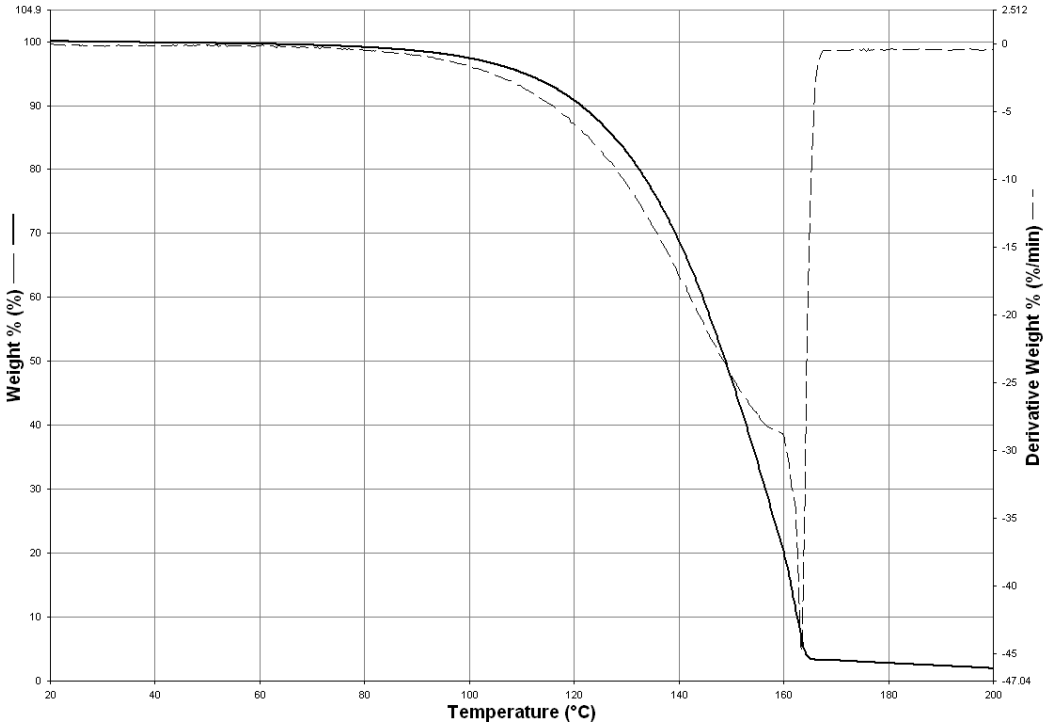

Figure E.8 TGA thermogram of powder 2-Amino-4-methylpyrimidine (AMP)

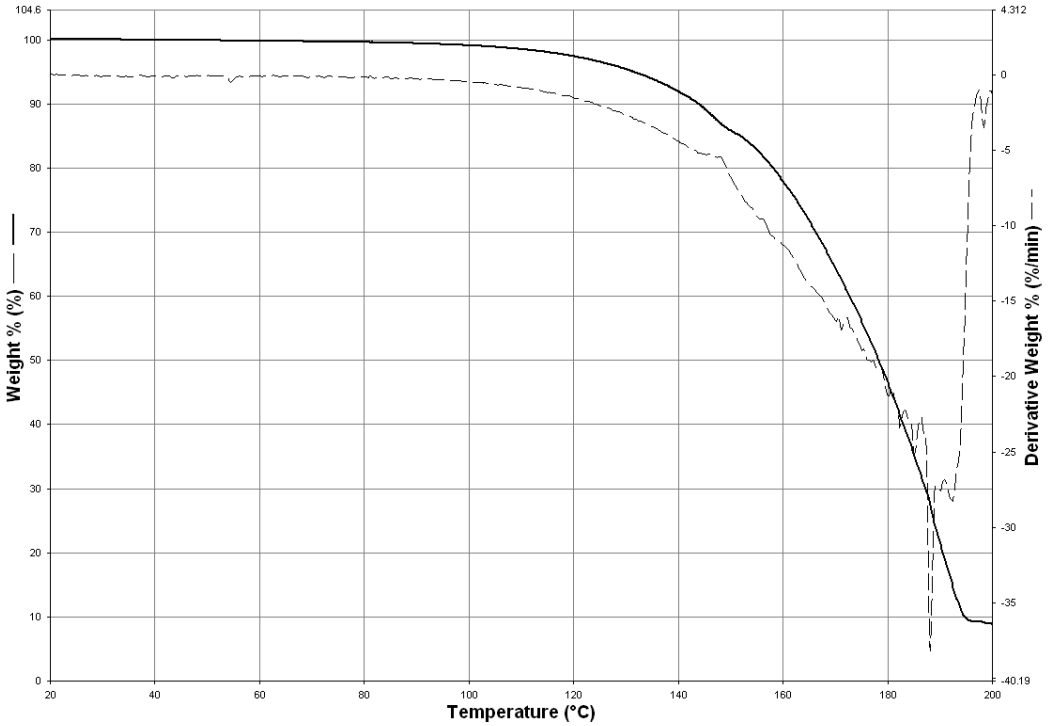

Figure E.9 TGA thermogram of powder 2-Methyldimidazole (Mia)

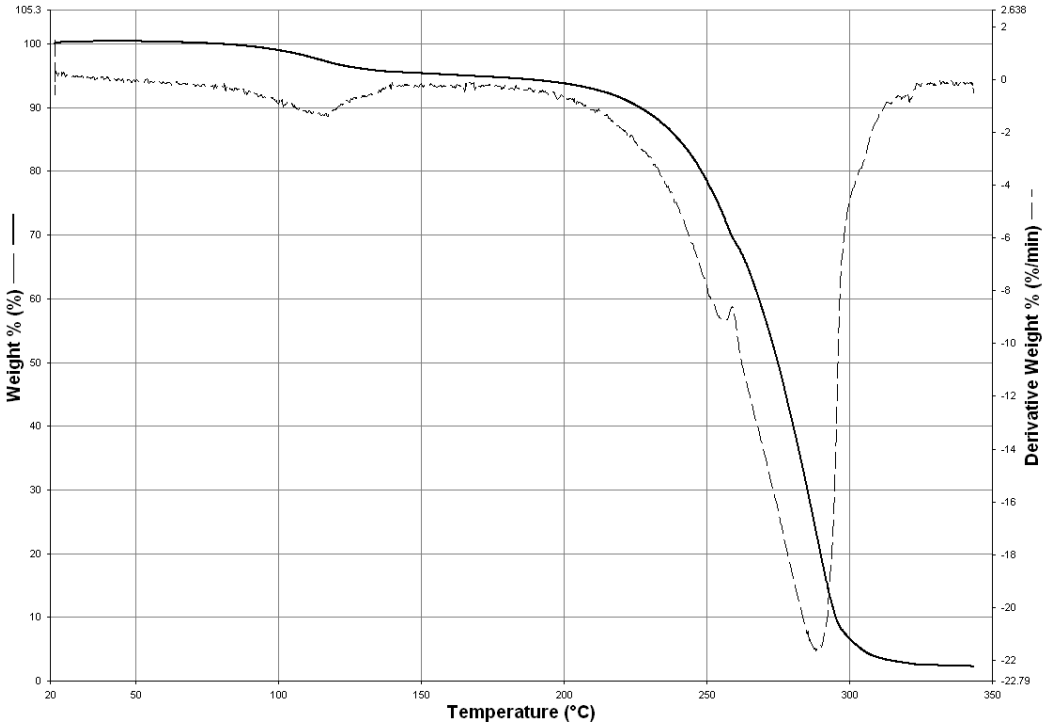

Figure E.10 TGA thermogram of powder 2,4,6 Triaminoprymidine (TAP)

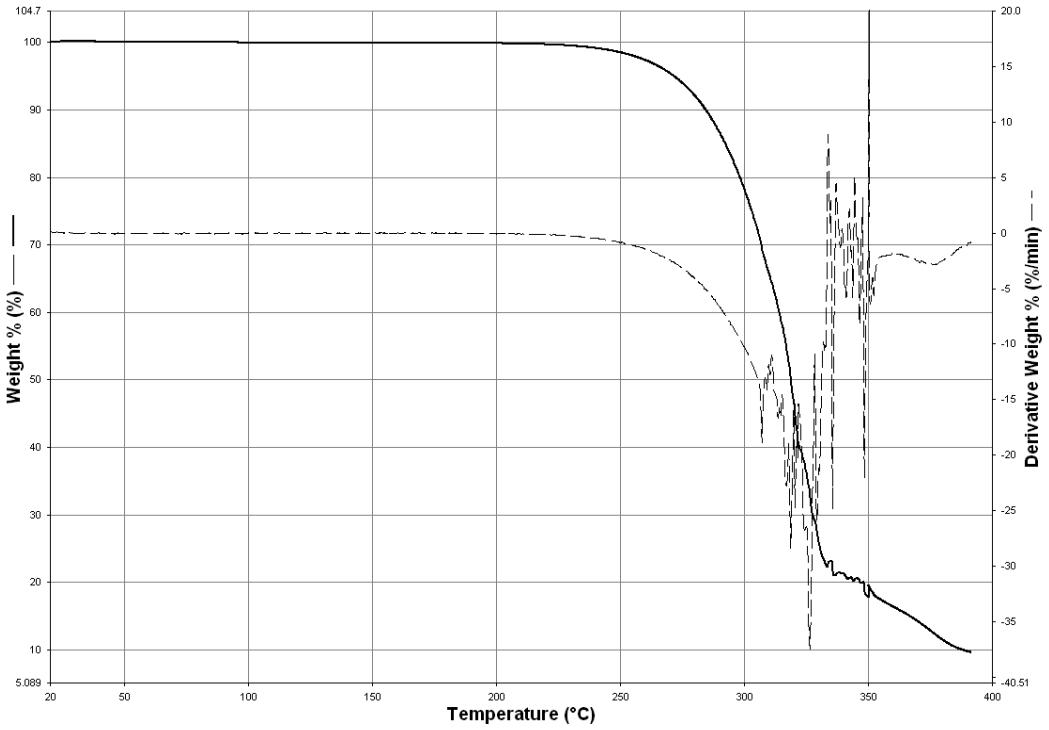

Figure E.11 TGA thermogram of powder 2-Amino-4-hydroxy-6 Methyl Pyrimidine (AHMP)

APPENDIX F

ELEMENTAL ANALYSIS

Table F.1 Carbon-Nitrogen-Sulphur Elemental Analysis Results

Membrane	% C	% N	% S
neat PES	61.57	-	14.00
	54.28	-	13.75
	65.21	-	14.10
	Avg: 60.35	-	Avg: 13.95
PES/HMA (4 w/w %)	63.93	0.20	13.7
	63.99	0.22	13.67
	57.95	0.19	13.39
	Avg: 61.96	Avg: 0.21	Avg: 13.57
PES/HMA (7 w/w %)	61.99	0.26	13.55
	59.31	0.24	13.48
	53.59	0.24	13.32
	Avg: 58.29	Avg: 0.25	Avg: 13.45
PES/HMA (10 w/w %)	64.80	0.33	13.51
	63.02	0.37	13.31
	63.02	0.25	13.33
	Avg: 63.61	Avg: 0.32	Avg: 13.38
un-annealed PES/HMA (25 w/w %)	59.94	1.91	13.74
	59.78	1.83	13.45
	53.66	1.85	13.51
	Avg: 57.79	Avg: 1.86	Avg: 13.57
PES/HMA (25 w/w %)	64.70	0.37	13.02

Sample calculation of expected weight percentage of nitrogen in PES/HMA membranes:

HMA has a chemical formula of C_7H_9NO, and a molecular weight of 123.16 gmole.

Nitrogen percentage in a single molecule of HMA is;

$$\%\ N_{in\ HMA} = \frac{14\frac{g}{mole} of\ N}{123.16\frac{g}{mole} of\ HMA} = \%\ 11.37$$

In a casting solution of PES/HMA (4 w/w %) membrane, 0.058 g of HMA and 1.45 g PES is dissolved in 7.25 ml DMSO. Assuming all of the solvent is evaporated during membrane fabrication, Amount of nitrogen element in the membrane is;

$$N_{(weight\ in\ membrane)} = 0.058\ g\ HMA * \frac{11.37}{100} = 6.59 * 10^{-3} g\ N$$

Weight percentage of nitrogen element in the membrane can be found dividing the weight of nitrogen by the weight of the membrane;

$$\%\ N_{in\ membrane} = \frac{6.59 * 10^{-3}\ gN}{(1.45\ gPES + 0.058\ g\ HMA)} * 100 = \%\ 0.437$$

Weight percentage of nitrogen element in the PES/HMA (4 % w/w) expected is % 0.437.

Sample calculation of estimated HMA/PES ratio in PES/HMA membranes from the CNS elemental analysis results:

Weight percentage of nitrogen element in the PES/HMA (4 % w/w) measured by CNS analysis is % 0.21. The weight of nitrogen element can be found from the weight percentage of N in the membrane measured from CNS analysis;

$$\frac{x\ g\ of\ N}{1.45 + \frac{x\ g\ of\ N}{0.1137}} * 100 = 0.21\ \rightarrow\ x = 3.10 * 10^{-3}\ g\ of\ N\ in\ membrane$$

$$HMA\ in\ the\ membrane = \frac{x}{0.1137}\ \rightarrow 0.027\ g\ of\ HMA\ in\ the\ membrane$$

$$\frac{HMA}{PES}\left(\frac{w}{w}\%\right) = \frac{0.027\ g\ HMA}{1.45\ g\ PES} * 100 = \%1.89$$

Sample calculation of weight percentages of elements in membranes:

Weight percentages of elements in PES and HMA are calculated. For PES, repeating unit is 788 g/unit, and carbon weight is 504 g/unit, sulphur weight is 96 g/unit, oxygen weight is 160 g/unit, hydrogen weight is 28 g/unit. For HMA, carbon weight is 84 gmole, oxygen weight is 16 gmole, hydrogen weight is 9 gmole, and nitrogen weight is 14 gmole. Using these amounts, weight percentages are calculated and tabulated in Table F.2.

Table F.2 Weight percentages of elements in polymer and additive

Elements	PES (% (w/w))	HMA (% (w/w))
C	63.96	68.20
S	12.18	0
O	20.31	12.99
H	3.55	7.31
N	0	11.37

The percentages tabulated in Table F.2 are used to find the weights of these elements in the membrane using the actual amounts of polymer and additive utilized during the preparation of this membrane. Sample is given in Table F.3 for PES/HMA (4 % (w/w)) membrane.

Table F.3 Amounts of elements in PES/HMA (4 % (w/w)) membrane.

Elements	In 1.45 g PES	In 0.058 g HMA	In Membrane
C (g)	0.93	0.0390	0.97
S (g)	0.18	0	0.18
O (g)	0.29	0.0075	0.30
H (g)	0.05	0.0042	0.056
N (g)	0	0.0065	0.0065

Table F.3 reveals that the weight of the overall membrane is 1.501 g, which is the addition of the weights of the elements. If the amount of carbon in membrane is divided by the weight of the membrane and multiplied by 100, the carbon percentage can be found to be 64. 12 %. Similarly, for the percentages of other elements, sulphur found to be 11.71 %, oxygen to be 20.02 %, hydrogen to be 3.69 %, nitrogen to be 0.44 %.